AD_____

Award Number: DAMD17-99-1-9408

TITLE: Measurement of the Electron Density Distribution of Estrogens-A First Step to Advanced Drug Design

PRINCIPAL INVESTIGATOR: Alan A. Pinkerton, Ph.D.

CONTRACTING ORGANIZATION: The University of Toledo
Toledo, Ohio 43606-3390

REPORT DATE: August 2001

TYPE OF REPORT: Annual

PREPARED FOR: U.S. Army Medical Research and Materiel Command
Fort Detrick, Maryland 21702-5012

REPORT DOCUMENTATION PAGE

Form Approved
OMB No. 074-0188

1. AGENCY USE ONLY (Leave blank)	2. REPORT DATE	3. REPORT TYPE AND DATES COVERED
	August 2001	Annual (15 Jul 00 - 14 Jul 01)

4. TITLE AND SUBTITLE
Measurement of the Electron Density Distribution of Estrogens-A First Step to Advanced Drug Design

5. FUNDING NUMBERS
DAMD17-99-1-9408

6. AUTHOR(S)
Alan A. Pinkerton, Ph.D.

7. PERFORMING ORGANIZATION NAME(S) AND ADDRESS(ES)
The University of Toledo
Toledo, Ohio 43606-3390

E-Mail: apinker@uoft02.utoledo.edu

8. PERFORMING ORGANIZATION REPORT NUMBER

9. SPONSORING / MONITORING AGENCY NAME(S) AND ADDRESS(ES)
U.S. Army Medical Research and Materiel Command
Fort Detrick, Maryland 21702-5012

10. SPONSORING / MONITORING AGENCY REPORT NUMBER

11. SUPPLEMENTARY NOTES
Report contains color.

12a. DISTRIBUTION / AVAILABILITY STATEMENT
Approved for Public Release; Distribution Unlimited

12b. DISTRIBUTION CODE

13. ABSTRACT *(Maximum 200 Words)*

Estradiol and related compounds bind as ligands to the estrogen receptor initiating biological reactions, which can cause either initiation/progress or inhibition of tumor growth. Slight structural variations in these molecules can change their carcinostatic potentials from agonistic to inhibitory. The principle objective of this proposal is to relate known biological reactions to physical properties such as point charges of atoms and the electrostatic potential.

We are obtaining information about these electronic properties of estrogen derivatives from experimental determination of their electron density using high quality single crystal X-ray crystallography. We derived electron density, electrostatic potential and related properties for two estrogen derivatives: 3,16α,17β-estriol and estrone. Though it is too early to make any predictions, these two compounds show a significant difference in the electrostatic potential distributions and atomic charges. We have developed the methodology of crystallization and X-ray experiments to obtain even more accurate results in a shorter period of time. For four other estrogen derivatives, charge density quality data have been collected. These experiments are currently at the stage of multipole refinements.

14. SUBJECT TERMS
Breast cancer, X-ray crystallography, estrogens, drug design

15. NUMBER OF PAGES
100

16. PRICE CODE

17. SECURITY CLASSIFICATION OF REPORT	18. SECURITY CLASSIFICATION OF THIS PAGE	19. SECURITY CLASSIFICATION OF ABSTRACT	20. LIMITATION OF ABSTRACT
Unclassified	Unclassified	Unclassified	Unlimited

Table of Contents

Introduction

The principal objective of this proposal is to obtain physico-chemical information on estrogen derivatives and correlate this knowledge to their known biological functionality. Slight chemical variation in these molecules can change the carcinostatic potentials from agonistic to inhibitory. Relating these biological reactions to physical properties such as point charges of atoms and the electrostatic potential is a logical first step in the intelligent design of therapeutical drugs. We are obtaining information about the electronic properties of estrogen derivatives from experimental determination of their electron density using high quality single crystal X-ray crystallography at low temperatures.

Body

Task 1. Preliminary Studies on a series of crystals of estrogen derivatives

- Feasibility study of already available crystals of estrogen derivatives

  The 2,3,17-estriol crystals appeared to be air and light sensitive. We are planning to work on crystallization of this compound under nitrogen atmosphere.

- Development of crystallization methods for the derivatives not yet available as high quality single crystals

  We have continued to develop crystallization methods for obtaining high quality crystals of several different estrogen derivatives. During the past year we succeeded to obtain high quality crystals of
  - 17α-estradiol (crystallized from ethanol),
  - 4-Hydroxyestradiol (crystallized from acetonitrile)

- Variable Temperature studies on each sample to define the appropriate temperature for the measurement

  Variable temperature studies were performed on the diffractometer on both above mentioned crystals. As our criterion for stability we chose the change in mosaicity of the respective crystal as identified by the broadening of the profiles of the diffraction intensities in comparison to a room temperature measurement. In our in-house experiments using Ag-radiation (0.56083 Å), both samples proved to be stable under nitrogen cooling to 100 K.
  The 3-Hydroxy-β-estradiol•MeOH, 3-Hydroxy-β-estradiol•urea•MeOH•H_2O, 3-Hydroxy-α-estradiol•MeOH, Hydroxy-α-estradiol•urea•MeOH•H_2O, β-estradiol •isopropanol, estrone•acetonitrile, estriol•acetone crystals were tested under helium temperature (about 15K). Contrary to our previous synchrotron results with 17 α-estradiol•1/2 H_2O, 17β-estradiol•urea, 17β-estradiol•1/2 MeOH, 17β-estradiol•2/3 MeOH•1/3 H_2O and estrone, we found no significant increase in the crystal's mosaicities

after slow cooling. We are continuing our investigations of the correlation between the final temperature of the crystal, speed of cooling, flux of the beam, wavelength etc. and the mosaicity observed from the diffracted beam in order to enhance the stability of the respective estrogen derivative.

- Routine X-ray crystal structure determination on uncharacterized derivatives

  - crystal structures of all studied compounds have been reported earlier

Task2. Electron density studies on the above mentioned estrogen analogues

- Electron density studies at nitrogen temperatures

  We have collected complete high quality data sets for charge density analyses on crystals of
  - 17α-estradiol
  - 3,16α,17β-estriol
  - 17β-estradiol•1/2 H_2O
  - 17β-estradiol•urea- two data sets were collected due to reflection overlapping problems in the first data set.

- Electron density studies at helium temperatures

  He-temperature studies have shown contradictory results with respect to crystal instability (see above) under extreme cooling. We are developing cooling techniques that will improve the stability of the crystals and therefore enable us to use the benefit of very low temperatures (a vast increase in scattering power) for our electron density data sets.

- Analysis of the experimental data, preparation of manuscripts

  - 3,16α,17β-estriol: The electron density study is completed, a manuscript for publication is in preparation. An optimized local atomic coordinate system was developed (Appendix A) in order to better compare the results from different estrogen analogs. The results (Appendix B) were presented at the Gordon Research Conference "Electron distribution and chemical bonding", Mount Holyoke College - South Hadley , MA July 8 - 12, 2001.
  - Estrone: A manuscript for publication has been prepared and is ready for submission (Appendix C).
  - 4-Hydroxyestradiol: Preliminary crystallographic studies have been performed, the crystals appeared to be good quality, the crystal structure (Appendix D), redetermined at 120K confirmed the results reported earlier from room temperature data.
  - 17α-estradiol•1/2 H_2O: The analysis of the electron density data is currently under investigation but incomplete.

- 17α-estradiol: The analysis of the electron density data is currently under investigation but incomplete.
- 17β-estradiol•1/2 MeOH: The analysis of the electron density data is currently under investigation but incomplete.
- 17β-estradiol•urea: The analysis of the electron density data is currently under investigation but incomplete.
- 17β-estradiol•2/3 MeOH•1/3 H_2O: The publication of the crystal structure is in preparation. Analyzing the electron density data has proven to be difficult, because the compound crystallizes in the space group $P2_1$ with three crystallographically independent estradiol molecules in the asymmetric unit. The number of parameters therefore triples compared to crystal structures with only one estrogen molecule in the asymmetric unit. We believe that the results of electron density determinations on similar derivatives will provide us with valuable starting values to further model the electronic properties of the crystal under investigation.
- 17β-estradiol•1/2 H_2O: The analysis of the electron density data, measured at 90K with Bruker's CCD-6000 detector showed an unsatisfactory quality of the data due to an unknown measurement/data integration problem. Currently, we are trying to understand the source of the poor quality of the data coming from the measurements with CCD-6000. Our preliminary recommendation is not to use this detector model for accurate charge density studies, at least in combination with a Ag X-ray tube. The data will to be recollected with CCD 2K.

Task 3. Extension of the above mentioned studies to the series of E_2 C-ring analogs.

The compounds have been ordered and we are planning to start the feasibility tests and try to crystallize these samples shortly.

Key Research Accomplishments

- Crystallization of high quality crystals
- Determination of electrostatic potential and other properties of 3,16α,17β-estriol and estrone
- Methodology development for electron density experiments and data treatment:
    a) optimized temperature conditions
    b) best detector type determination
    c) best local atomic coordinate system

Reportable Outcomes

1. American Crystallographic Association Meeting, St. Paul, MN, July 22-17, 2000.
2. 19th European Crystallographic Meeting, Nancy, France, August 25-31, 2000.
3. Gordon research conference "Electron distribution and chemical bonding", Mount

Holyoke College - South Hadley , MA July 8 - 12, 2001.

4. Bruker Area Detector Users Group Meeting, Madison, WI, May 21-22, 2001.

Conclusion

We have derived the electron density, electrostatic potential and related properties for two estrogen derivatives: 3,16α,17β-estriol and estrone. Though it is too early to make any predictions, these two compounds show a significant difference in the electrostatic potential distributions and atomic charges. We have developed the methodology of crystallization and X-ray experiments to obtain even more accurate results in a shorter period of time. For four other estrogen derivatives charge density quality data have been collected. These data are currently under multipole refinements.

References:

1. D.Parrish, N.Wu & A.A.Pinkerton "Charge Density Distribution of Estrone". American Crystallographic Association Meeting, St. Paul, MN, July 22-17, 2000.
2. D.Parrish, N.Wu & A.A.Pinkerton "Charge Density Distribution of Estrone". 19th European Crystallographic Meeting, Nancy, France, August 25-31, 2000.
3. P.Kumaradhas & A.A.Pinkerton "A Charge Density and Electrostatic Potential Study on Estrogen Molecules: Estriol". Gordon research conference "Electron distribution and chemical bonding", Mount Holyoke College - South Hadley , MA July 8 - 12, 2001 (Appendix B).
4. A.A.Pinkerton "Just How Good Is Your Data". Bruker Area Detector Users Meeting, Madison, WI, May 21-22, 2001.

Appendix A.

An Optimized Atomic Local Coordinate System for Estrogen Molecules

Charge Density 'Rules':

1. Non-hydrogen atoms, always label the first vector (v1) **x**. (unless it's a linear atom, then v1 should be **z**).
2. Always label the second vector (v2) **y**.
3. Hydrogen atoms, always label the first vector (v1) **z**.

What to populate first:

sp	20, possibly 40 (watch pi-density)	
sp2	33+, 20	
sp3	32-	bisect 2 pairs of atoms for dummy atom positions

Remember: always make the bond distance of the atoms equal.
For example, if you want to bisect the angle of a H atom and C atom, push the H to the C distance, or your vector will not be a true bisection.

Treat lone pairs like bonds when determining hybridization.

The top side, or side containing the methyl group, is the β side. Therefor all hydrogens on this side are to be named with a "b". All hydrogens on the bottom side, or α side, will be labeled with an "a".

ENANTIOMERS

All estradiol derivatives are chiral, which means there are two possible enantiomers. To test to see if you have the correct one, go into XP and type the following command:

tors c11 c12 c13 c18

This will calculate the torsion angle of these 4 atoms. The angle should be about 70°. If the angle is negative (-), you have the correct enantiomer, if the angle is positive (+), you have the wrong enantiomer.

TOP

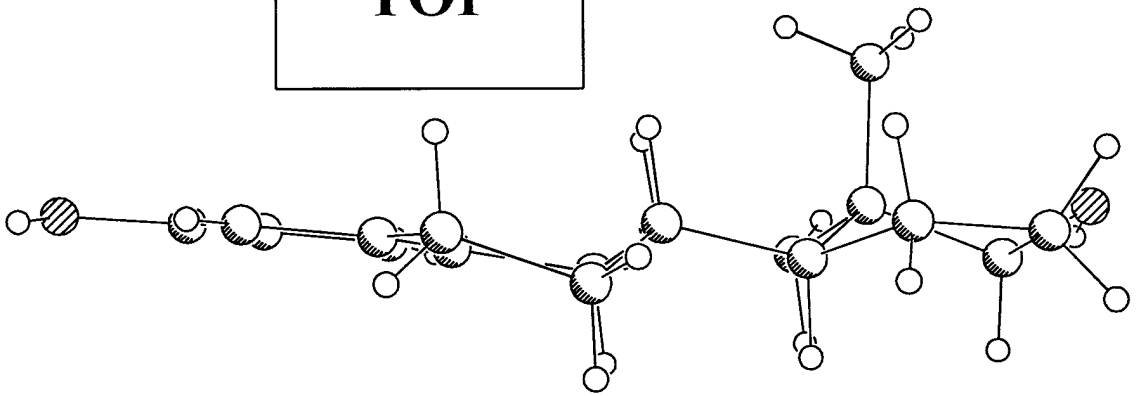

BOTTOM

R_2CH_2 Hydrogens

These include the hydrogens on the following C atoms.
(C6,C7,C11,C12,C15,C16)

This example is of C6.

Point v2 at the other hydrogen on the carbon.

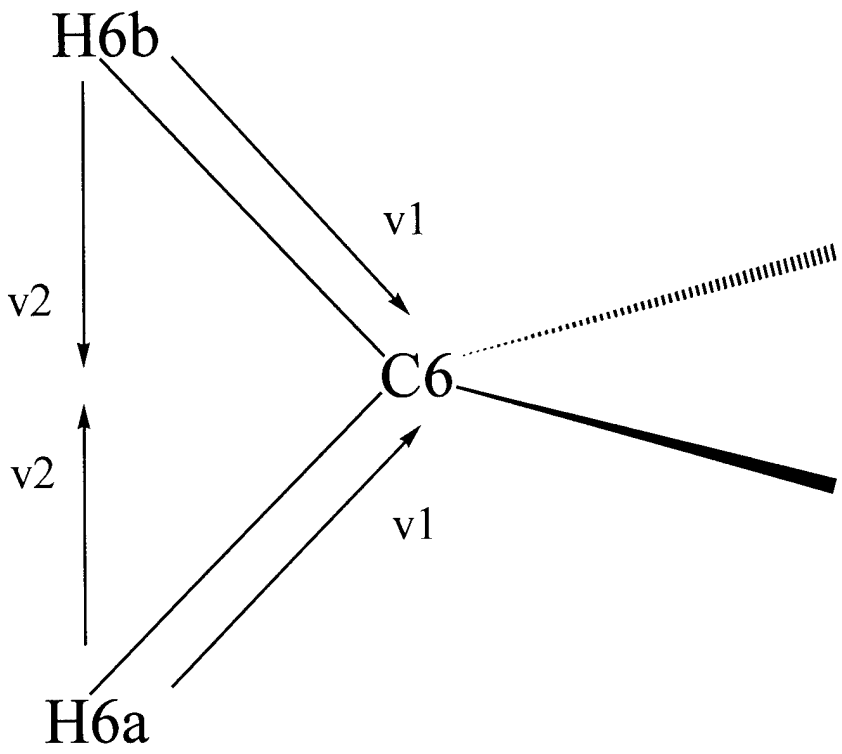

H8, H9, and H14

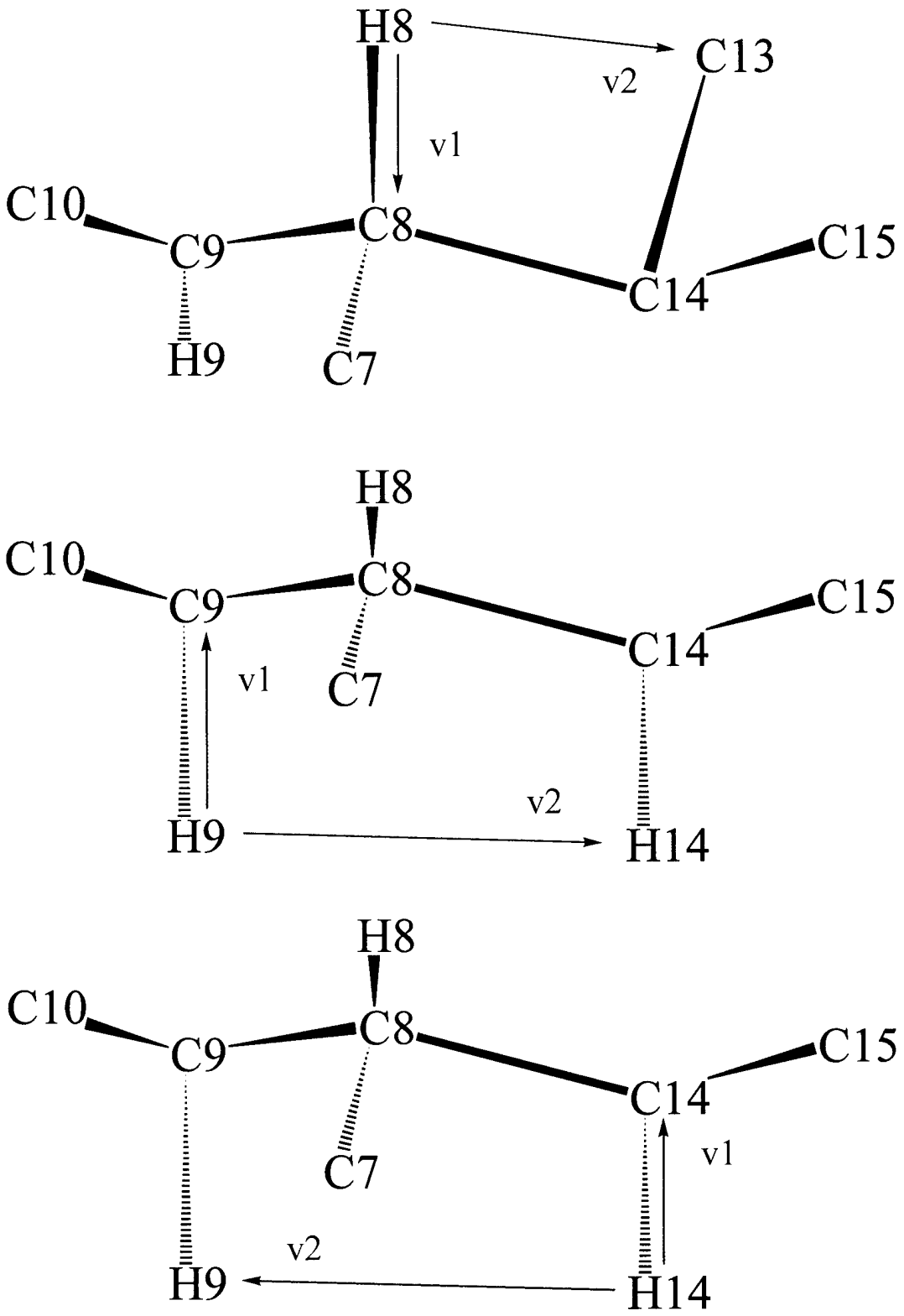
H8
C13
v2
v1
C10
C8
C15
C9
C14
H9
C7
H8
C10
C8
C9
C15
C14
v1
C7
v2
H9
H14
H8
C10
C8
C9
C15
C14
C7
v1
v2
H9
H14

Hydroxy Group

This diagram can be used for any hydroxy group (X= C, N, etc.)

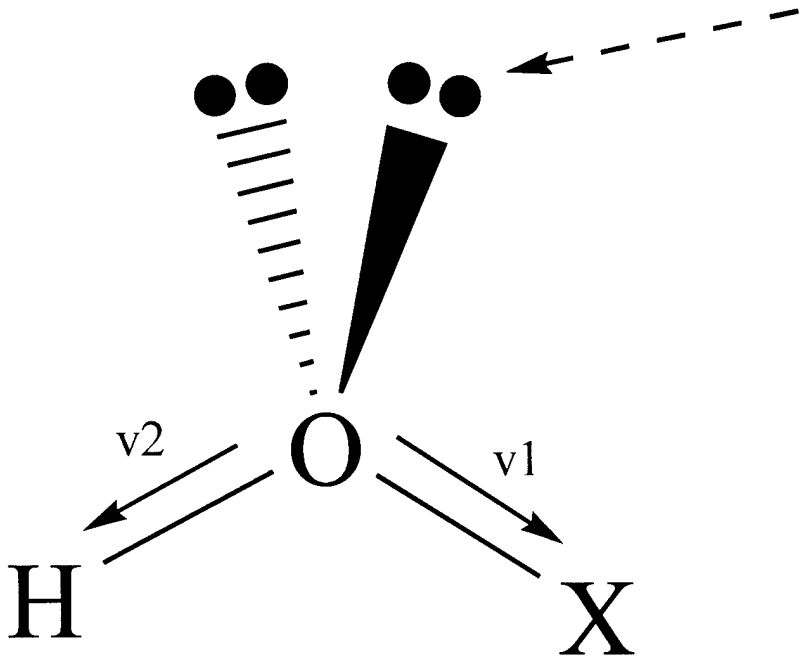

To calculate the bisection, place a hydrogen atom at the lone pair position, then push it to the same distance as the O-X bond.
Remember to pay attention to the geometry. Sometimes the oxygens can appear to be shaped more like sp3 than sp2.

C18 with Hydrogens

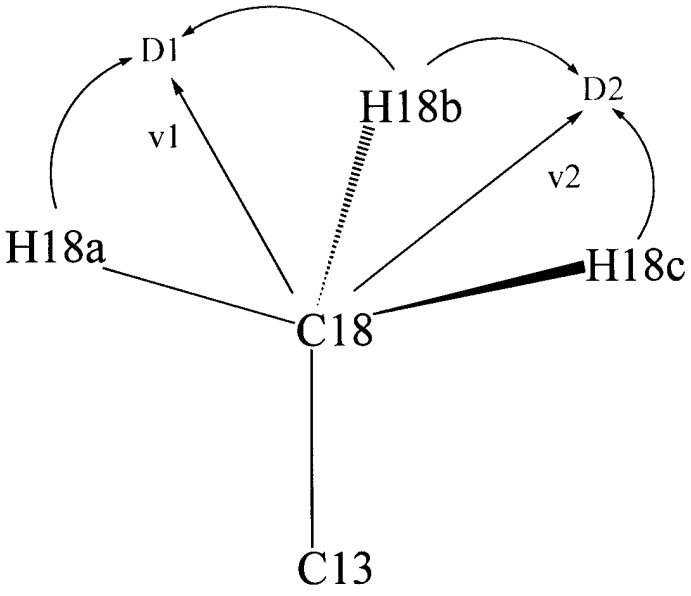

Looking down the 3-fold axis of C18.

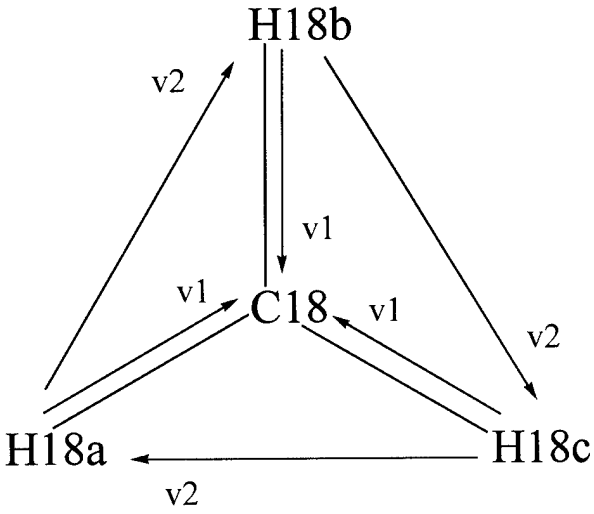

A Ring

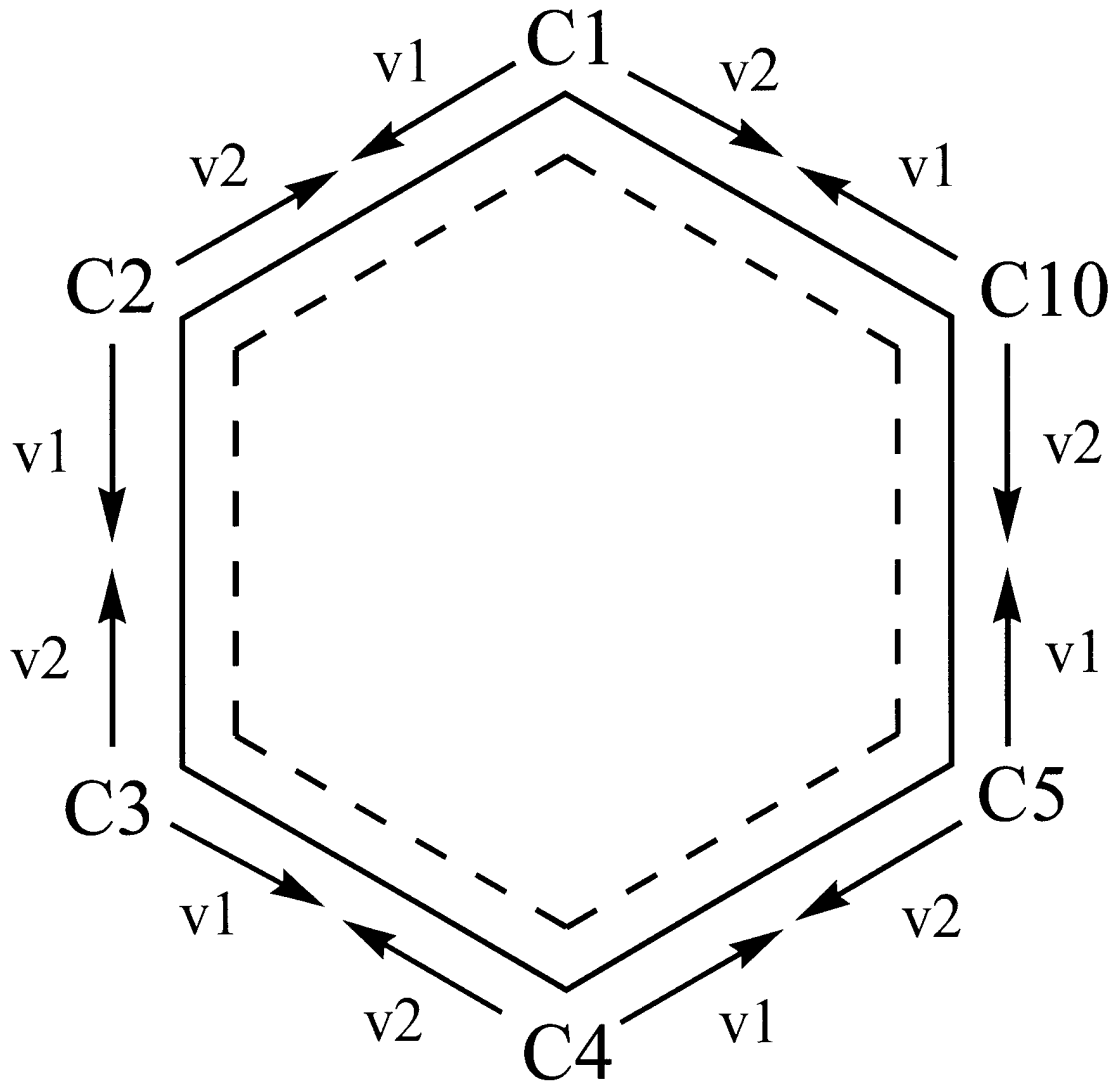

B Ring

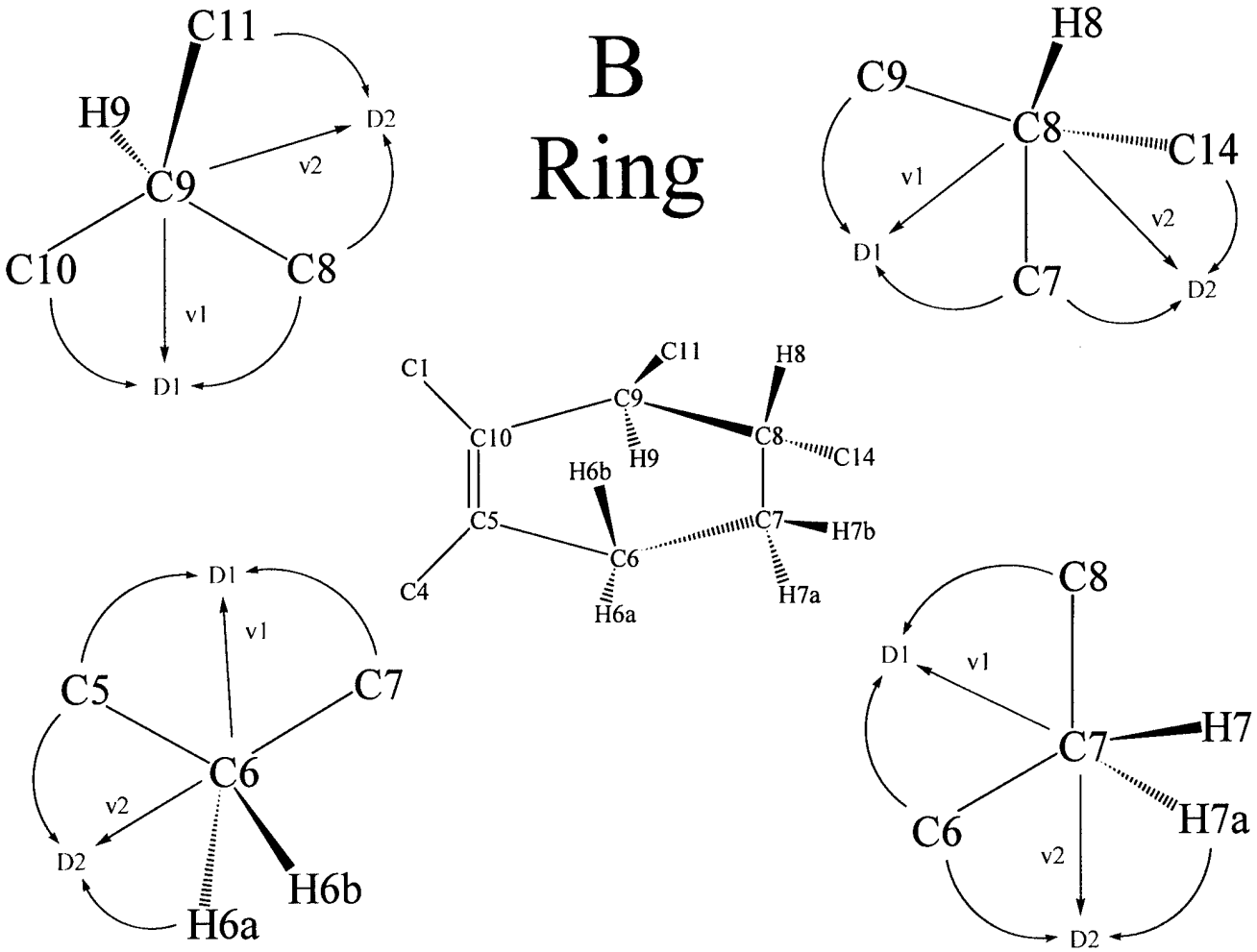
C11
H9
D2
C9
v2
C10
C8
v1
D1
H8
C9
C8
C14
v1
v2
D1
C7
D2
C1
C11
H8
C9
C10
C8
C14
H9
H6b
C5
C7
H7b
C6
C4
H7a
H6a
D1
v1
C5
C7
C6
v2
D2
H6b
H6a
C8
D1
v1
C7
H7
H7a
C6
v2
D2

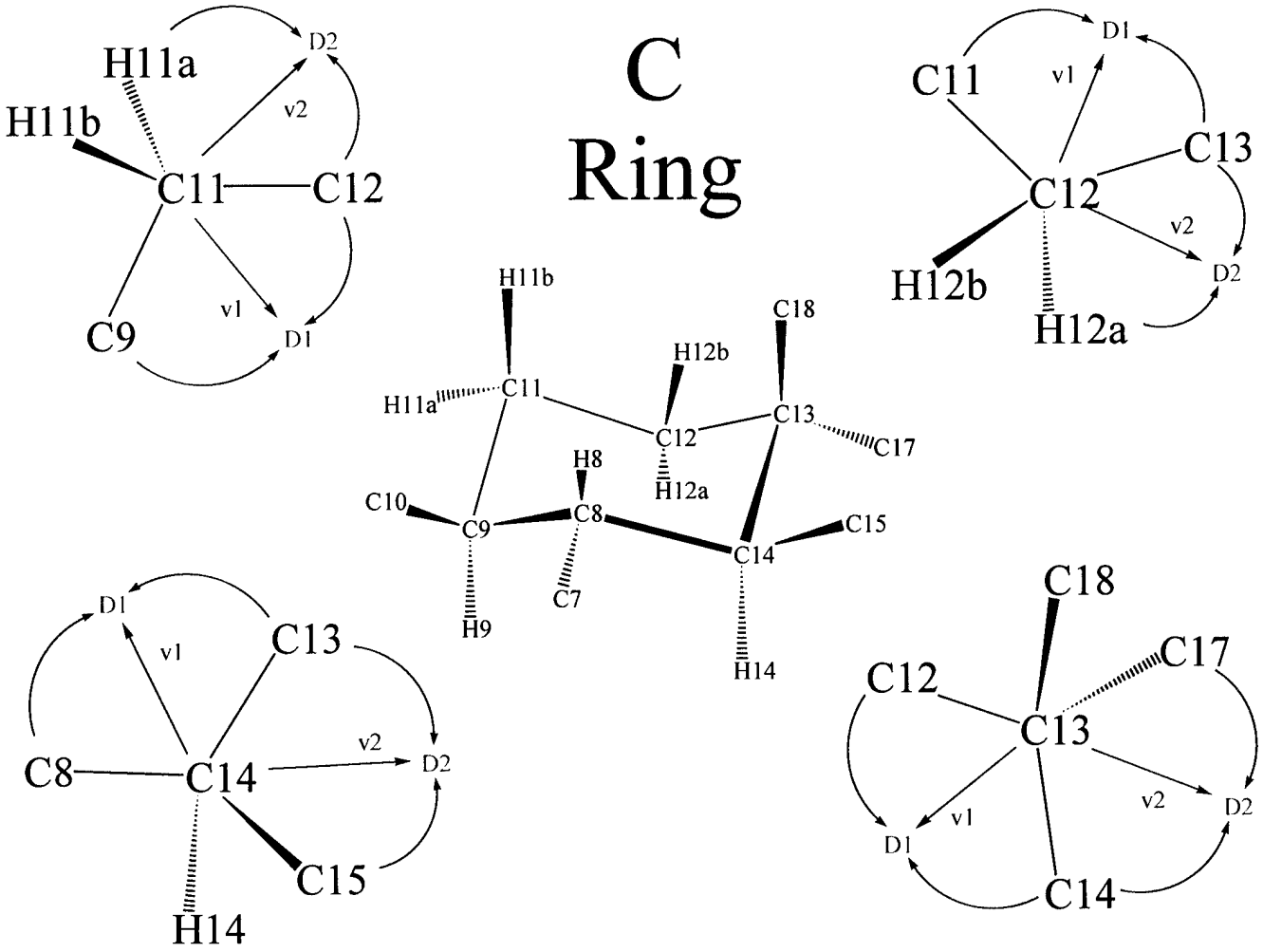
C
Ring
H11a
H11b
C11
C12
C9
D2
v2
v1
D1
C11
v1
D1
C13
C12
v2
H12b
D2
H12a
H11b
C18
H12b
H11a
C11
C12
C13
C17
H8
H12a
C10
C9
C8
C15
C14
C7
H9
H14
D1
v1
C13
C8
C14
v2
D2
C15
H14
C18
C12
C17
C13
v1
v2
D2
D1
C14

This diagram is for 17β–estradiol. If you have a different derivative, C16 & C17 might differ. If C16 & C17 remain sp^3 the current scheme will work by simply substituting the different atoms. If they are a different hybridization, scheme must change to support the appropriate multipoles.

D Ring

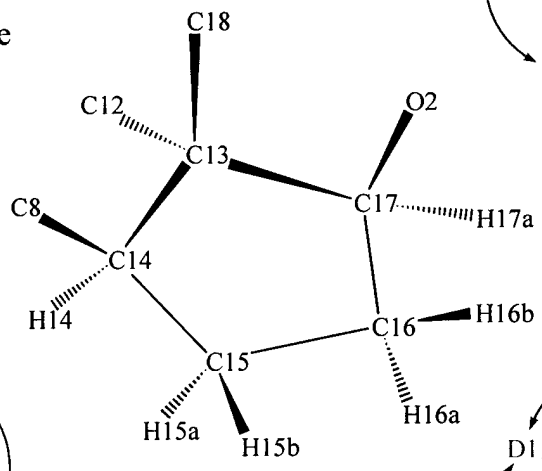

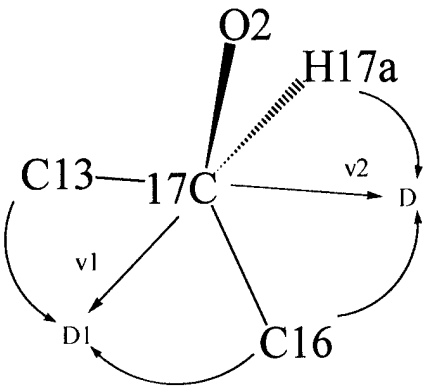

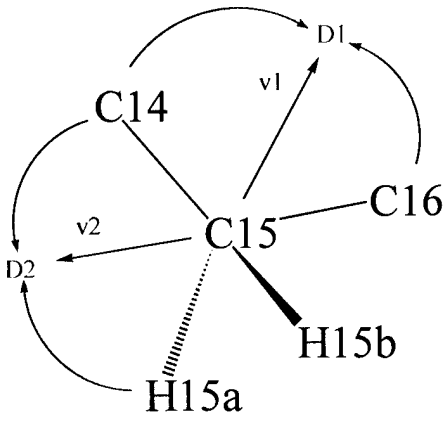

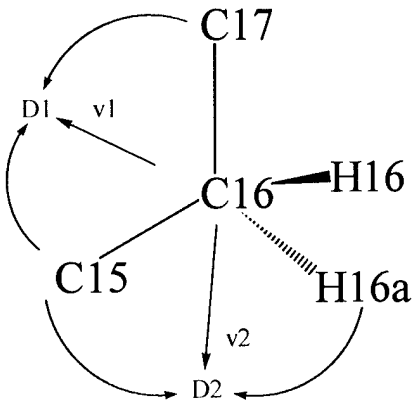

A Ring Hydrogens

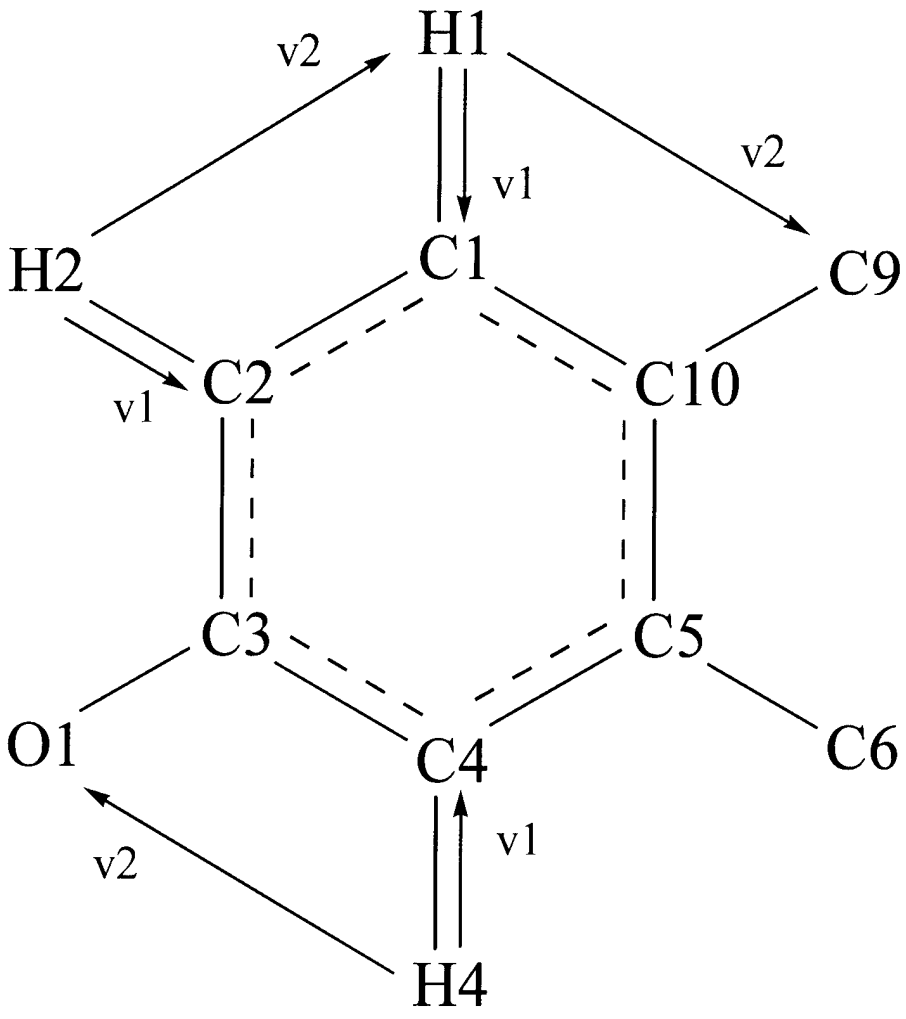

Coordinate System Atom List

If there are 2 atoms in parenthesis (), the vector should point to a dummy atom bisecting these 2 atoms

Atom	v1	v2
C1	C2	C10
C2	C3	C1
C3	C4	C2
C4	C5	C3
C5	C10	C4
C6	(C5-C7)	(C5-H6a)
C7	(C6-C8)	(C6-H7a)
C8	(C7-C9)	(C7-C14)
C9	(C8-C10)	(C8-C11)
C10	C1	C5
C11	(C9-C12)	(C12-H11a)
C12	(C11-C13)	(C13-H12a)
C13	(C12-C14)	(C14-C17)
C14	(C8-C13)	(C8-C15)
C15	(C14-C16)	(C14-H15a)
C16	(C15-C17)	(C15-H16a)
C17	(C13-C16)	(C16-O2)
C18	(H18a-H18b)	(H18b-H18c)

Atom	v1	v2
H1	C1	C9
H2	C2	H1
H4	C4	O1
H6a	C6	H6b
H6b	C6	H6a
H7a	C7	H7b
H7b	C7	H7a
H8	C8	C13
H9	C9	H14
H11a	C11	H11b
H11b	C11	H11a
H12a	C12	H12b
H12b	C12	H12a
H14	C14	H9
H15a	C15	H15b
H15b	C15	H15a
H16a	C16	H16b
H16b	C16	H16a
H17a	C17	O2
H18a	C18	H18b
H18b	C18	H18c
H18c	C18	H18a

Hydrogen Neutron Distances

-CH3 = 1.059
-C2-CH2 = 1.092
-Car-H = 1.083
-C3-CH = 1.099
-C-OH = 0.967

Appendix B.

A Charge Density and Electrostatic Potential Study on Estrogen Molecules: 16α, 17β-Estriol

A Charge Density and Electrostatic Potential Study on Estrogen Molecules : 16α, 17β-Estriol

P. KUMARADHAS and A. ALAN PINKERTON

Department of Chemistry, University of Toledo

Toledo, Ohio 43606-3390

A charge density and electrostatic potential study on estrogen molecules: 16α, 17β - Estriol

Abstract

The measurement of the electron density distribution of the principal members of the estrogen family, the derivatives estriol, estradiol and estrone are in progress. As a part of our study the electron density distribution of 16α,17β-estriol ($C_{18}H_{24}O_3$) was determined from high resolution single crystal x-ray diffraction measurements at 100 K. Estriol crystallizes with two molecules in the asymmetric unit. Intensity data were collected using a SMART 2K CCD area detector with Ag Kα radiation to a resolution corresponding to $(\sin\theta/\lambda)_{max}$=1.29 $Å^{-1}$. The structure was solved and a conventional spherical atom refinement was carried out. A multipole pseudo atom refinement was then performed using the XD program. The electron density multipolar parameters were used to calculate the electrostatic potential around the molecule removed from the crystal lattice. Strong electro negative regions were found in the vicinity of the oxygen atoms in both the molecules. Net atomic charges were calculated from a kappa refinement. The topological analysis of the hydrogen bond indicates the strength of the intermolecular interactions.

Introduction

More than 60% of all breast cancers are known to be hormone dependent, ie., initiation and progress can be influenced by estrogens and related compounds. These molecules bind as ligands to the estrogen receptor and hereby initiate a series of events resulting in the activation or repression of selective genes. Subtle changes in the structure of the estrogen affect their chemical/biological behavior and can result in the development of growth inhibitors for tumors. For example moving the hydroxy group from C(3) (estradiol) to one of the adjacent C-atoms can change the carcinostatic potentials from agonistic (estradiol) to inhibitory (2-and 4-hydroxy estratrien -17β-ol). While most changes modify the affinity of the ligand for the estrogen

receptor, this does not necessarily correlate with the stimulation ability of the transcription of estrogen responsive genes. The mechanism by which the ligands regulate the gene expression is currently unknown, however it has been suggested that the differences in electrostatic potential are responsible for the variation in the regulation of hormone dependent genes. This information can be obtained from studies of the electronic properties of estrogen derivatives. Experimental determination of the electron density distribution of molecules by x-ray diffraction methods leads directly to the determination of properties such as charges of atoms and the electrostatic potential, which in turn aid in the prediction of how this molecule might react with a given environment.

We have begun a systematic study of such compounds by investigating crystals of the derivatives of the principal estrogens, estriol, estradiol and estrone. The second study in this series, on estra-1,3,5(10)-triene-3,16α,17β-triol, is reported here. Estriol is the one of the active estrogens found in the body. The main source of estriol is the placenta, which produces a large amount of estriol during pregnancy. The commercially available estriol has been crystallized from acetonitrile. The geometry and electronic structure of the two molecules in the asymmetric unit as described below.

Experimental Section

1. Data collection:

The estriol was crystallized from acetonitrile by slow evaporation at room temperature. The crystals were found to be colorless and prismatic. In order to find a sample with good reflection profiles several crystals were examined on the diffractometer for low and high angle scattering. A well shaped 0.48 x 0.26 x 0.24 mm size crystal was selected and mounted on a Bruker SMART 2K CCD diffractometer using graphite monochromatized Ag Kα (λ=0.56089Å) radiation (50V, 35mA). As a preliminary check a room temperature data set was collected for a hemisphere. Refinement of the structure from this data gave results comparable to the reported structure. Then the crystal was cooled to 100 K using an Oxford Cryostream N_2 open flow cryostat. When the crystal was cooled, no significant unit cell modification was observed and it was very stable over the period of the entire data collection.

Initially the orientation matrix and the unit cell parameters were obtained from a least-squares refinement using 88 well centred reflections measured in three sets of matrix runs of each 20 frames. The low temperature cell thus obtained is ~2 % smaller than that at room temperature. A full sphere of low and high angle reflection intensities were measured using two detector settings at $2\theta = 0°$ and $2\theta = -50°$, using the ω scan method for different φ angles (0, 45, 90, 135, 180, 225, 270 and 315°). The CCD detector was placed at 5.1 cm from the crystal where the reflection overlap was minimal. A total of 600 frames were collected for each φ angle with a scan width of 0.3°. The frame times for low (40 sec) and high angles (160 sec) were decided after careful observation of the most intense reflection thus avoiding detector overflow but utilizing the full dynamic range. The crystal decay was monitored by re-measuring the initial 50 frames at the end of each data collection, and it was found to be negligible. The data collection strategy was checked with the ASTRO program incorporated into the SMART software. We obtained 100% coverage for a resolution of $(\sin\theta/\lambda)_{max} = 1.1$ Å^{-1} with good redundancy. A total of 9600 frames were collected over the period of two weeks.

2. Data reduction and Averaging

The best unit cell and the orientation matrix were determined by thresholding [$I/\sigma(I) \geq 20$] of reflections from each run of the data set. This orientation matrix fits well with the entire reciprocal space observed. The data has been integrated and corrected for background, Lorentz and polarization effects using SAINT sofware's advanced integrating procedures. The method of integration of the collected frames was as described by Kabch (1993) for area detectors. During the integration the orientation matrix and unit cell were not allowed to vary. Appropriate three dimensional box sizes were used in low and high angle integrations to account for the $K\alpha_1$ and $K\alpha_2$ splitting in high order reflections. No absorption correction was applied because of the low value of the absorption coefficient (0.055 mm^{-1}). All the corrected reflection intensities were scaled and averaged based on the point group symmetry using the program SORTAV. A total of 278184 reflections were measured to $\sin\theta/\lambda = 1.1$ Å^{-1}. 33019 are unique reflections with an average redundancy of 7.3. Of these, 179 unique data were measured only once , 829 twice and 31992 three or more times. We note that, in the complete set of unique reflections, 25899 reflections were found to be greater than $3\sigma(I)$. The internal agreement factors based on the

averaging of symmetry equivalent reflections are R1 = 0.042, R2 = 0.031, wR = 0.114 and S=1.4. The unit cell parameters, data collection, averaging and other crystallographic parameters are summarized in table 1.

3. Conventional Refinement

The room temperature crystal structure of 16α,17β-estriol has been previously reported. We solved the 100 K low temperature structure by direct methods using the program SHELXS97 and the spherical atom least squares refinement was carried out using the program SHELXTL. All the hydrogen atoms were located from a difference fourier synthesis. In the least squares refinement, all non hydrogen atoms were treated anisotropically and the hydrogen atoms were isotropic. The refinement converged with all data to R=0.058, wR=0.151 GOF=1.01. Comparison of F_0 and Fc values of the largest structure factors gave no indication of the effect of extinction in the data. A thermal ellipsoid diagram (figure 1.) shows the two molecules in the asymmetric unit and the standard atom numbering scheme.

4. Multipole refinement

In order to model the deformation electron density and explore the bond topological characteristics like $\rho(\mathbf{r})$, $\nabla^2\rho(\mathbf{r})$, bond ellipticity (ε), molecular electrostatic potential etc., a multipole aspherical atom refinement was carried out using the Hansen-Coppens multipole formalism implemented in the XD program. According to this formalism the total electron density of an aspherical atom is parameterized using an atom-centered multipole expansion

$$\rho_{atom}(\mathbf{r}) = P_c\,\rho_c + P_v\,\kappa^3\,\rho_v(\kappa\mathbf{r}) + \Sigma\,\kappa'^3_l\,R_l\,(\kappa'_l\mathbf{r})\Sigma\,P_{lm\pm}\,d_{lm\pm}\,(\theta,\varphi)$$

The first two terms ρ_c and $\rho_v(\kappa\mathbf{r})$ are the spherically averaged Hartree-Fock atomic core and valence densities normalized for one electron. The third term describes the aspherical part of the pseudo atom. $R_l(\mathbf{r}) = [\alpha_l{}^{n_l+3}/(n_l+2)!]r^{nl}\,e^{-\alpha_l r}$ are the normalized radial distribution functions. α_l are the Hartree Fock optimized single zeta values. κ and κ' are radial expansion /contraction

parameters which are optimized in the least-square refinement along with P_v and P_{lm}. P_{lm} are the multipole population coefficients. $d_{lm\pm}$ are density normalized real spherical harmonic angular functions and r, θ and φ are user defined local atom centered coordinates expressed in a polar coordinate system. In the multipole refinement all carbon and oxygen atoms were allowed to expand up to the hexadecapole and hydrogen atoms to the dipole level. The κ and κ' parameters of all non-H atoms were refined, but hydrogen atoms κ' was fixed at 1.2.

In order to obtain accurate positional and thermal parameters for the non-hydrogen atoms, a high angle refinement was carried out using the data with $\sin\theta/\lambda > 0.7$ Å^{-1}. All sp^2, sp^3 and hydroxyl hydrogen atoms were then reset to neutron bond lengths [C_{sp2}–H=1.083, C_{sp3}–H=1.099(CH), 1.092(CH_2), 1.059(CH_3) & O–H = 0.967Å] as given in the international table. This refinement converged without any significant change of scale factor, thus indicating the quality of the high angle data. The multipole refinement was carried out on 25520 reflections [$I>3\sigma(I)$] with the resolution $(\sin\theta/\lambda)_{max}$=1.1Å^{-1}. The refinement strategy was as follows: In the first step P_v, κ and scale factor were refined; second step P_{lm}, κ'; third step xyz, U_{ij}, scale factor were. Finally xyz, U_{ij} and all electronic parameters were refined together. Since there are two molecules in the asymmetric unit, their multipole parameters were constrained to be equal at the beginning of the refinement except the O–H group atoms as these are involved in strong hydrogen bonding. In addition, to avoid the phase problem, all chemically equivalent atoms were initially constrained to be equal but no site symmetry was imposed on any atoms in the molecules. At the later stages of the refinement, the chemical atom constraints within the molecules were released but not between the molecules. The residual index from the final refinement is given in table 1. An attempt was made to refine the two molecules independently after the final refinement. This refinement did not give a meaningful result so we did not proceed further. The net atomic charges were calculated from a κ-refinement (P_v, κ, and scale). During the refinements the unit cell was constrained to be neutral and no charge transfer was allowed between the molecules. The featureless residual density maps of the two molecules (figure 2) from the Fourier summation ($Fo-F_{mul}$) indicates the adequacy of the model refinement.

It is essential to test the physical significance and the correctness of the thermal parameters obtained from the model refinement. To accomplish this, Hirshfeld's "rigid bond"

test was performed for both the molecules leading to a satisfactory result. The maximum difference $\Delta_{A,B}$ between the atomic mean square displacement amplitudes along the interatomic vectors was 0.0012 Å. The fractional atomic coordinates and thermal parameters are given in table 2 and 3.

Result and Discussion

1. Structural aspects

The report of the room temperature crystal structure indicated significant conformational differences between the two molecules in the asymmetric unit. We observe some notable differences between the reported room temperature and current low temperature structure, so it is worth revisiting the structural analysis. Figure 1. shows the thermal ellipsoid representation of estriol with two independent molecules in the asymmetric unit obtained from the low temperature 100 K measurement. The geometrical comparison of the two molecules explicitly indicates how the two molecules are conformationally different. On comparing the bond distances between the two molecules no significant difference were observed in contrast to the previous report. The maximum deviation in the bond lengths of the ring (A-D) systems between the two molecules is 0.01 Å (table 4a). There is no evidence for C(2)–C(3) bond shortening in the A-ring systems as the room temperature structure reports. The average C_{ar}–C_{ar} bond distances of A-ring atoms of molecule 1 and 2 are 1.3995 and 1.3990 Å respectively. The CH_3 group of the second molecule lies above the aromatic ring of the first producing distortion in the aromatic ring. This effect is reproduced here producing a folding in the A-ring of molecule 1 with a dihedral angle of 2.99°. There is no such effect in the second molecule where the A-ring system is planar (0.52°). There are differences in bond angles between the molecules 1 and 2 around the atoms C(9), C(13) and C(14) [table 4b] . However, we observe a maximum deviation of 2.5° compared to 3.9° as previously reported. The torsion angles in the table 4 indicate the distortion of the B and C ring systems. The steric hindrance between the C-ring equatorial hydrogen atom at C(11) and the hydrogen atom at C(1) produce different conformations of the B and C ring systems in the two molecules. Comparison of torsion angles between the molecules

shows the major distortion appears at the head and tail part of the molecules (table 5). This is attributed to the different environment of intermolecular interactions of the molecules (1 and 2) with their neighbors. The relative strengths of the hydrogen bonds to O(3) in the two molecules was previously discussed on the basis of 0.04 Å difference in the C(16)-O(3) bond length. We observe less than 0.01 Å difference in this distance between molecules 1 and 2. Hydrogen bonding does, however, have an effect on the geometry of the hydroxyl groups. In the second molecule the 16α and 17β-hydroxyl C–O–H bond angles are systematically less compared with the first, the maximum difference being 8.8°. There is less of a differentiation in the 3-hydroxyl bonds, the deviation being 2.1°. The structure is characterized by strong hydrogen bonding. Figure 2. depicts the hydrogen bonding environment of the two molecules in the asymmetric unit. Each hydroxyl group is involved in at least two hydrogen bonds. O(1') has one additional hydrogen bond resulting in a tetrahedral coordination of the O-atom. The head to tail hydrogen bonds link the molecules into chains. The hydrogen bond geometrical parameters are given in table 6.

2. Charge density

The model static deformation density map in figure 3 clearly shows the bonding features of the different atoms in the estriol molecule. All chemical bonds show an increase in electron density with respect to neutral spherical atoms as well as density associated with the lone pair regions of the oxygen atoms. The featureless residual electron density map was computed using the XDFOUR program after the multipole refinement. The featureless residual maps (figure 2a and b) of the two molecules in the asymmetric unit, confirms the validity and the adequacy of the model refinement and the quality of the data set. The minimum and maximum residual density calculated for the molecules are 0.21, -0.29 (molecule1) and 0.22, -0.27eÅ^{-3} (molecule 2) respectively. This values are very close to the requirement of the average error (±0.05) eÅ^{-3} in the experimental difference density maps. As specified earlier, in the multipole refinement, the respective chemically equivalent ring atoms of the two molecules were constrained pair wise. No constraint was imposed on the hydroxyl groups, because they involved strong hydrogen bonding. All further discussions are based on this constraint model. In order to further characterize the interaction of atoms in the molecule a bond topological analysis was performed

based on Bader's theory of "atoms in molecules" implemented in XDPROP. This analysis includes the determination of electron density $\rho_c(r)$ at the bond critical point (CP) where $\nabla\rho(r) = 0$ between the bonded atoms, its Laplacian $\nabla^2\rho_c(r)$ and bond ellipticity [$\varepsilon = (\lambda_1/\lambda_2)-1$]. Also, the eigenvalues of the second derivatives of $\rho(r)$ was calculated to characterize the nature of the bond critical point. The bond path analysis gives information about the amount of deviation of the bond critical point from the internuclear axis, thus obtaining an additional measure of strain. All these results including the length of bond paths and internuclear distances are listed in table 7.

A-ring system: The topological analysis results reported in table 7, such as λ_1, λ_2, λ_3, $\rho_c(r)$, $\nabla^2\rho_c(r)$, ε reveal electronic insight into the estriol molecules. The magnitude of $\rho_c(r)$ at the bond critical point is a clear indicator of chemical bond strength. The electron density $\rho_c(r)$ at the critical points of the aromatic ring ($C_{sp2}-C_{sp2}$) bonds range from 2.04 to 2.16 eÅ^{-3}. The average value (2.11 eÅ^{-3}) is a typical value for aromatic bonds. The Laplacian $\nabla^2\rho_c(r)$ is a very sensitive parameter which identifies the areas where charge is concentrated (negative value) or depleted (positive value) in the bonding region. In this respect we observe the maximum negative Laplacian in the A-ring bonds is –22.2(1) eÅ^{-5} and this value appears less in the bonds linked to B ring atoms. However the average value is –18.72 eÅ^{-5} which is very close to an earlier observation for the benzene molecule. The dispersion of bond ellipticity is attributed to the preferential charge accumulation in the bond. Bader's theory on ellipticity emphasis the concept of the σ-π character of the bond. Explicitly, it is the measure of deviation of charge density from spherical symmetry (at the critical point). In this aspect the average value (0.17) of ellipticity of $C_{sp2}-C_{sp2}$ bonds indicates significant π (aromatic) character. The $\rho_c(r)$'s in the C_{sp2}-H bonds ranges from 1.78(4) to 1.89(1) eÅ^{-3} and this density is consistent with one would expect for single C-H bonds. The Laplacian the of C(1)-H(1) bond is small compared with the other two C-H bonds, perhaps indicating weakening of the bond due to steric interactions with hydrogen atoms at C(11). The small ellipticity of C_{sp2}-H bonds is consistent with only a σ contribution in the single bonds.

B and C– ring systems: The density of chemically equivalent $C_{sp2}-C_{sp3}$ bonds in the B-ring are equal and their Laplacian's are very close (see the table 7). In both ring systems, the average values (1.70 and 1.68 eÅ^{-3}) of $\rho_c(r)$'s in the $C_{sp3}-C_{sp3}$ bonds are not very different and a

similar trend appears for the Laplacian. The $\rho_c(r)$'s and Laplacian for these bonds are significantly less than the aromatic ring system in agreement with their single bond character. In the C-ring the ellipticity of the bonds C(11)-C(12) and C(12)-C(13) are unexpectedly larger compared to the similar bonds having small values (see the table 7) indeed the values approach those of the aromatic ring. In all C_{sp3} –H (CH_2) bonds the density ranges from 1.64 to 1.87 eÅ^{-3} and C_{sp3} –H (CH) bonds 1.75 to 1.77 eÅ^{-3}. The average effect is same in both types of bonds. The Laplacian of these bonds is consistently smaller than for the C_{sp2} –H bonds. The maximum and minimum values are –8.8(2), -18.3(1) eÅ^{-5}.

D-ring system: Due to this being a 5 membered ring and to the different hydrogen bonding environments this ring is highly strained in the geometry of both molecules (1 and 2). Although its geometry is strained, no significant difference was observed in the $\rho_c(r)$'s at the bond critical points except for C(14)-C(15) = 1.57 eÅ^{-3} implying a weakening of this bond. The average value of the Laplacian is -12.78 eÅ^{-5}. We observe the ellipticity of this five membered system is close to B-ring bonds and they are small consistent with single bonds. The electron density (1.95 eÅ^{-3}) and Laplacian of C(16)-H(16) bond is surprisingly higher than the similar C(17)-H(17) bond in this ring (see the table 7).

C-O and O-H groups: These groups play a significant role in the whole geometry of both the molecules. The $\rho_c(r)$'s of C_{sp2} – O [A-rings] bonds of both the molecules(1 and 2) are larger than C_{sp3} –O bonds of D-ring in agreement with conjugation of O(1) to the aromatic ring. The average values are 2.11 and 1.91 eÅ^{-3}. The Laplacians of the C_{sp2} – O bonds are not equal to C_{sp3} – O bonds and also indicate a strengthening of the bond to the aromatic ring. Whereas the ellipticity of the O(1)-C(3) bond in molecule 1 is a strong indicator of a π component to the bond, that in molecule 2 is closer to the value observed for the D ring. We attribute this to the difference in the hydrogen bonding in the two molecule.

The small values at the ellipticity (0.06-0.1) in the C_{sp3} – O bonds for both molecules indicates an unperturbed pure σ bonds.

Hydrogen bonding: Table 8 reports the hydrogen bond topology. There are three intermolecular hydrogen bonds in each molecule that meet Bader's criteria for polar non-bonded interaction of the type H· · · A by observing a CP along the H· · ·A path. Of the three hydrogen bonds from molecule 1, the two bonds [O(1)–H(1A)· · · O(3) and O(3)–H(3A)· · · O(1')] display

approximately linear hydrogen bonding, 171.7, 170.5° respectively. The corresponding electron densities of these bonds at the CP are similar with values of 0.23 and 0.20 $eÅ^{-3}$ respectively. Both of these bonds have a positive Laplacian $\nabla^2\rho$ at the CP. This is characteristic of closed shell interactions which are governed by the contraction of the electro density towards each of the interacting atoms. In molecule 2 we observe similar electron densities and Laplacians for the bonds O(1')–H(1'A)· · · O(3') and O(2')–H(2'A)· · · O(2'). The hydrogen bond O(2')–H(2'A)· · · O(2') in molecule 1 shows moderate electron density at the CP (0.11 $eÅ^{-3}$) with a positive Laplacian. Although the hydrogen bond O(2')–H(2'A)· · · O(1') is approximately linear (169.2°) the electron density is very small at the CP (0.05 $eÅ^{-3}$). This may be attributed to the longer H(2'A)· · ·O(1'A) distance and the fact that O(1'A) accepts one additional hydrogen bond.

3. Electrostatic Potential

An additional important application of the multipole model is that it provides an opportunity to understand the chemical reactivity of molecules. That is, to identify the places where nucleophilic or electrophilic attack may take place. The regions of positive potential will attract nucleophilic reagents and the electronegative regions of the molecule will determine the approach of electrophilic reagents. The electrostatic potential (ESP) not only plays an important role in directing chemical attack, but also for molecular recognition (drug receptor interaction). This is because electrostatic forces are long range interactions which determine the most stable geometrical orientation of two molecules. To investigate this aspect we have calculated the electrostatic potential around the molecules by the method of Su and Coppens based on the populations obtained from the multipole refinement. The figures 4a and 4b show a contour plot of the electrostatic potential of the molecule 1 and 2 in the molecular plane. The positive contours around the aromatic rings are more diffuse than those of the saturated rings. The negative contours around the 16α, 17β oxygen atoms are much more pronounced than for the A ring. The potential around molecule 1 is more symmetric than for molecule 2. Figure 5 shows the electrostatic potential in the hydrogen bonding environment of each oxygen atom of the molecule.

Figure 6 displays the 3D isosurface representation of the electrostatic potential computed from the molecule extracted from the crystal. The strong extended electro negative regions are

evident at the head and tail portion of the molecule. The shape and direction of polarization is attributed to the intermolecular interaction.

4. Net atomic charges

The net atomic charges (table 9) were calculated from from a κ-refinement (κ, Pv, scale). In this refinement the chemically equivalent atoms were constrained as described in the multipole refinement. All oxygen atoms carry significant negative charges in the range –0.63 to –0.87e. Similarly all hydroxyl hydrogen atoms carry high positive charges, approximately double the amount of charge of the other hydrogen atoms in the molecules. A group charge calculation on both molecules indicates that the central regions are close to neutral, whereas the head and tail regions form charged units.

Conclusion

The present study on estriol gives information on both the structural and electronic properties of the molecule. The differences in hydrogen bonding, molecular packing environment, and interamolecular steric effects are responsible for small differences in the two molecules in the asymmetric unit. The significant differences as reported for the room temperature structure were not confirmed here. The comparison of torsion angles between the two molecules shows that the major differences at the head and tail portions of the molecules may be attributed to the different hydrogen bonding environment, both molecules being involved in strong hydrogen bonding.

The electron densities at the CP of the aromatic C-C bonds is larger than for the C_{sp3} –C_{sp3} bonds of the B,C and D ring systems. The additional electron density accumulation in the aromatic bonds along with the ellipticity indicates a π contribution. The unconstrained refinement of the hydroxyl groups between the two molecules shows differences in both C-O and O-H bond electron densities at the CP. The average C_{sp3} –O bond densities significantly less than C_{sp2} –O. The charge accumulation in the O-H (16α,17β position) bond is slightly larger than in the 3-hydroxy O-H bond. The bond path calculation reveals a deviation of the CP from the internuclear axis for several C-O bonds. The CP of C_{sp2}–O bond in the first molecule deviates by 0.03 Å from the internuclear axis, while in molecule 2 it lies very close (0.006 Å). In molecule 1 C(17)-O(2) and C(16)- O(3) deviate 0.03 and 0.01Å respectively. But these

deviations are exactly opposite in the bonds C(17')-O(2') [0.01Å] and C(16')- O(3') [0.03Å] of molecule 2. Strong electronegative regions were found in the electrostatic potential maps at the vicinity of the oxygen atoms of both molecules. The extension of positive and negative contours in both molecules explicitly indicates the electrostatic interaction with the neighboring molecules. The large electron density at the hydrogen bond CP's implies the very strong nature of hydrogen bonding in the estriol crystal. Net atomic charges computed from the κ-refinement gave a reasonable charge distribution. The oxygen atoms O(2),O(3) (molecule 1) and O(2'),O(3') (molecule 2) carry a higher negative charge than O(1) and O(1').

Table 1. Crystal data and experimental conditions

Crystal data	
Empirical formula	$C_{18}H_{24}O_3$
Formula weight	288.37
Crystal system	Monoclinic
Space group	$P2_1$
a (Å)	7.5077(4)
b (Å)	23.0809(12)
c (Å)	9.1632(5)
β (°)	110.957(2)
V ($Å^3$)	1482.8
Z	4
F(000)	624
Dx (Mg/m^3)	1.292
μ (mm^{-1})	0.055
Data collection	
Diffractometer	Bruker's SMART 2K CCD
Radiation, λ (Å)	Ag Kα, 0.56087
Scan method	ω-scan
No. of reflections measured	278184
$Sin(\theta/\lambda)_{max}$ ($Å^{-1}$)	1.29
R_{int}	0.042
No. of unique data	43918
Refinement	
No. of relections ($F \geq 3\sigma$, $Sin(\theta/\lambda)_{max}$=1.1 $Å^{-1}$)	25520
R (F), wR(F)	0.031, 0.035
GOF	0.98
N_{obs}/N_{par}	27.3

Table 2. Fractional coordinates, equivalent displacement parameters after multipole refinement.

Atom	x	y	z	U_{eq}
O(1)	0.51770(10)	0.85356(11)	0.52121(11)	0.018
O(2)	0.79922(9)	1.32165(11)	0.40946(9)	0.015
O(3)	1.19063(9)	1.28093(11)	0.40370(9)	0.015
O(1')	0.98786(9)	1.26564(11)	1.07236(8)	0.013
O(2')	0.74949(10)	0.79559(11)	1.08082(9)	0.016
O(3')	0.31380(9)	0.81946(11)	0.90942(8)	0.015
C(1)	0.45781(8)	1.00734(11)	0.42503(8)	0.014
C(2)	0.41441(8)	0.94973(11)	0.44369(8)	0.016
C(3)	0.56256(8)	0.91063(11)	0.51232(7)	0.012
C(4)	0.75074(7)	0.93008(11)	0.56559(6)	0.011
C(5)	0.79387(7)	0.98793(11)	0.54672(6)	0.010
C(6)	1.00171(8)	1.00583(11)	0.60532(7)	0.013
C(7)	1.03656(7)	1.06196(11)	0.53177(7)	0.013
C(8)	0.89490(7)	1.10848(11)	0.53903(6)	0.010
C(9)	0.69129(7)	1.08934(11)	0.43668(6)	0.010
C(10)	0.64663(7)	1.02776(11)	0.47412(6)	0.010
C(11)	0.54264(8)	1.13511(11)	0.43758(7)	0.013
C(12)	0.58776(7)	1.19498(11)	0.38487(7)	0.012
C(13)	0.78968(7)	1.21489(11)	0.48383(6)	0.010
C(14)	0.93243(7)	1.16705(11)	0.47887(6)	0.010
C(15)	1.12818(8)	1.19669(11)	0.55148(8)	0.015
C(16)	1.08802(7)	1.26095(11)	0.49991(7)	0.012
C(17)	0.87053(7)	1.26406(11)	0.41297(6)	0.010
C(18)	0.80161(10)	1.23053(11)	0.65010(7)	0.017
C(1')	1.04605(7)	1.11001(11)	1.03189(7)	0.013
C(2')	1.08893(7)	1.16882(11)	1.05868(7)	0.013
C(3')	0.94251(7)	1.20772(11)	1.04701(6)	0.010
C(4')	0.75671(7)	1.18775(11)	1.01090(6)	0.010
C(5')	0.71459(7)	1.12879(11)	0.98527(6)	0.009
C(6')	0.51022(7)	1.11048(11)	0.95314(8)	0.013
C(7')	0.47065(7)	1.04732(11)	0.90308(7)	0.012
C(8')	0.63561(7)	1.00870(11)	0.99990(6)	0.009
C(9')	0.81329(7)	1.02458(11)	0.96111(6)	0.009
C(10')	0.86000(7)	1.08864(11)	0.99458(6)	0.010
C(11')	0.98225(7)	0.98344(11)	1.03926(7)	0.012
C(12')	0.92731(7)	0.91897(11)	1.00723(7)	0.012
C(13')	0.75706(7)	0.90430(11)	1.05525(6)	0.009
C(14')	0.59062(7)	0.94491(11)	0.96631(6)	0.009
C(15')	0.41988(8)	0.91953(11)	0.99962(8)	0.014
C(16')	0.46121(8)	0.85359(11)	1.01718(7)	0.012
C(17')	0.65667(8)	0.84561(11)	0.99893(6)	0.011
C(18')	0.81623(9)	0.90818(11)	1.23339(6)	0.015
H(1A)	0.63209	0.82990	0.55330	0.034
H(2A)	0.69428	1.32373	0.44686	0.012
H(3A)	1.13395	1.27295	0.29273	0.025
H(1)	0.34450	1.03712	0.36414	0.029
H(2)	0.26604	0.93672	0.39812	0.044
H(4)	0.86510	0.89941	0.61941	0.021
H(6A)	1.09283	0.97171	0.58700	0.037

H(6B)	1.04093	1.01387	0.73024	0.020
H(7A)	1.01476	1.05396	0.40896	0.015
H(7B)	1.18207	1.07730	0.59177	0.021
H(8)	0.89840	1.11151	0.65964	0.017
H(9)	0.68554	1.08694	0.31532	0.016
H(11A)	0.40304	1.12061	0.35796	0.024
H(11B)	0.53292	1.13757	0.55336	0.020
H(12A)	0.57626	1.19302	0.26278	0.018
H(12B)	0.48167	1.22649	0.38902	0.019
H(14)	0.90581	1.15747	0.35520	0.014
H(15A)	1.23477	1.17769	0.51002	0.022
H(15B)	1.18913	1.19417	0.67908	0.024
H(16)	1.12808	1.29047	0.60016	0.025
H(17)	0.84636	1.25096	0.29187	0.011
H(18A)	0.76328	1.19583	0.70939	0.033
H(18B)	0.70167	1.26365	0.64136	0.026
H(18C)	0.94099	1.24472	0.71651	0.025
H(1'A)	0.87426	1.28653	1.06698	0.027
H(2'A)	0.84956	0.78829	1.03968	0.022
H(3'A)	0.28464	0.83420	0.80471	0.020
H(1')	1.15901	1.07987	1.03660	0.026
H(2')	1.23032	1.18590	1.08056	0.026
H(4')	0.64298	1.21784	1.00111	0.021
H(6'C)	0.41147	1.14015	0.87102	0.027
H(6'D)	0.48205	1.11487	1.06167	0.014
H(7'C)	0.44868	1.04194	0.77938	0.024
H(7'D)	0.33470	1.03427	0.91168	0.021
H(8')	0.66573	1.01546	1.12513	0.012
H(9')	0.77340	1.01922	0.83423	0.011
H(11C)	1.09205	0.99035	0.98873	0.020
H(11D)	1.04447	0.99134	1.16493	0.017
H(12C)	0.89389	0.91066	0.88280	0.018
H(12D)	1.05438	0.89402	1.07392	0.029
H(14')	0.56308	0.93793	0.84142	0.012
H(15C)	0.28167	0.92827	0.90891	0.023
H(15D)	0.40421	0.93935	1.10220	0.016
H(16')	0.48007	0.83935	1.13620	0.015
H(17')	0.62869	0.84147	0.87314	0.014
H(18D)	0.86807	0.94995	1.27305	0.017
H(18E)	0.92207	0.87636	1.28493	0.022
H(18F)	0.70244	0.89942	1.27329	0.032

Table 3. Anisotropic thermal parameters of non-Hydrogen atoms ($Å^2$) and estimated standard deviations.

Atom	U_{11}	U_{22}	U_{33}	U_{12}	U_{13}	U_{23}
O(1)	0.0125(2)	0.0088(2)	0.0312(3)	-0.0001(2)	0.0108(2)	0.0022(2)
O(2)	0.0146(2)	0.0087(2)	0.0217(3)	0.0028(1)	0.0102(2)	0.0011(2)
O(3)	0.0113(2)	0.0137(2)	0.0187(2)	-0.0035(2)	0.0066(2)	-0.0017(2)
O(1')	0.0118(2)	0.0071(1)	0.0182(2)	-0.0011(1)	0.0073(2)	-0.0007(1)
O(2')	0.0171(2)	0.0093(2)	0.0200(3)	0.0028(2)	0.0096(2)	0.0024(2)
O(3')	0.0144(2)	0.0111(2)	0.0168(2)	-0.0051(2)	0.0065(2)	-0.0028(2)
C(1)	0.0083(2)	0.0112(2)	0.0211(2)	0.0005(1)	0.0039(2)	0.0020(2)
C(2)	0.0094(2)	0.0109(2)	0.0250(3)	-0.0003(1)	0.0062(2)	0.0016(2)
C(3)	0.0108(2)	0.0089(1)	0.0164(2)	0.0002(1)	0.0071(1)	0.0008(1)
C(4)	0.0103(2)	0.0096(1)	0.0120(2)	0.0005(1)	0.0048(1)	0.0009(1)
C(5)	0.0087(1)	0.0086(1)	0.0103(2)	0.0005(1)	0.0029(1)	0.0007(1)
C(6)	0.0085(2)	0.0104(2)	0.0167(2)	0.0010(1)	0.0015(1)	0.0032(1)
C(7)	0.0083(2)	0.0104(2)	0.0170(2)	0.0018(1)	0.0041(1)	0.0024(1)
C(8)	0.0080(1)	0.0089(1)	0.0104(2)	0.0008(1)	0.0024(1)	0.0010(1)
C(9)	0.0077(1)	0.0086(1)	0.0108(2)	0.0011(1)	0.0023(1)	0.0008(1)
C(10)	0.0080(1)	0.0090(1)	0.0112(2)	0.0005(1)	0.0026(1)	0.0007(1)
C(11)	0.0085(2)	0.0099(2)	0.0193(2)	0.0014(1)	0.0054(1)	0.0017(1)
C(12)	0.0086(1)	0.0094(2)	0.0162(2)	0.0014(1)	0.0034(1)	0.0016(1)
C(13)	0.0091(1)	0.0085(1)	0.0106(2)	0.0005(1)	0.0042(1)	-0.0005(1)
C(14)	0.0078(1)	0.0087(1)	0.0110(2)	0.0011(1)	0.0028(1)	0.0008(1)
C(15)	0.0082(2)	0.0115(2)	0.0214(2)	0.0006(1)	0.0020(2)	0.0023(2)
C(16)	0.0097(2)	0.0096(2)	0.0147(2)	-0.0005(1)	0.0041(1)	-0.0009(1)
C(17)	0.0097(2)	0.0080(1)	0.0123(2)	0.0010(1)	0.0048(1)	0.0001(1)
C(18)	0.0216(2)	0.0145(2)	0.0123(2)	-0.0001(2)	0.0089(2)	-0.0018(2)
C(1')	0.0082(1)	0.0087(1)	0.0217(2)	0.0000(1)	0.0066(1)	-0.0009(2)
C(2')	0.0092(2)	0.0083(2)	0.0211(2)	-0.0007(1)	0.0067(2)	-0.0005(1)
C(3')	0.0097(1)	0.0073(1)	0.0128(2)	-0.0004(1)	0.0053(1)	-0.0003(1)
C(4')	0.0089(1)	0.0069(1)	0.0134(2)	0.0002(1)	0.0041(1)	0.0002(1)
C(5')	0.0074(1)	0.0070(1)	0.0125(2)	0.0004(1)	0.0032(1)	0.0001(1)
C(6')	0.0071(1)	0.0089(1)	0.0212(2)	0.0007(1)	0.0034(1)	-0.0006(1)
C(7')	0.0075(1)	0.0087(2)	0.0175(2)	0.0003(1)	0.0008(1)	-0.0019(1)
C(8')	0.0072(1)	0.0073(1)	0.0115(2)	-0.0001(1)	0.0034(1)	-0.0016(1)
C(9')	0.0085(1)	0.0068(1)	0.0112(2)	0.0003(1)	0.0041(1)	-0.0006(1)
C(10')	0.0078(1)	0.0076(1)	0.0123(2)	0.0004(1)	0.0040(1)	0.0000(1)
C(11')	0.0080(1)	0.0085(1)	0.0174(2)	0.0008(1)	0.0047(1)	0.0005(1)
C(12')	0.0103(2)	0.0083(1)	0.0156(2)	0.0014(1)	0.0069(1)	0.0002(1)
C(13')	0.0090(1)	0.0083(1)	0.0089(1)	0.0000(1)	0.0040(1)	-0.0007(1)
C(14')	0.0080(1)	0.0073(1)	0.0113(2)	-0.0003(1)	0.0032(1)	-0.0021(1)
C(15')	0.0099(2)	0.0091(2)	0.0220(2)	-0.0015(1)	0.0077(2)	-0.0035(2)
C(16')	0.0119(2)	0.0080(1)	0.0144(2)	-0.0017(1)	0.0066(1)	-0.0019(1)
C(17')	0.0117(2)	0.0076(1)	0.0121(2)	-0.0003(1)	0.0060(1)	-0.0013(1)
C(18')	0.0175(2)	0.0149(2)	0.0095(2)	-0.0022(2)	0.0044(2)	-0.0009(1)

Table 4a. Selected bond lengths (Å)

Atoms	Molecule(1)	Molecule(2)
C(1)-C(2)	1.3939(8)	1.3962(7)
C(2)-C(3)	1.3953(8)	1.3936(7)
C(3)-C(4)	1.3938(7)	1.3920(7)
C(4)-C(5)	1.3991(7)	1.3978(6)
C(5)-C(10)	1.4084(7)	1.4110(7)
C(1)-C(10)	1.4063(7)	1.4035(7)
O(1)-C(3)	1.3692(8)	1.3784(7)
C(5)-C(6)	1.5147(7)	1.5154(7)
C(6)-C(7)	1.5256(7)	1.5252(7)
C(7)-C(8)	1.5293(7)	1.5263(7)
C(8)-C(9)	1.5446(7)	1.5425(6)
C(9)-C(10)	1.5274(7)	1.5252(6)
C(9)-C(11)	1.5389(7)	1.5407(7)
C(11)-C(12)	1.5408(7)	1.5442(7)
C(12)-C(13)	1.5324(7)	1.5311(7)
C(13)-C(14)	1.5508(7)	1.5413(7)
C(13)-C(17)	1.5360(7)	1.5464(7)
C(13)-C(18)	1.5368(8)	1.5333(7)
C(14)-C(15)	1.5399(7)	1.5360(7)
C(14)-C(8)	1.5237(7)	1.5172(7)
C(15)-C(16)	1.5529(7)	1.5501(7)
C(16)-(17)	1.5412(7)	1.5462(7)
C(16)-O(3)	1.4386(9)	1.4278(8)
C(17)-O(2)	1.4291(7)	1.4167(8)

Table 4b. Selected bond angles (°)

Bonds	Molecule (1)	Molecule(2)
C(2) - C(1) - C(10)	122.2(1)	122.1(1)
C(1) - C(2) - C(3)	119.2(1)	199.1(1)
O(1) - C(3) - C(2)	118.4(1)	118.1(1)
O(1) - C(3) - C(4)	122.0(1)	121.8(1)
C(2) - C(3) - C(4)	119.6(1)	120.0(1)
C(3) - C(4) - C(5)	121.0(1)	120.6(1)
C(4) - C(5) - C(6)	118.1(1)	117.2(1)
C(4) - C(5) - C(10)	120.3(1)	120.4(1)
C(6) - C(5) - C(10)	121.6(1)	122.4(1)
C(5) - C(6) - C(7)	113.1(1)	113.6(1)
C(6) - C(7) - C(8)	110.2(1)	110.7(1)
C(7) - C(8) - C(9)	109.0(1)	108.4(1)
C(7) - C(8) - C(14)	112.7(1)	111.9(1)
C(9) - C(8) - C(14)	107.8(1)	109.4(1)
C(8) - C(9) - C(10)	112.3(1)	109.9(1)
C(8) - C(9) - C(11)	111.3(1)	112.5(1)
C(10) - C(9) - C(11)	114.8(1)	114.3(1)
C(1) - C(10) - C(5)	117.6(1)	117.7(1)
C(1) - C(10) - C(9)	121.1(1)	121.8(1)
C(5) - C(10) - C(9)	121.0(1)	120.5(1)
C(9) - C(11) - C(12)	111.9(1)	112.7(1)
C(11) - C(12) - C(13)	111.4(1)	110.6(1)
C(12) - C(13) - C(14)	108.5(1)	108.4(1)
C(12) - C(13) - C(17)	115.4(1)	117.1(1)
C(12) - C(13) - C(18)	110.6(1)	109.8(1)
C(14) - C(13) - C(17)	97.6(1)	98.6(1)
C(14) - C(13) - C(18)	113.6(1)	113.5(1)
C(17) - C(13) - C(18)	110.7(1)	109.1(1)
C(8) - C(14) - C(13)	113.7(1)	113.8(1)
C(8) - C(14) - C(15)	120.6(1)	118.1(1)
C(13) - C(14) - C(15)	103.5(1)	103.9(1)
C(14) - C(15) - C(16)	104.0(1)	104.2(1)
O(3) - C(16) - C(15)	113.9(1)	113.1(1)
O(3) - C(16) - C(17)	111.6(1)	113.0(1)
C(15) - C(16) - C(17)	104.8(1)	105.6(1)
O(2) - C(17) - C(13)	119.7(1)	116.6(1)
O(2) - C(17) - C(16)	112.0(1)	110.2(1)
C(13)- C(16) - C(17)	104.6(1)	103.2(1)
C(3) - O(1) - H(1A)	110.5(2)	108.4(2)
C(17) - O(2) - H(2A)	112.6(2)	103.8(2)
C(16) - O(3) - H(3A)	116.8(1)	109.7(2)

Table 4b (continued). H-atom bond angles (°)

Bonds	Molecule (1)	Molecule (2)
C(3) - O(1) - H(1A)	110.5(2)	108.4(2)
C(17) - O(2) - H(2A)	112.6(2)	103.8(2)
C(16) - O(3) - H(3A)	116.8(1)	109.7(2)
C(2) - C(1) - H(1)	119.6(2)	119.2(2)
C(10) - C(1) - H(1)	118.0(2)	118.7(2)
C(1) - C(2) - H(2)	118.1(2)	122.4(2)
C(3) - C(2) - H(2)	122.6(2)	118.3(2)
C(3) - C(4) - H(4)	119.1(2)	120.2(2)
C(5) - C(4) - H(4)	119.9(2)	119.2(2)
C(5) - C(6) - H(6A)	111.7(1)	110.5(2)
C(5) - C(6) - H(6B)	106.0(1)	108.0(1)
C(7) - C(6) - H(6A)	109.1(1)	112.5(2)
C(7) - C(6) - H(6B)	107.1(2)	106.4(2)
H(6A) - C(6) - H(6B)	109.5(2)	105.4(2)
C(6) - C(7) - H(7A)	109.0(2)	111.2(2)
C(6) - C(7) - H(7B)	110.6(2)	109.1(2)
C(8) - C(7) - H(7A)	108.2(1)	109.1(1)
C(8) - C(7) - H(7B)	109.7(2)	112.4(2)
H(7A) - C(7) - H(7B)	109.1(1)	104.2(1)
C(7) - C(8) - H(8)	108.8(1)	110.2(1)
C(9) - C(8) - H(8)	106.9(1)	109.6(1)
C(14) - C(8) - H(8)	111.5(2)	107.3(2)
C(8) - C(9) - H(9)	107.5(1)	106.6(1)
C(10) - C(9) - H(9)	104.4(2)	106.1(2)
C(11) - C(9) - H(9)	105.9(1)	106.8(1)
C(9) - C(11) - H(11A)	108.1(2)	109.5(2)
C(9) - C(11) - H(11B)	110.0(2)	111.0(2)
C(12) - C(11) - H(11A)	109.3(2)	104.5(2)
C(12) - C(11) - H(11B)	110.9(2)	110.2(2)
H(11A)- C(11) - H(11B)	106.5(1)	108.6(1)
C(11) - C(12) - H(12A)	109.8(2)	108.3(2)
C(11) - C(12) - H(12B)	110.0(2)	106.3(2)
C(13) - C(12) - H(12A)	108.5(1)	110.9(1)
C(13) - C(12) - H(12B)	111.1(1)	111.9(1)
H(12A)- C(12) - H(12B)	105.8(2)	108.6(2)
C(8) - C(14) - H(14)	101.8(2)	107.4(2)
C(13) - C(14) - H(14)	107.5(1)	106.0(1)
C(15) - C(14) - H(14)	109.1(1)	106.9(1)
C(14) - C(15) - H(15A)	112.1(1)	114.3(1)
C(14) - C(15) - H(15B)	114.1(1)	111.5(1)
C(16) - C(15) - H(15A)	111.4(2)	111.2(2)

C(16) - C(15) - H(15B)	109.7(2)	113.7(2)
H(15A)- C(15) - H(15B)	105.8(1)	102.3(2)
O(3) - C(16) - H(16)	105.5(1)	108.3(2)
C(15) - C(16) - H(16)	111.9(2)	110.3(2)
C(17) - C(16) - H(16)	109.1(1)	106.3(1)
O(2) - C(17) - H(17)	107.9(2)	111.0(2)
C(13) - C(17) - H(17)	106.0(2)	108.3(2)
C(16) - C(17) - H(17)	105.7(1)	106.9(1)
C(13) - C(18) - H(18A)	113.5(1)	110.5(1)
C(13) - C(18) - H(18B)	107.9(1)	108.6(1)
C(13) - C(18) - H(18C)	109.8(1)	113.1(1)
H(18A)- C(18) - H(18B)	105.6(1)	110.7(1)
H(18A)- C(18) - H(18C)	109.4(2)	107.4(2)
H(18B)- C(18) - H(18C)	110.5(3)	106.4(2)

Table 5. Selected torsion angles (°)

bonds	Molecule 1	Molecule 2
A-ring		
C(10)-C(1)-C(2)-C(3)	-0.5(2)	-0.5(2)
C(1)-C(2)-C(3)-C(4)	2.1(2)	0.8(2)
C(2)-C(3)-C(4)-C(5)	-2.1(2)	-0.3(2)
C(3)-C(4)-C(5)-C(10)	0.5(2)	-0.4(2)
C(4)-C(5)-C(10)-C(1)	1.1(2)	0.7(2)
C(5)-C(10)-C(1)-C(2)	-1.1(2)	-0.3(2)
B-ring		
C(10)-C(5)-C(6)-C(7)	-19.2(2)	-10.5(2)
C(5)-C(6)-C(7)-C(8)	48.4(2)	41.1(2)
C(6)-C(7)-C(8)-C(9)	-64.9(2)	-66.0(2)
C(7)-C(8)-C(9)-C(10)	50.6(2)	57.7(2)
C(8)-C(9)-C(10)-C(5)	-22.2(2)	-27.9(2)
C(9)-C(10)-C(5)-C(6)	6.2(2)	4.2(2)
C-ring		
C(8)-C(9)-C(11)-C(12)	56.1(2)	51.8(2)
C(9)-C(11)-C(12)-C(13)	-55.2(2)	-54.7(2)
C(11)-C(12)-C(13)-C(14)	54.4(2)	56.8(2)
C(12)-C(13)-C(14)-C(8)	-58.7(2)	-60.2(2)
C(13)-C(14)-C(8)-C(9)	59.3(2)	56.9(2)
C(14)-C(8)-C(9)-C(11)	-56.5(2)	-51.4(2)
D-ring		
C(13)-C(14)-C(15)-C(16)	-33.3(2)	-31.2(2)
C(14)-C(15)-C(16)-C(17)	4.2(2)	2.0(2)
C(15)-C(16)-C(17)-C(13)	26.7(2)	27.6(2)
C(16)-C(17)-C(13)-C(14)	-45.9(2)	-45.8(2)
C(17)-C(13)-C(14)-C(15)	48.6(2)	47.7(2)
C(13)-C(17)-C(16)-O(3)	150.4(2)	151.8(2)
C(15)-C(16)-C(17)-O(2)	157.7(2)	152.9(2)
C(13)-C(17)-O(2)-H(2A)	-4.7(2)	-78.2(2)
C(15)-C(16)-O(3)-H(3A)	84.4(2)	50.8(2)
C(2)-C(3)-O(1)-H(1A)	169.7(2)	-171.3(2)
C(4)-C(3)-O(1)-H(1A)	-8.5(2)	3.6(2)

Table 6. Hydrogen bonds

Bonds	O–H [Å]	O···O [Å]	H···O [Å]	O–H···O Angle[°]
molecule 1				
O(1)–H(1A)···O(3)[1]	0.97	2.646(2)	1.682(2)	171.7(1)
O(2)–H(2A)···O(1)[2]	0.97	2.773(2)	1.851(1)	158.6(1)
O(3)–H(3A)···O(1')[3]	0.97	2.890(1)	1.930(1)	170.5(1)
molecule 2				
O(1')–H(1'A)···O(3')[4]	0.97	2.640(2)	1.684(1)	169.9(1)
O(2')–H(2'A)···O(1')[5]	0.97	2.884(1)	1.927(1)	169.2(1)
O(3')–H(3'A)···O(2)[6]	0.97	2.736(1)	1.857(1)	149.9(1)

Symmetry codes: (1) –x+2, y-1/2, -z+1; (2) –x+1, y+1/2, -z+1; (3) x, y, z-1 ;
(4) –x+1, y+1/2, -z+2; (5) –x+2, y-1/2, -z+2; (6) –x+1, y-1/2, -z+1

Table 7. Analysis of the properties of the bond critical points for molecule 1 and 2

Bond	λ_1	λ_2	λ_3	ρ_c (eÅ^{-3})	$\nabla^2\rho_c$ (eÅ^{-5})	R_{ij} (Å)	d_1(Å)	d_2(Å)	ε
A-ring									
C(1)-C(2)	-14.91	-13.13	9.86	2.14(1)	-18.2(1)	1.3941	0.7093	0.6848	0.14
C(2)-C(3)	-16.56	-14.23	8.59	2.20(2)	-22.2(1)	1.3968	0.6823	0.7145	0.16
C(3)-C(4)	-15.95	-13.53	8.27	2.16(1)	-21.2(1)	1.3944	0.7586	0.6357	0.18
C(4)-C(5)	-14.99	-12.74	9.40	2.06(1)	-18.3(1)	1.3993	0.6995	0.6997	0.18
C(5)-C(10)	-14.50	-12.39	9.76	2.06(1)	-17.1(1)	1.4085	0.7184	0.6901	0.17
C(10)-C(1)	-13.90	-11.46	10.05	2.04(1)	-15.3(1)	1.4064	0.7400	0.6664	0.21
C(1)-H(1)	-15.76	-14.68	16.12	1.81(1)	-14.3(1)	1.0810	0.7043	0.3767	0.07
C(2)-H(2)	-17.47	-15.97	11.67	1.89(1)	-21.8(1)	1.0835	0.6892	0.3943	0.09
C(4)-H(4)	-16.13	-15.02	12.13	1.78(4)	-19.0(1)	1.0856	0.6953	0.3903	0.07
C(3)-O(1)	-18.43	-14.58	11.15	2.06(3)	-21.9(9)	1.3704	0.8338	0.5366	0.26
	-17.69	-16.37	11.96	2.15(2)	-22.1(5)	1.3785	0.8625	0.5160	0.08
O(1)-H(1A)	-42.54	-41.68	28.43	2.06(8)	-55.8(8)	0.9705	0.8183	0.1523	0.02
	-39.51	-38.86	33.10	2.19(8)	-45.3(7)	0.9656	0.7918	0.1738	0.02
B-ring									
C(5)-C(6)	-11.17	-10.68	10.59	1.71(1)	-11.3(1)	1.5150	0.7758	0.7392	0.05
C(6)-C(7)	-11.42	-10.53	11.01	1.74(1)	-10.9(1)	1.5260	0.7649	0.7611	0.08
C(7)-C(8)	-11.08	-10.19	10.42	1.66(1)	-10.9(1)	1.5294	0.7811	0.7482	0.09
C(8)-C(9)	-11.97	-11.24	9.55	1.69(1)	-13.7(1)	1.5449	0.7774	0.7675	0.06
C(9)-C(10)	-11.72	-10.64	10.03	1.70(1)	-12.3(1)	1.5278	0.7819	0.7459	0.10
C(6)-H(6A)	-15.27	-13.50	13.17	1.81(4)	-15.6(1)	1.0949	0.6650	0.4299	0.13
C(6)-H(6B)	-13.83	-13.26	18.27	1.64(4)	-8.8(2)	1.0919	0.7474	0.3446	0.04
C(7)-H(7A)	-17.45	-16.39	15.50	1.87(4)	-18.3(1)	1.0934	0.7486	0.3447	0.06
C(7)-H(7B)	-16.40	-15.11	15.05	1.83(4)	-16.5(1)	1.0918	0.7198	0.3721	0.08
C(8)-H(8)	-16.66	-15.88	15.86	1.75(4)	-16.7(2)	1.0987	0.7747	0.3240	0.05
C(9)-H(9)	-16.00	-15.43	15.47	1.77(4)	-16.0(1)	1.0988	0.7529	0.3460	0.04
C-ring									
C(9)-C(11)	-10.88	-10.22	10.44	1.66(1)	-10.7(1)	1.5392	0.7584	0.7807	0.06
C(11)-C(12)	-11.08	-9.82	10.55	1.64(1)	-10.4(1)	1.5409	0.7602	0.7807	0.13
C(12)-C(13)	-12.51	-10.91	9.88	1.74(1)	-13.5(1)	1.5326	0.7590	0.7737	0.15
C(13)-C(14)	-11.25	-10.40	9.44	1.61(1)	-12.2(1)	1.5511	0.7811	0.7701	0.08
C(14)-C(8)	-12.82	-11.67	9.11	1.73(1)	-15.4(1)	1.5240	0.7471	0.7769	0.10
C(11)-H(11A)	-15.07	-14.54	15.84	1.75(4)	-13.8(1)	1.0940	0.7254	0.3686	0.04
C(11)-H(11B)	-16.42	-15.68	14.56	1.81(4)	-17.6(1)	1.0910	0.7252	0.3658	0.05
C(12)-H(12A)	-15.89	-15.29	17.28	1.76(4)	-13.9(2)	1.0918	0.7609	0.3309	0.04
C(12)-H(12B)	-15.43	-14.39	13.44	1.79(4)	-16.4(1)	1.0895	0.6880	0.4015	0.07
C(14)-H(14)	-17.00	-16.69	15.47	1.77(4)	-18.2(2)	1.1014	0.7906	0.3108	0.02
D-ring									
C(14)-C(15)	-10.55	-10.14	9.96	1.57(1)	-10.7(1)	1.5407	0.7822	0.7585	0.04
C(15)-C(16)	-12.44	-11.26	9.30	1.72(1)	-14.4(1)	1.5545	0.7425	0.8120	0.10
C(16)-C(17)	-12.55	-11.96	9.60	1.78(1)	-14.9(1)	1.5415	0.7855	0.7560	0.05
C(17)-C(13)	-11.07	-10.22	9.64	1.65(1)	-11.7(1)	1.5388	0.7186	0.8202	0.08
C(15)-H(15A)	-17.48	-15.46	12.88	1.81(4)	-20.1(1)	1.0932	0.7318	0.3614	0.13
C(15)-H(15B)	-15.96	-15.02	16.09	1.69(5)	-14.9(2)	1.0949	0.7720	0.3229	0.06
C(16)-H(16)	-19.64	-18.95	13.21	1.95(5)	-25.4(2)	1.0963	0.7781	0.3182	0.04
C(17)-H(17)	-17.60	-17.14	15.35	1.79(4)	-19.4(2)	1.1012	0.7941	0.3071	0.03
C(13)-C(18)	-11.21	-10.71	10.49	1.71(1)	-11.4(1)	1.5369	0.7884	0.7485	0.05
C(18)-H(18A)	-16.66	-15.94	16.28	1.88(5)	-16.3(2)	1.0637	0.7103	0.3533	0.05
C(18)-H(18B)	-16.33	-15.85	13.99	1.88(5)	-18.2(2)	1.0542	0.6786	0.3756	0.03
C(18)-H(18C)	-16.25	-14.78	15.99	1.85(5)	-15.0(1)	1.0574	0.6869	0.3706	0.10
C(17)-O(2)	-14.87	-14.01	13.67	1.95(2)	-15.2(8)	1.4309	0.8536	0.5773	0.06
	-14.13	-13.07	14.41	1.93(3)	-12.8(6)	1.4168	0.8365	0.5803	0.08
O(2)-H(2A)	-47.56	-44.89	24.94	2.26(6)	-67.5(7)	0.9664	0.8096	0.1569	0.06
	-45.49	-42.90	24.61	2.36(8)	-63.8(7)	0.9684	0.7946	0.1738	0.06
C(16)-O(3)	-14.88	-14.01	13.82	1.90(2)	-15.1(7)	1.4387	0.8574	0.5813	0.06
	-14.17	-12.85	14.64	1.86(2)	-12.4(1)	1.4296	0.8351	0.5945	0.10
O(3)-H(3A)	-35.49	-34.31	42.26	2.36(7)	-27.4(5)	0.9696	0.7579	0.2118	0.03
	-40.78	-39.22	34.73	2.25(7)	-45.3(6)	0.9678	0.7921	0.1757	0.04

λ_1, λ_2 and λ_3 are the eigenvalues of Hessian matix. ρ_c -electron density; $\nabla^2\rho_c$ - Laplacian at the CP; d_1 & d_2 are the distances from the critical point; R_{ij} – Sum of d_1 & d_2; ε- bond ellipticity.

Table 8. Topological characteristics of the electron density at the hydrogen Bond critical point.

Bond	ρ_c (eÅ^{-3})	$\nabla^2\rho_c$ (eÅ^{-5})	R_{ij} (Å)	d_1(Å)	d_2(Å)	ε
molecule 1						
O(1)–H(1A)· · · O(3)[1]	0.23(5)	5.01(6)	1.6854	1.1482	0.5372	0.17
O(2)–H(2A)· · · O(1)[2]	0.11(2)	3.00(1)	1.9290	1.2552	0.6738	0.82
O(3)–H(3A)· · · O(1')[3]	0.20(3)	2.93(1)	1.9308	1.2247	0.7061	0.17
molecule 2						
O(1')–H(1'A)· · · O(3')[4]	0.23(5)	4.96(5)	1.6861	1.1194	0.5668	0.20
O(2')–H(2'A)· · · O(1')[5]	0.05(2)	2.24(1)	2.0792	1.3508	0.7284	1.42
O(3')–H(3'A)· · · O(2')[6]	0.20(2)	3.33(2)	1.8746	1.2160	0.6586	0.15

Symmetry codes: (1) –x+2, y-1/2, -z+1; (2) –x+1, y+1/2, -z+1; (3) x, y, z-1 ;
(4) –x+1, y+1/2, -z+2; (5) –x+2, y-1/2, -z+2; (6) –x+1, y-1/2, -z+1

λ_1, λ_2 and λ_3 are the eigenvalues of Hessian matix. ρ_c -electron density; $\nabla^2\rho_c$ - Laplacian at the CP; d_1 & d_2 are the distances from the critical point; R_{ij} – Sum of d_1 & d_2 ; ε- bond ellipticity.

Table 9. Net atomic charges (e)

Atom	charge	Atom	charge
C(1)	-0.21(3)	H(1)	0.16(2)
C(2)	-0.06(3)	H(2)	0.29(2)
C(3)	0.16(3)	H(4)	0.31(2)
C(4)	-0.06(3)	H(6A)	0.20(2)
C(5)	-0.00	H(6B)	0.12(2)
C(10)	-0.04(2)	H(7A)	0.20(2)
C(6)	-0.36(3)	H(7B)	0.24(2)
C(7)	-0.48(3)	H(8)	0.16(2)
C(8)	-0.12(3)	H(9)	0.20(2)
C(9)	-0.29(3)	H(11A)	0.20(2)
C(11)	-0.31(3)	H(11B)	0.22(2)
C(12)	-0.47(3)	H(12A)	0.08(2)
C(13)	-0.00	H(12B)	0.26(2)
C(14)	-0.07(3)	H(14)	0.17(2)
C(15)	-0.24(3)	H(15A)	0.30(2)
C(16)	0.05(3)	H(15B)	0.21(2)
C(17)	-0.08(3)	H(16)	0.21(2)
C(18)	-0.61(3)	H(17)	0.16(2)
		H(18A)	0.20(2)
		H(18B)	0.27(2)
		H(18C)	0.19(2)
O(1)	-0.63(3)	H(1A)	0.43(3)
	-0.79(3)		0.35(3)
O(2)	-0.86(3)	H(2A)	0.48(2)
	-0.87(3)		0.46(2)
O(3)	-0.84(3)	H(3A)	0.25(2)
	-0.77(3)		0.46(2)

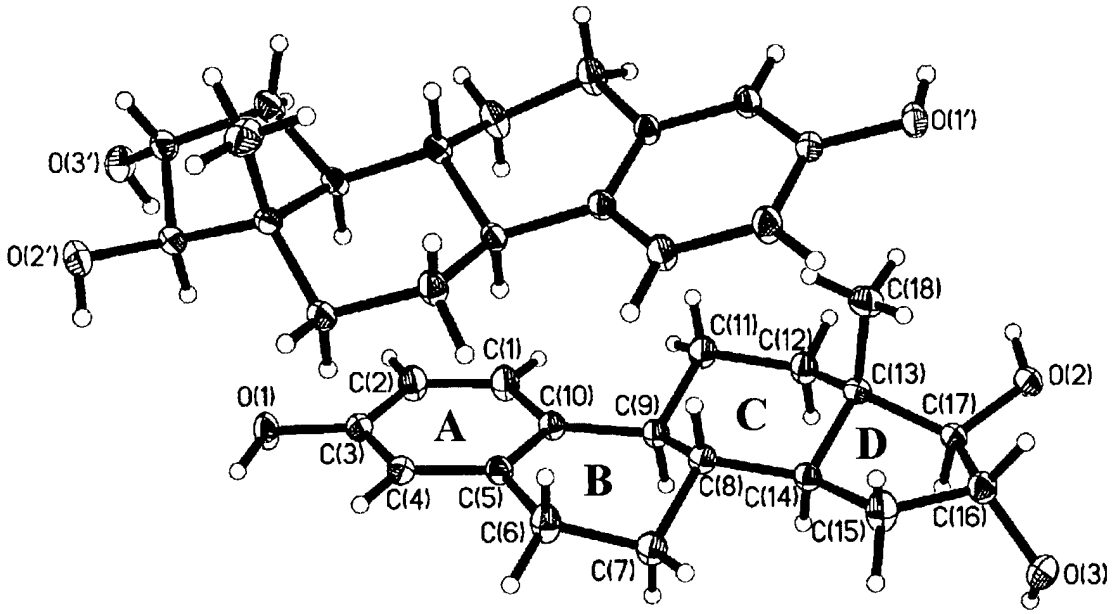

Figure 1. ORTEP view of two molecules in the asymmetric unit showing 75% probability thermal ellipsoids.

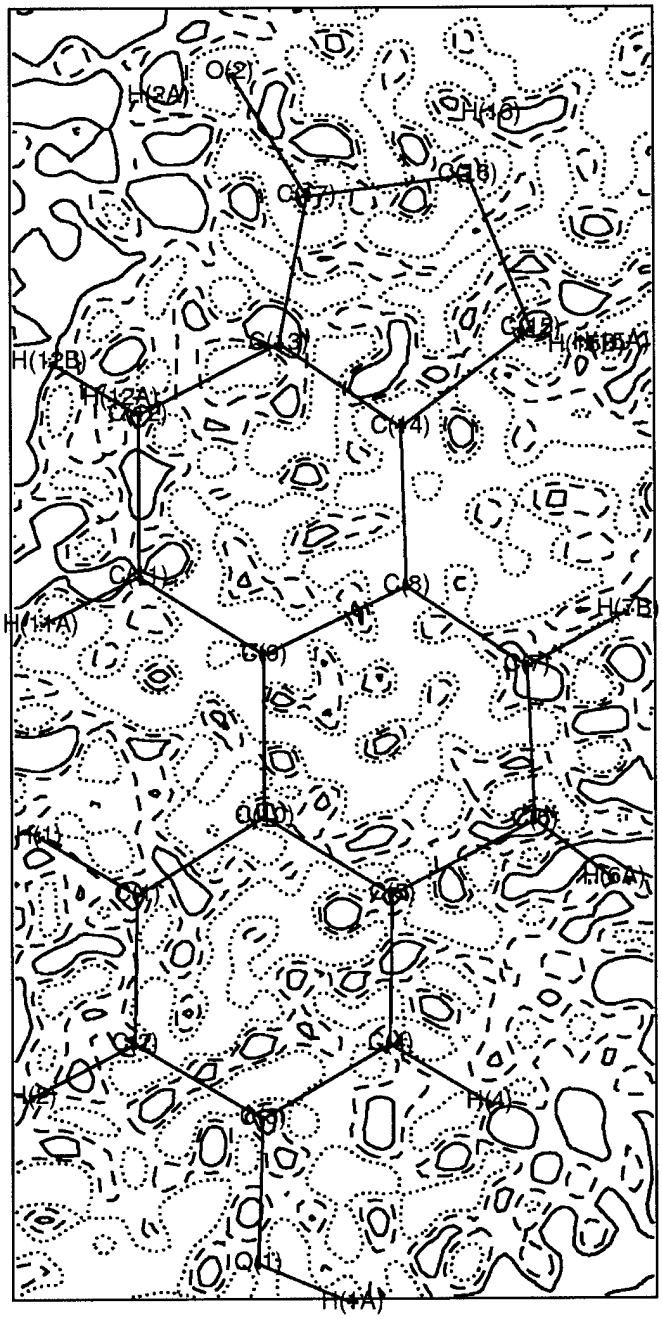

Figure 2a. Residual electron density ($\delta\rho_{resid}=\rho_{exper} - \rho_{mult}$) map for the molecule 1. Contour interval is 0.05 eÅ^{-3}. The solid lines show positive values, the negative contours are dashed lines, the zaro one is dashed.

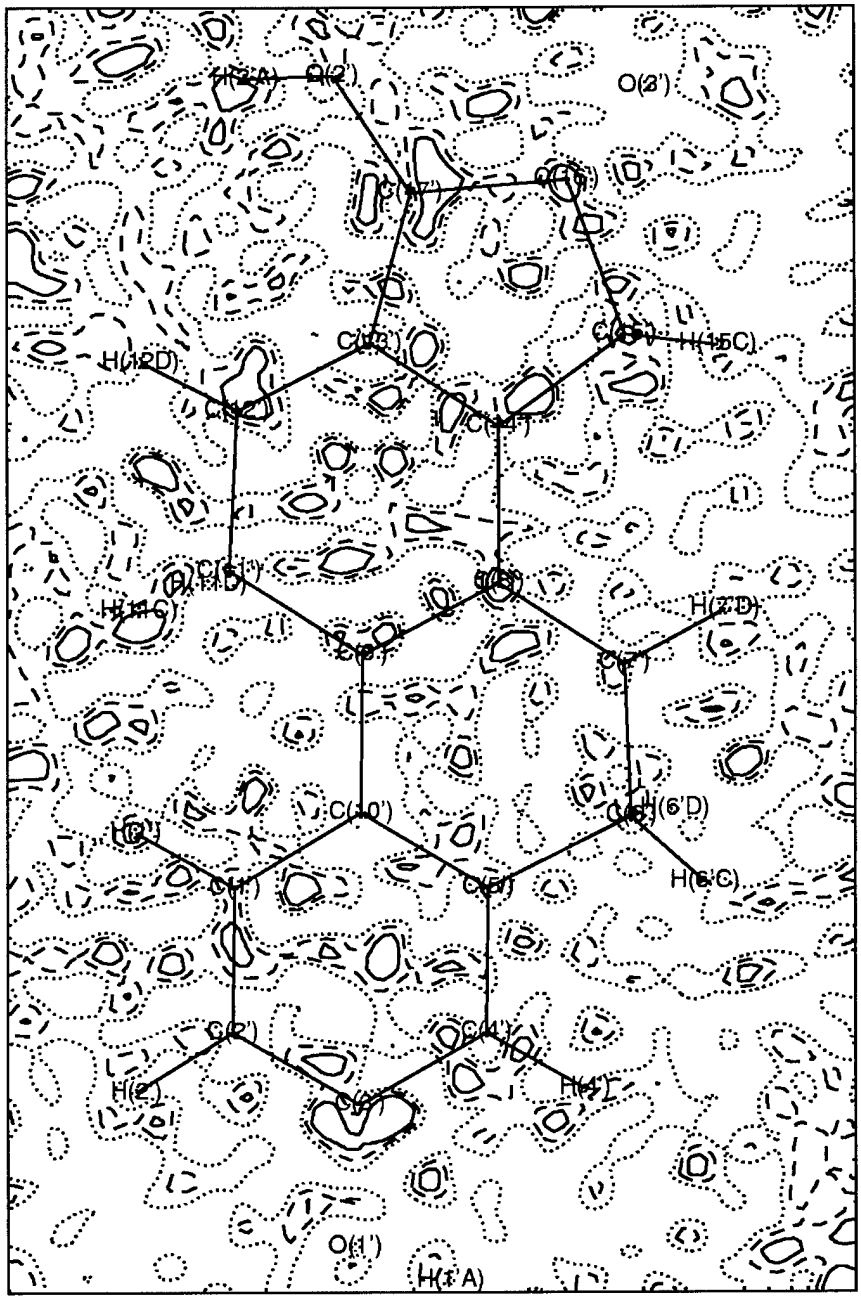

Figure 2b. Residual electron density ($\delta\rho_{resid}=\rho_{exper} - \rho_{mult}$) map for the molecule 2. Contour interval is 0.05 eÅ^{-3}. The solid lines show positive values, the negative contours are dashed lines, the zaro one is dashed.

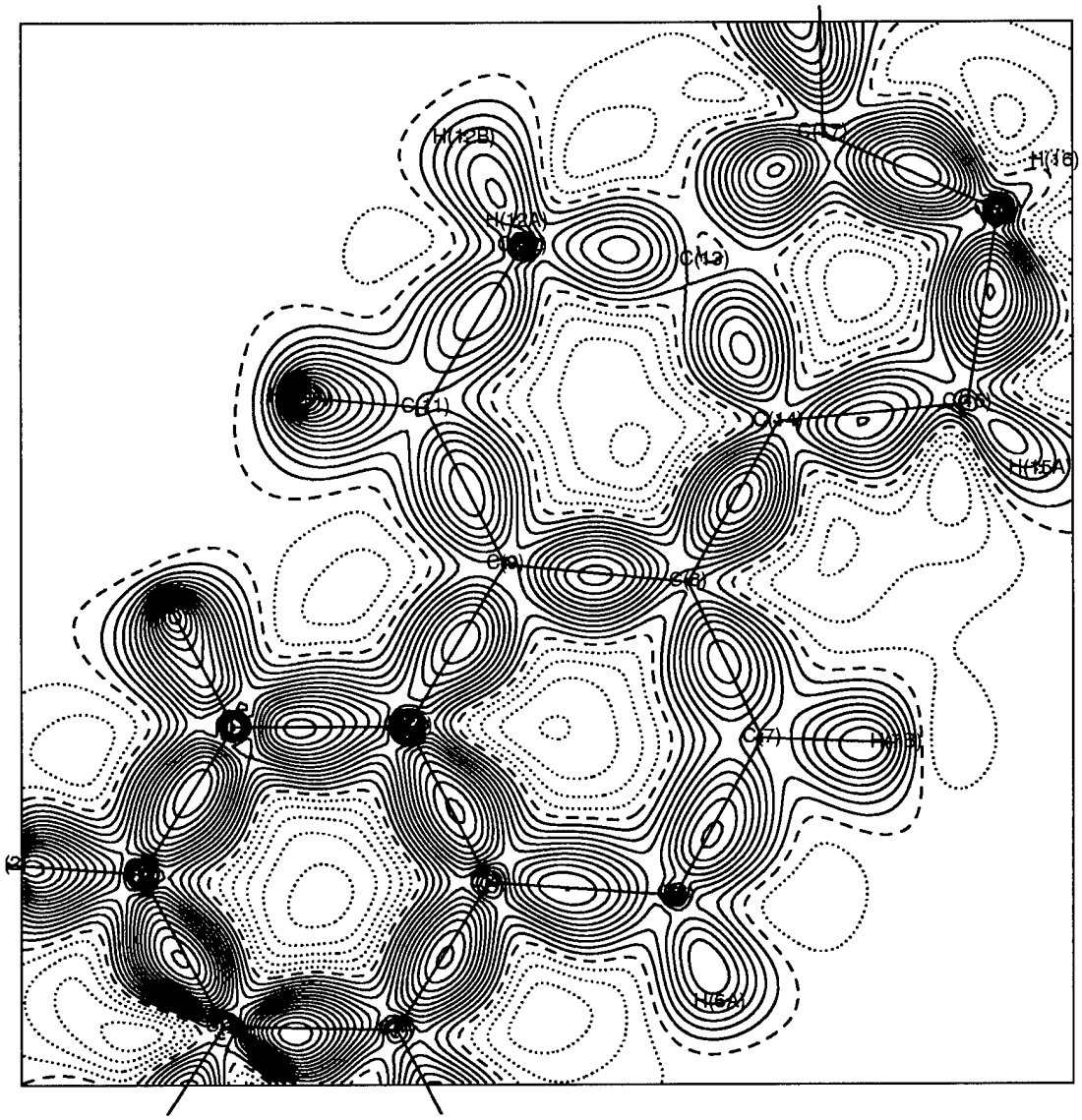

Figure 3. The multipole deformation electron density ($\delta\rho_{mult}=\rho_{mult} - \rho_{sph}$) map in the aromatic ring plane. Contours are the same as in Fig. 2.

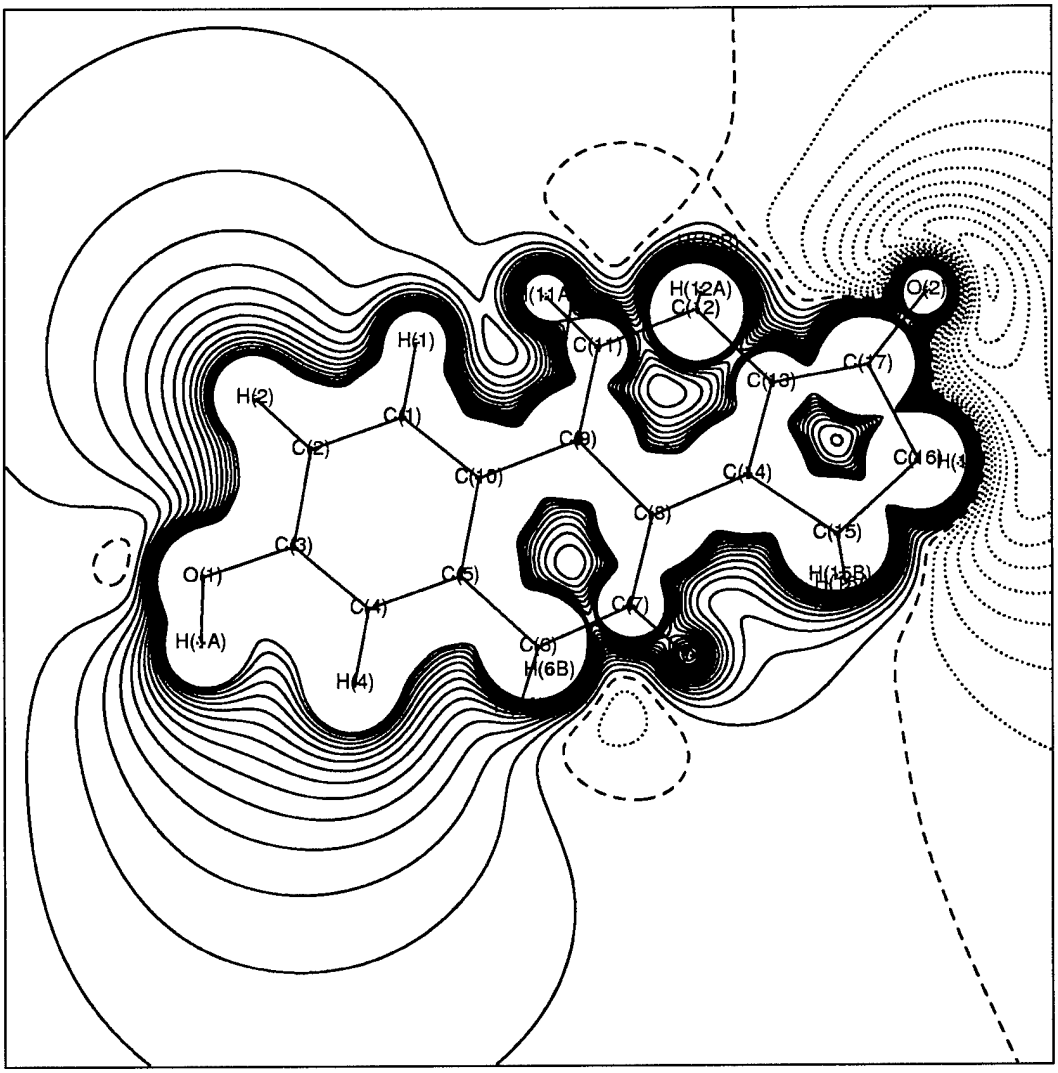

Figure 4a. Electrostatic potential of molecule (1) in the plane of O(1), C(5) & C(16) atoms. Contour interval is 0.05 eÅ^{-1}. Positive contours are solid lines, negative contours are dotted lines, and zero contour is dashed.

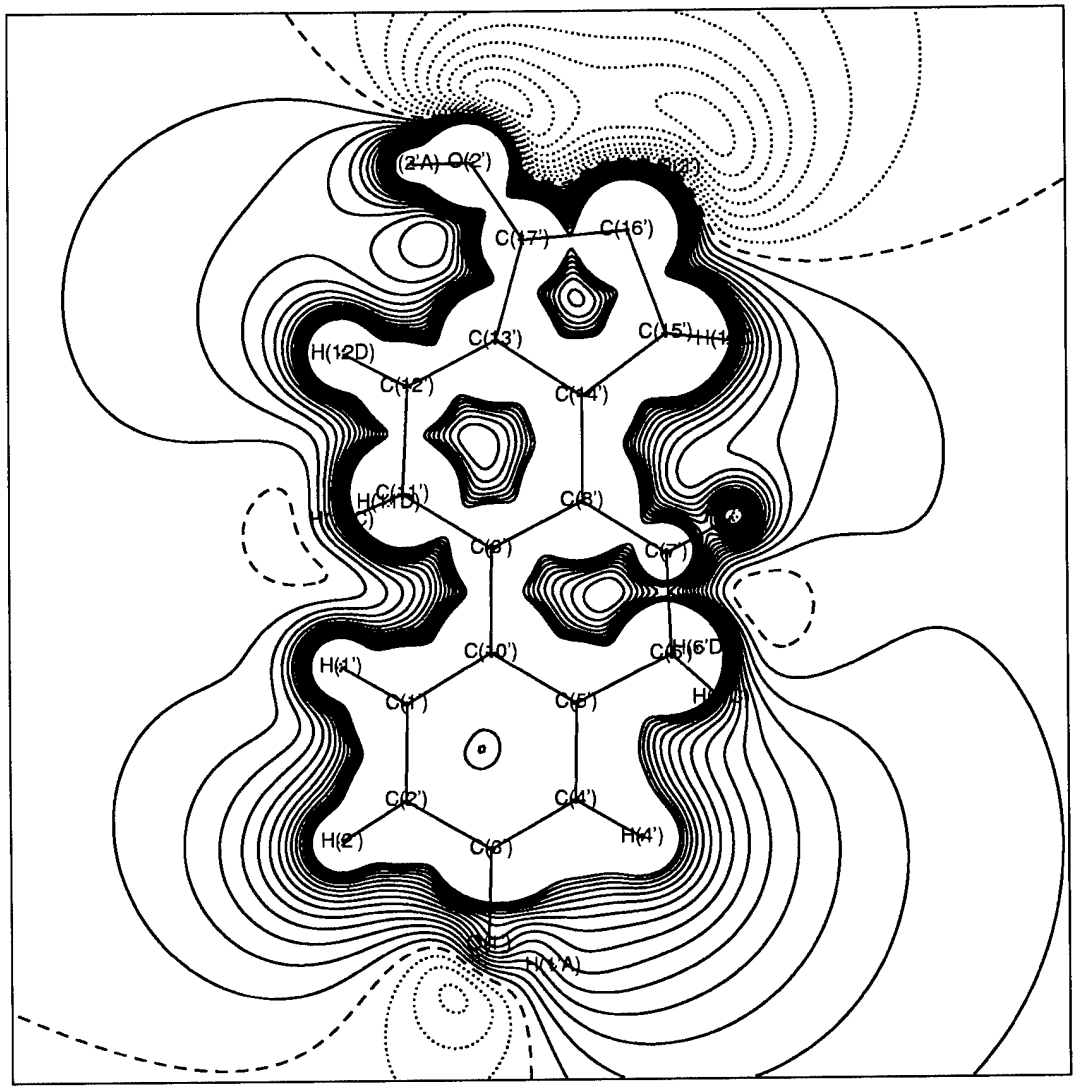

Figure 4b. Electrostatic potential of molecule (2) in the plane of C(1'), C(5') & C(16'). Contour are the same as in Fig4a.

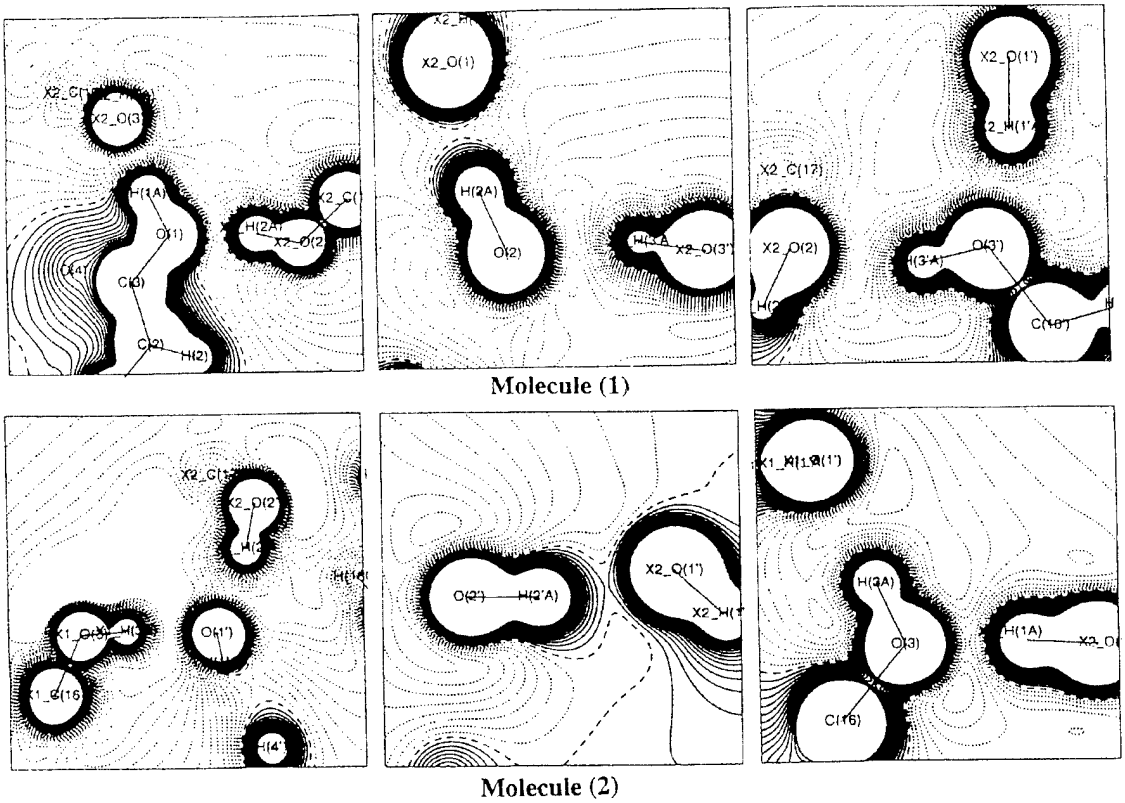

Figure 5. The electrostatic potential in the hydrogen bonding environment of oxygen atoms of molecule (1) & (2). Contour interval 0.05e/Å; Positive solid line, negative dashed line, zero contour as dotted lines.

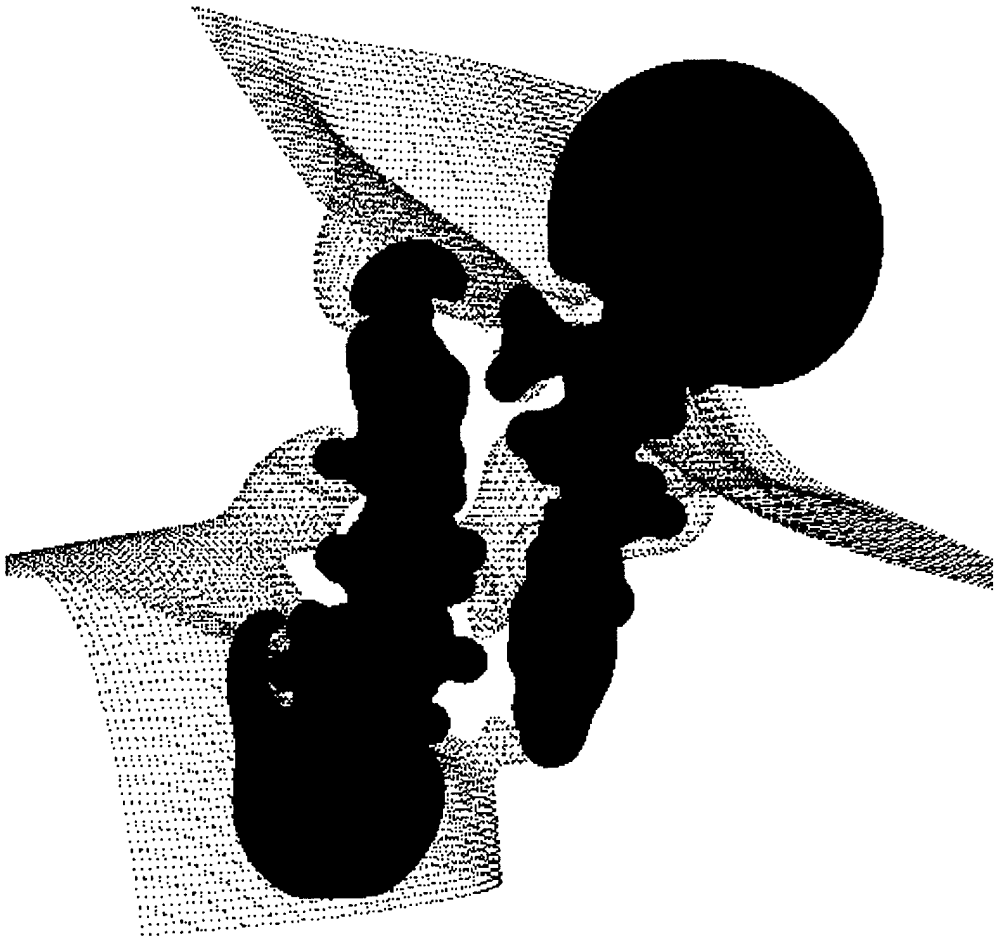

Figure 6. Isosurface representation of electrostatic Potential of molecule 1 (right) and molecule 2 (left). Surfaces are drawn at constant positive and negative potentials of 0.5 e/Å (red) and –0.1 e/Å (green). Gray dots are zero surface.

Appendix C.

Electron density study of estrone

Electron Density Study of Estrone

by

Nan Wu, Elizabeth A. Zhurova and A. Alan Pinkerton*

Department of Chemistry, University of Toledo, Toledo, OH 43606, USA

Abstract

Many breast cancers are known to be hormone dependent, i.e. the activation or inhibition of tumor growth can be influenced by estrogens. Minor chemical changes in the estrogens structures are known to cause fundamental changes in the biological reactions. The reason for this is unknown, however, it has been suggested (Vander Kuur, J.A.; Hafner, M.S.; Christman, J.K.; Brooks, S.C. Biochemistry, 1993, 32, 7016-7021) that the behavior of different estrogen analogs can be related to the physical properties such as the distribution of electron density and the electrostatic potential. In this work we present the first electron density study of an estrone molecule based on low-temperature X-ray diffraction experimental data. The parameterization of the electron density in terms of a multipole expansion allowed the direct space calculation of the estrone electrostatic potential. It exhibits negative regions around both oxygen atoms, more narrow for the O atom bonded to hydrogen. There are also significant negative regions above and below the aromatic ring. These areas represent the sites of the possible electrophilic attack or the sites which match the electropositive regions of the estrogen receptor during the activated complex formation. Chemical bonding in the estrone molecule as well as the hydrogen bonding is discussed in terms of Bader's topological theory.

Introduction

Estrogens and their derivatives have been extensively investigated since the agonistic effect of estradiol on most breast cancer tumors was determined[1]. Estrogens and related compounds bind as ligands to the estrogen receptor (ER) forming an activated complex. A series of events are initiated by the ER complex resulting in the activation or

repression of selective genes and subsequent induction or suppression of production of characteristic proteins. In order to better understand the role of the ligand in ER mediated processes, extensive research into the influence of the different estrogen derivatives on the regulation of hormone responsive genes has been performed[2-6]. Even though most changes in the estrogen ligand affect its affinity for the receptor, this does not necessarily correlate with the stimulation ability of the transcription of estrogen responsive genes. The mechanism by which these structurally altered ligands regulate the differential induction of gene expression is currently unknown. However, it has been suggested that the differences in electrostatic potential generated by the lone pair electrons of the phenolic oxygen and π- electrons of the aromatic ring are responsible for the variation in the regulation of hormone dependent genes[5]. It is obvious, that the binding ability of the ligand to the receptor is not the only important factor in the biological activity of a potential drug, secondary interactions and several domains of the receptor are involved. But the initial driving force towards binding to a receptor is due to the match between topography of the electrostatic potential (ESP) of the pharmaceutical molecule and that of the binding site.

In principle, the ESP distributions can be calculated theoretically. But the calculations of reliable ESP's from high level ab initio methods are only possible for relatively small molecules because extended basis sets are required in order to obtain meaningful results. A recent approach[7] has to be mentioned, which uses large basis sets for small fragments which in turn are used as building blocks for larger molecules. In spite of the computational advantage of this method, it can be only a rough approximation to the real object.

A better approach is to map the ESP experimentally by interpretation of single crystal X-ray diffraction data. Until recently, this type of measurement was very time consuming, even for smaller molecules. The recently developed new generation of CCD Platform Diffractometers with an appropriate cooling system allow us to measure a precise complete set of data in 2-3 weeks, even for such large molecules, as estrogens. The developed multipole method[8-9] allows the parameterization of the electron density in a crystal and a subsequent calculation of the ESP distribution[10].

Another novel approach that can be used in the analysis of the electron density (ED) and related properties is Bader's topological theory[11]. This theory is based on quantum mechanics and describes a crystal in terms of the ED $\rho(\mathbf{r})$, its gradient vector field $\nabla\rho(\mathbf{r})$, ED curvature, critical point (CP) positions and their characteristics[12]. The CP, the point at which $\nabla\rho(\mathbf{r}_c)=0$, is determined by it's rank, the number of non-zero eigenvalues of the diagonalized Hessian (or curvature) matrix λ_i, and signature, the sum of the algebraic signs of λ_i. The ED exhibits four kinds of non-degenerate CP's of rank 3: maxima (3,-3), minima (3,+3) and two types of saddle points, (3,+1) and (3,-1). They correspond to nuclear positions, cages, rings and bonds in the crystal or molecule. In the $\nabla\rho(\mathbf{r})$ field, there are pairs of gradient lines that originate at a (3,-1) CP and terminate at two neighboring nuclei. They are determined by the eigenvector corresponding to the only positive eigenvalue of the Hessian λ_3 at this point and they form the atomic interaction lines along which the ED decreases for any lateral displacements. At equilibrium, this line is named as a bond path and the associated (3,-1) point is termed a bond CP. The negative eigenvalues λ_1 and λ_2 at the bond CP correspond to the directions normal to the bond path and measure the degree of ED contraction towards this point; $\lambda_3>0$ measures the degree of ED contraction towards each of the neighboring nuclei. The spatial distribution of the Laplacian of the ED, $\nabla^2\rho(\mathbf{r})$ characterizes the concentration and depletion of electrons in each point $\mathbf{r}$ of the system. The sign of the Laplacian of the ED at the bond (3,-1) CP depends on the relation between the principal curvatures of the ED at the CP and, therefore reflects the character of the atomic interactions. If the electrons are locally concentrated in the bond CP ($\nabla^2\rho(\mathbf{r}_c)<0$), then ED is shared by both nuclei (shared interactions). This is typical for the covalent type of bonds. If electrons are concentrated in each of the atomic basins separately ($\nabla^2\rho(\mathbf{r}_c)>0$), the interaction type is closed-shell, and it is typical of ionic and hydrogen bonds, as well as van der Waals interactions[13]. Each bond path is homeomorphically mirrored by a virial path, a line of maximally negative potential energy density linking the same nuclei. The presence of a bond path and its associated virial path provide a 'universal indicator of bonding between the atoms so linked'.[14]

At this early state of experimental ED investigations on estrogens, it is very difficult to formulate a precise hypothesis. However, we believe, we can derive parameters from experimental data which will identify physical properties of regions of a ligand that are related to certain biological functions. This is the information needed in order to intelligently design therapeutically improved drugs. The ED investigation of estrone, one of the natural estrogens, is a very first step towards the solution of this task.

Experimental

A colorless rectangular crystal (Table 1) was re-crystallized from an ethanol: ethyl acetate solvent system. It was mounted on a 0.1 mm capillary with epoxy resin and slowly cooled down to 92K with an Oxford Cryostream. The X-ray diffraction experiment was performed with a Bruker platform diffractometer with a 2K CCD detector using Ag-K_α radiation. 0.2° ω -scans were performed at a detector distance of 6 cm. Two detector settings of 2θ= -20° and –65° and 4 different φ settings were used. The exposure time of 88 sec for the low-angle data and 180 sec for the high-angle data allowed the use of the full dynamic range of the detector. The first 100 frames were repeated at the end of the measurement to check the X-ray intensity decay. Other experimental details are in Table 1.

The integration was performed with the program SAINT[15]. An empirically chosen integration box size of 1.8×1.8×0.7° for low-angle data and 1.5×1.5×0.7° for high-angle data and the profile fitting procedure based on strong ($I > 10\sigma$) reflections allowed us to obtain the best internal consistency (R_{int}=0.0478) and preliminary refinement R factors. After the integration process, the unit cell parameters were refined with all reflections with $\sin\theta/\lambda < 0.84$ Å^{-1} since all of the high-angle reflections were relatively weak. The integration process was repeated twice until convergence in cell parameters was obtained. An empirical absorption correction with the program SADABS[16] was performed. The data were averaged with the program SORTAV [17].

Refinements and results

The crystal structure was solved by direct methods and a preliminary least-squares refinement was carried out with the SHELXTL program suite[18]. The positions of hydrogen atoms were determined from the difference Fourier peaks. Anisotropic thermal motion was considered for all non-hydrogen atoms, and the latter were refined as isotropic. The estrone molecule with 50% probability thermal ellipsoids for non-hydrogen atoms is shown in Fig.1a. The atomic coordinates, atomic thermal parameters and the scale factor were refined at this stage with all data. Then, the so-called Hansen-Coppens multipole refinement[8] using the XD program package[9] was performed with the low-angle data ($\sin\theta/\lambda < 1.0$ Å^{-1}). In this model the ED is approximated as a sum of the core and valence pseudo-atomic electron densities in the form

$$\rho_{atomic}(\mathbf{r}) = \rho_{core}(r) + P_v \kappa'^3 \rho_{valence}(\kappa' r) + \sum_{l=1}^{4} \kappa''^3 R_l(\kappa'' r) \sum_{m=-l}^{l} P_{lm} y_{lm}(\mathbf{r}/r). \qquad \textbf{(1)}$$

Here P_v and P_{lm} are monopole and higher multipole populations; R_l are normalized Slater-type radial functions; y_{lm} are real spherical harmonic angular functions; κ' and κ'' are the valence shell contraction\expansion parameters. Hartree-Fock densities[19] are used for the spherically averaged core and valence shells. The drawing of the local multipole coordinate systems for each atom has been deposited (Fig. D1). For the hydrogen atoms the x-axis was chosen to be directed towards neighboring carbon or oxygen atom. Only dipole population along this direction was refined for hydrogen atoms, other populations were set to zero. Since the molecule is rather large and the crystallographic space group ($P2_12_12_1$) is non-centrosymmetric, the X-ray phase problem arises[20]. Therefore, chemical and symmetry constraints were applied at the initial stages of the multipole refinement as follows. Hydrogen atoms attached to the same carbon were considered to be chemically the same, i.e. having the same monopole and dipole populations and kappa sets, but different thermal motion. H(1), H(2) and H(4) were also taken the same. Carbons C(1) – C(4); C(5) & C(10); C(6), C(7), C(11)-C(13), C(15),C(16), C(18); C(8),C(9) & C(14) were considered to be the same. Atoms C(1)-C(5), C(10) & C(17) were considered to have the sp^2 hybridization state, therefore only multipoles directed same as the σ-bonds and multipoles perpendicular to the aromatic ring were refined. An additional mirror symmetry constraint for the aromatic ring was imposed. A totally of 8 κ' and κ'' sets were used (see Table 2). κ' and κ'' parameters were fixed to 1.2 and 1.0 correspondingly

for all hydrogen atoms. Reasonable values for the initial κ′ and κ″ parameters, close to the final ones were picked up to get better X-ray phases in the initial refinement. The multipole parameters were refined up to the hexadecapole level (l=4) for all non-hydrogen atoms. The molecular electroneutrality constraint was also applied. For hydrogen atoms, all the parameters including positional and displacement ones were refined with sin $\theta/\lambda < 0.5$ Å^{-1}. The O-H and C-H bond lengths were fixed to the tabulated values[21] according to their hybridization state.

The model, described above was refined with all reflections together with atomic coordinates, thermal parameters and scale factor. Then, all the constraints, except those for hydrogen atoms attached to sp^3 carbons were removed gradually and the model was refined again. The highly correlated parameters were refined in the separate groups, so that the highest correlation coefficient was 0.54. In the final cycles, parameters with values less than one standard deviation were fixed to zero. The rigid-bond test[22] showed that the differences of mean-square displacement amplitudes along the interatomic vectors were less than 1.3×10^{-3} Å^2. The resulting multipole and κ parameters have been deposited (tables D1 and D2). The atomic coordinates, thermal parameters and interatomic distances are deposited as a cif file.

Then, in order to get the correct values of atomic charges[23], all the multipole parameters were set to zero, and the so-called κ- refinement was performed. Only P_v and κ' parameters together with the scale factor, positional and thermal atomic parameters were refined. The resulting atomic charges and κ' values are in the Table 2.

The residual ED ($\delta\rho_{resid} = \rho_{exper} - \rho_{mult}$) and model multipole deformation ED ($\delta\rho_{mult} = \rho_{mult} - \rho_{sph}$) maps were calculated with the low-angle data (sin $\theta/\lambda < 0.9$ Å^{-1}). They are presented in Figs. 2 and 3.

The ESP is a crystal (or molecular) property directly related to the ED:

$$V(\mathbf{r}) = \sum_A \frac{Z_A}{|\mathbf{R}_A - \mathbf{r}|} - \int \frac{\rho(\mathbf{r}')}{|\mathbf{r}' - \mathbf{r}|} d\mathbf{r}', \qquad \textbf{(2)}$$

where Z_A is the charge of nucleus A located at $\mathbf{R}_A$, $\rho(\mathbf{r}')$ is the total ED. The partition of the ED into pseudoatomic fragments in the form of a multipole expansion **(1)** allows the direct space calculation of the ESP distribution[10], recently becoming popular in such

crystallographic studies[24,9]. The ESP for the isolated molecule taken from the crystal is shown in Fig.4.

The topological analysis of the estrone ED was performed. The Laplacian map is reported in Fig.5. The bond CP's in the molecule were found as well as those representing the hydrogen bonding in the crystal. They are reported in Table 3. The dipole moment of the molecule in the crystal after the multipole refinement (10.2(3) D) corresponding to the geometrical center of the molecule was also calculated.

Discussion

The estrone crystal unit cell parameters were measured by Vanden Bossche[25] and structure was solved first by Busetta et al.[26] in 1973. In the solid state, the estrone molecules are linked into zig-zag chains by hydrogen bonds (Fig. 1b). Though their refinement was performed up to R=0.039 (estrone II in their nomenclature), all atomic thermal parameters β_{22} were too small compared with β_{11} and β_{33}, which reflects, probably the lack of the experimental data. Our unit cell parameters (Table 1) only approximately match those previously published[25-26] with the largest difference being 0.09 Å. This is a first electron density investigation of a molecule belonging to the class of estrogens, to the best of our knowledge. The molecule is rather large and the space group $P2_12_12_1$ is non-centrosymmetric. This created some problems in the least-squares refinement due to the high correlations between the refined parameters and the possible wrong reflection phases. The applied chemical and symmetry constraints on the atomic multipole parameters (see above) allowed us to solve this problem[20] and get the reasonable results reported herein.

The atomic charges calculated as a difference between the actual monopole population number and the number of outer shell electrons in the neutral atoms are reported in Table 2. They all look reasonable, being negative for the oxygens, positive for the carbons next to the oxygens, negative for the carbons in the aromatic ring and positive for all hydrogens. At the same time, these numbers are far from the formal charges one could expect (for example, +1 for hydrogen atom), which, generally is not a surprise for a covalent crystal. These charges are consistent with those for other organic molecules obtained by multipole analysis[27-28].

The residual electron density (the difference between the experimental ED and the calculated aspherical multipole ED) map in the aromatic ring plane is presented in Fig.2. This map, as well as the maps in the other planes (not presented in this paper), does not contain any feature greater than ± 0.1 eÅ^{-3}, which can be considered as a random noise. This is one of the indications of the quality of the experimental data and least-squares fitting of the model. Fig.3. contains the model deformation electron density (DED) maps, which is a difference between the calculated multipole (aspherical) ED and the calculated ED of neutral spherical atoms at the same positions in the crystal. Each expected chemical bond (in the plane of the map) is represented by a well-shaped DED peak, though the both lone pairs of O1 (Fig.3a) and one of the O2 atoms (Fig.3b) are shifted from the plane. A slightly negative region was found inside the aromatic ring. The polarization of the DED on the H1A-O1 bond towards O1 atom is evident when comparing to the DED on the H1-C1, H2-C2 and H4-C4 bonds. This also could be expected[29] since the H1A atom is involved in the hydrogen bonding with the O2 atom of the neighboring molecule (Fig.1b).

The electrostatic potential isosurfaces of the isolated estrone molecule taken from the crystal are shown in Fig.4. The positive isosurface of 0.5 eÅ^{-1} repeats the shape of the estrone molecule (green color). The red areas represent the negative isosurface of –0.2 eÅ^{-1} (Fig.4a) and of –0.1 eÅ^{-1} (Fig.4b). The negative regions are located around both oxygen atoms, smaller for the O1 atom bonded to the hydrogen. The O2 ESP negative area is enveloping the H12A atom. There are also considerable negative regions above and below the aromatic ring, where the π- electrons are expected to be. Tiny negative ESP regions were found inside the aromatic, C(5)-C(7)-C(10) and C(8)-C(12)-C(14) rings. Their existence could be caused by the chosen hydrogen κ- set[30] (κ'=1.2 and κ''=1.0), not refined in this work. All these negative ESP areas represent the sites of possible electrophilic attack or the sites which match electropositive regions of the estrogen receptor during the activated complex formation.

The topological analysis[11] gives us a more complete view of the chemical bonding in the crystals. Fig.5 contains the Laplacian map in the aromatic ring plane. It was calculated for the cluster of 6 neighboring molecules to include the hydrogen bonding. The Laplacian is an important function of ED, defined as[24]

$$\nabla^2\rho(\mathbf{r})=\partial^2\rho(\mathbf{r})/\partial x^2 + \partial^2\rho(\mathbf{r})/\partial y^2 + \partial^2\rho(\mathbf{r})/\partial z^2. \qquad (3)$$

It is invariant under a rotation of the coordinate system, and it is equal to the trace of the Hessian matrix **H(r)** with elements $\partial^2\rho/\partial x_i\partial x_j$. The Laplacian is also reference-state independent, it characterizes the actual concentration (negative values) and depletion (positive values) of electrons in the crystal. In Fig.5 the contours with the same **negative** Laplacian values are shown as the solid contours to make it analogous to the DED distribution maps. For all the carbons the concentration of electrons is mainly around the atoms and along the chemical bonds, though for the hydrogens it is almost spherical. The local ED depletions along the chemical bonds and the contractions in the perpendicular directions indicates the positions of the bond critical points. For the oxygens this concentrations is also in the non-bonding directions, which is a quite common[31-33] and associated with lone pairs. Some ED depletion areas are found inside the aromatic ring and around it.

The positions of the critical points of the ED and their characteristics contain a lot of information about the character of the chemical bonding in the crystal. Table 3 presents the bond (3,-1) CP's found in the estrone molecule and the one belonging to the hydrogen bond. The Table contains the values of the ED ρ and Laplacian $\nabla^2\rho$ at each CP, eigenvalues λ_1, λ_2, λ_3, interatomic distances R_{ij} and the distances from the CP to the bonding atoms d_1 and d_2. As it might be expected, the ED values at the CP on the double bond O(2)-C(17) and on the aromatic ring bonds are generally higher than those for the single bonds. The ED value at the O(1)-H(1A) of 2.07 $e\text{Å}^{-3}$ is also high compared to the C-H bonds. The polarization of C-O, O-H and C-H bonds is also evident, since the CP is located much closer to the more electropositive atom, i.e. electrons are shifted towards the more electronegative atom. The C-C bonds are less polarized. A quite short hydrogen bond (1.852 Å) contains values of the ρ and $\nabla^2\rho$[33] considered typical for strong bonds. Therefore, the hydrogen bonding in the estrone crystal can not be considered as a weak one, as it was supposed by Busetta et al.[26]

Conclusion

We have performed a low-temperature X-ray diffraction investigation of the electron density and related properties of the estrone crystal. The molecular electrostatic potential exhibits the negative regions around both oxygen atoms, more narrow for the O atom bonded to hydrogen. There are also significant negative regions above and below the aromatic ring. The quantitative comparison of these regions as well as the atomic charges and the dipole moments between different estrogens with different biological activities would be necessary information for the intelligent design of new drugs. This will be the task of our future work.

Acknowledgement

We appreciate the financial support of the US Army through grant number DAMD17-99-1-9408.

References

(1) Wakeling, A.E.; Bowler, J. J.Eddocrinol., **1987**, 112, R7-R10.

(2) Davis, M.D.; Butler, W.B.; Brooks, S.C. J. Steroid Biochem.Molec.Biol., **1995**, 52, 421-430.

(3) Vander Kuur, J.A.; Wiese, T.; Brooks, S.C. Biochemistry, 1993, **32**, 7002-7008.

(4) Pilat, M.J.; Hafner, M.S.; Kral, L.G.; Brooks, S.C. Biochemistry, 1993, **32**, 7009-7015.

(5) Vander Kuur, J.A.; Hafner, M.S.; Christman, J.K.; Brooks, S.C. Biochemistry, 1993, **32**, 7016-7021.

(6) Adams, J.; Garcia, M.; Rochefort, H. Cancer Res., 1981, **41**, 4720-4726.

(7) Borman, S. Chem.& Eng.News, 1995, **73**, 29-29.

(8) Hansen, N.; Coppens, P. Acta Cryst. 1974, **A34**, 909-921.

(9) Koritsanszky, T.; Howard, S.; Mallison, P.R.; Su, Z.; Ritcher, T.; Hansen, N.K. *XD. A computer Program Package for Multipole Refinement and Analysis of Electron Densities from Diffraction Data. User's Manual.* University of Berlin, Germany, 1995.

(10) Su, Z.; Coppens, P. Acta Cryst., 1992, **A48**, 188-197.

(11) Bader, R.F.W. *Atoms in Molecules: A Quantum Theory*. The International Series of Monographs of Chemistry, 1990, ed. by J.Halpen & M.L.H.Green. Oxford: Clarendon Press, p.1-438.

(12) Tsirelson, V.; Ivanov, Yu.; Zhurova, E.; Zhurov, V.; Tanaka, K. Acta Cryst., 2000, **B56**, 197-203.

(13) Bader, R.F.W.; Essen, H. J. Chem. Phys.,1984, **80**, 1943-1960.

(14) Bader, R.W.F. J.Phys. Chem., 1998, **A102**, 7314-7323.

(15) Siemens. *SAINT. Program to Integrate and Reduce Raw Crystallographic Area Detector Data,* 1996, Siemens Analytical X-ray Instruments Inc., Madison, Wisconsin, USA.

(16) Sheldrick, G.M. SADABS, 1996, Univ. of Göttingen.

(17) Blessing, R., SORTAV '99, 1999, Hauptman-Woodward Institute, USA.

(18) Sheldrick, G.M. *SHELXTL Vers.5.1. An Integrated System for Solving, Refining and Displaying Crystal Structures from Diffraction Data*, Univ. of Göttingen: Germany, 1997.

(19) Clementi, E.; Roetti, C. Atomic Data and Nuclear data Tables, 1974, **14,** 177-478.

(20) Haouzi, A.E.; Hansen, N.K.; Henaff C.L.; Protas, J. Acta Cryst., 1996, **A52**, 291-301.

(21) International Tables for Crystallography, v.C., Wilson, A.J.C., Ed.; Dordrecht: Kluwer Academic Publishers, 1995, p. 1-992.

(22) Hirshfeld, F.L. Acta Cryst., 1976, **A32**, 239-244.

(23) Coppens, P.; Guru Row, T.N.; Leung, P.; Stevens, E.D.; Becker, P.J.; Yang, Y.W. Acta Cryst., 1979, **A35**, 63-72.

(24) Coppens, P. *X-ray Charge Densities and Chemical Bonding*, 1997. Oxford University Press, p. 1-358.

(25) Vanden Bossche, G. Bull.Soc.R.Sci.Liege, 1971, **40**, 614-627.

(26) Busetta, B.; Courseille, C.; Hospital, M. Acta Cryst., 1973, **B29**, 298-313.

(27) Volkov, A.; Gatti, C.; Abramov, Yu.; Coppens, P. Acta Cryst., 2000, **A56**, 252-258.

(28) Pichon-Pesme, V.; Lachekar, H.; Souhassou, M.; Lecomte, C. Acta Cryst., 2000, **B56**, 728-737.

(29) Krijn, M.P.C.M.; Graafsma, H.; Feil, D. Acta Cryst., 1988, **B44**, 609-616.

(30) Chen, L.; Craven, B.M. Acta Cryst., 1995, **B51**, 1081-1097.

(31) Zhurova, E.A.; Pinkerton, A.A. (2001) Acta Cryst., **B57**, 359-365.

(32) Chen, Yu.Sh.; Pinkerton, A.A. In preparation. 2000.

(33) Flaig, R.; Koritsanszky, T.; Zobel, D.; Luger, P. J.AmChem.Soc. 1998, **120**, 2227-2238.

(34) Espinosa, E.; Souhassou, M; Lachekar, H.; Lecomte, C. Acta Cryst., 1999, **B55**, 563-572.

Table 1. Experimental

Compound name:	estrone
Chemical formula:	$C_{18}H_{22}O_2$
Chemical formula weight:	270.36
Crystal density:	1.263
Crystal size, mm	0.2×0.25×0.30
μ, mm^{-1}	0.05
Unit cell parameters:	
a (Å)	7.7618(1)
b (Å)	9.9536(1)
c (Å)	18.4055(1)
V (Å)	1421.97(2)
Z	4
F(000)	584
Space group	$P2_12_12_1$
Temperature:	92.0(2)
Radiation(Å):	Ag K_α (λ=0.56086 Å)
h_{min}/h_{max}	-20/20
k_{min}/k_{max}	-26/25
l_{min}/l_{max}	-48/48
$\theta_{min}/\theta_{max}$	1.75/48.26
Intensity decay	0 %
Total No. of reflections	119720
No. of independent reflections	25945
R_{int}	0.0478
No. of reflections used	8384
Criterion	$I>2\sigma$ for $\sin\theta/\lambda \leq 0.7$ $Å^{-1}$
	$I>6\sigma$ for $\sin\theta/\lambda > 0.7$ $Å^{-1}$
Refinement on	F
Total No. of parameters	810

Weighting scheme	$w=1/\sigma^2$
Multipole refinement:	
R	0.0224
R_w	0.0149
S	0.62
κ- refinement:	
R	0.0445
R_w	0.0611
S	1.54

Table 2. Estrone: atomic charges and κ' parameters

Atom	O(1)	O(2)	C(1)	C(2)	C(3)	C(4)	C(5)	C(6)	C(7)	C(8)	C(9)
q, e	-0.546(8)	-0.390(8)	-0.41(1)	-0.45(1)	+0.33(1)	-0.44(1)	-0.19(1)	-0.33(1)	-0.42(1)	-0.14(1)	-0.11(1)
κ'	0.953(1)	0.954(1)	0.941(2)	0.941(2)	0.992(4)	0.941(2)	0.960(3)	0.977(1)	0.977(1)	0.977(1)	0.977(1)

Table 2 (continued)

Atom	C(10)	C(11)	C(12)	C(13)	C(14)	C(15)	C(16)	C(17)	C(18)	H(1A)	H(1)
q, e	-0.19(1)	-0.43(1)	-0.42(1)	+0.01(1)	-0.11(1)	-0.33(1)	-0.44(1)	+0.17(1)	-0.56(1)	+0.422(8)	+0.206(8)
κ'	0.960(3)	0.977(1)	0.977(1)	0.977(1)	0.977(1)	0.977(1)	0.977(1)	0.991(4)	0.977(1)	1.2	1.2

Table 2 (continued)

Atom	H(2)	H(4)	H(6A)	H(6B)	H(7A)	H(7B)	H(8)	H(9)	H(11A)	H(11B)
q, e	+0.244(8)	+0.311(8)	+0.318(6)	+0.318(6)	+0.272 (6)	+0.272(6)	+0.215(8)	+0.192(8)	+0.212(6)	+0.212(6)
κ'	1.2	1.2	1.2	1.2	1.2	1.2	1.2	1.2	1.2	1.2

Table 2 (continued)

Atom	H(12A)	H(12B)	H(14)	H(15A)	H(15B)	H(16A)	H(16B)	H(18A)	H(18B)	H(18C)
q, e	+0.141(6)	+0.141(6)	+0.205(8)	+0.245(6)	+0.245(6)	+0.216(6)	+0.216(6)	+0.254(5)	+0.254(5)	+0.254(5)
κ'	1.2	1.2	1.2	1.2	1.2	1.2	1.2	1.2	1.2	1.2

Table 3. The properties of bond critical points in estrone.

Bond	ρ, eÅ^{-3}	$\nabla^2\rho$, eÅ^{-5}	λ_1	λ_2	λ_3	R_{ij}, Å	d_1, Å	d_2, Å
O(1)-C(3)	2.29(1)	-27.09(5)	-19.40	-17.54	9.85	1.367	0.837	0.530
O(2)-C(17)	2.90(1)	-7.59(7)	-27.48	-23.91	43.80	1.228	0.821	0.407
C(1)-C(2)	2.319(8)	-24.06(3)	-15.03	-14.71	5.68	1.395	0.702	0.693
C(1)-C(10)	2.32(1)	-25.74(3)	-16.63	-15.23	6.12	1.404	0.706	0.698
C(2)-C(3)	2.32(1)	-25.93(3)	-17.40	-14.74	6.21	1.399	0.738	0.661
C(3)-C(4)	2.34(1)	-24.62(4)	-17.09	-14.03	6.50	1.397	0.644	0.753
C(4)-C(5)	2.26(1)	-23.07(1)	-15.00	-13.77	5.70	1.404	0.628	0.776
C(5)-C(10)	2.17(1)	-21.01(4)	-14.94	-13.32	7.25	1.412	0.673	0.739
C(5)-C(6)	1.84(1)	-14.87(3)	-12.23	-11.34	8.70	1.518	0.772	0.746
C(6)-C(7)	1.695(8)	-11.08(2)	-10.61	-9.75	9.28	1.531	0.786	0.745
C(7)-C(8)	1.704(8)	-11.90(2)	-10.58	-10.12	8.80	1.528	0.801	0.727
C(8)-C(9)	1.688(9)	-11.64(3)	-10.85	-9.68	8.89	1.547	0.743	0.804
C(8)-C(14)	1.852(9)	-16.38(3)	-12.84	-11.96	8.43	1.526	0.780	0.746
C(9)-C(10)	1.76(1)	-15.18(3)	-11.85	-11.64	8.31	1.528	0.702	0.825
C(9)-C(11)	1.660(9)	-11.24(3)	-10.65	-9.73	9.14	1.541	0.753	0.788
C(11)-C(12)	1.672(9)	-11.25(3)	-10.50	-10.05	9.30	1.546	0.758	0.788
C(12)-C(13)	1.780(9)	-14.79(3)	-12.11	-11.19	8.51	1.528	0.792	0.736
C(13)-C(14)	1.70(1)	-13.63(3)	-11.03	-10.75	8.16	1.545	0.756	0.789
C(13)-C(17)	1.82(1)	-14.34(4)	-12.17	-11.49	9.32	1.518	0.780	0.738
C(13)-C(18)	1.722(9)	-14.30(3)	-11.64	-11.04	8.39	1.546	0.731	0.815
C(14)-C(15)	1.705(9)	-12.56(3)	-11.29	-10.26	8.99	1.540	0.767	0.773
C(15)-C(16)	1.667(9)	-10.27(3)	-10.23	-9.76	9.71	1.549	0.754	0.795
C(16)-C(17)	1.80(1)	-13.92(3)	-12.03	-11.72	9.88	1.528	0.766	0.762
O(1)-H(1A)	2.07(1)	-39.73(3)	-39.34	-38.20	37.81	0.967	0.806	0.161
C(1)-H(1)	1.844(6)	-18.39(2)	-16.35	-15.76	13.73	1.077	0.729	0.348
C(2)-H(2)	1.800(6)	-17.96(2)	-16.62	-14.76	13.42	1.077	0.730	0.347
C(4)-H(4)	1.736(7)	-17.83(2)	-15.99	-14.75	12.91	1.077	0.733	0.344
C(6)-H(6A)	1.713(7)	-18.26(2)	-15.99	-15.18	12.91	1.092	0.744	0.348
C(6)-H(6B)	1.682(8)	-16.91(2)	-15.19	-14.90	13.18	1.092	0.745	0.347
C(7)-H(7A)	1.726(8)	-16.49(2)	-15.72	-14.77	13.99	1.092	0.737	0.355
C(7)-H(7B)	1.723(7)	-16.00(2)	-15.61	-14.89	14.50	1.092	0.743	0.349

C(8)-H(8)	1.686(7)	-15.26(2)	-15.17	-14.63	14.54	1.099	0.745	0.354
C(9)-H(9)	1.746(8)	-15.42(3)	-15.08	-14.73	14.39	1.099	0.726	0.373
C(11)-H(11A)	1.682(7)	-13.85(2)	-14.93	-14.25	15.33	1.092	0.736	0.356
C(11)-H(11B)	1.613(7)	-11.24(2)	-14.34	-13.04	16.14	1.092	0.742	0.350
C(12)-H(12A)	1.779(8)	-15.47(3)	-16.39	-13.97	14.88	1.092	0.715	0.377
C(12)-H(12B)	1.725(8)	-12.49(3)	-14.54	-13.38	15.42	1.092	0.718	0.374
C(14)-H(14)	1.690(8)	-14.04(3)	-15.05	-13.75	14.76	1.099	0.734	0.365
C(15)-H(15A)	1.638(8)	-12.42(2)	-13.78	-13.53	14.88	1.099	0.739	0.360
C(15)-H(15B)	1.648(9)	-12.87(2)	-15.19	-13.46	15.78	1.099	0.752	0.347
C(16)-H(16A)	1.778(8)	-17.11(3)	-16.29	-14.88	14.07	1.092	0.728	0.364
C(16)-H(16B)	1.724(8)	-16.28(3)	-14.96	-14.63	13.31	1.092	0.715	0.377
C(18)-H(18A)	1.725(8)	-14.31(2)	-15.74	-13.94	15.36	1.059	0.708	0.351
C(18)-H(18B)	1.689(8)	-13.34(2)	-14.99	-14.12	15.78	1.059	0.714	0.345
C(18)-H(18C)	1.794(8)	-15.90(2)	-16.98	-14.30	15.38	1.059	0.711	0.348
H(1A)...X2_O(2)	0.204(2)	3.143(2)	-1.33	-1.23	5.71	1.852	0.614	1.238

Figure captions

Fig.1. a- The estrone molecule with 50% probability thermal ellipsoids for non-hydrogen atoms. b- Packing diagram showing the hydrogen bonds.

Fig.2. Residual electron density ($\delta\rho_{resid} = \rho_{exper} - \rho_{mult}$) map in the aromatic ring plane. Contour interval is 0.05 $eÅ^{-3}$. The solid lines show positive $\delta\rho_{resid}$ values, the negative contours are dotted lines, the zero one is dashed.

Fig.3. The multipole model deformation electron density ($\delta\rho_{mult} = \rho_{mult} - \rho_{sph}$) maps: a- in the aromatic ring plane; b- in the O(2), C(17), C(16) plane. Contours are the same as in Fig.2.

Fig.4. Isosurfaces of the electrostatic potential of the isolated estrone molecule taken from the crystal. Green is the surface of 0.5 $eÅ^{-1}$, red is the one of –0.2 $eÅ^{-1}$ (a) and of –0.1 $eÅ^{-1}$ (b).

Fig.5. The Laplacian of the electron density of estrone in the aromatic ring plane. The solid lines show the negative Laplacian values, i.e. they present the accumulation of electrons in the crystal. The contours are: -125, -110, -95, -80, -65, -50, -45, -40, -35, -30, -25, -20, -15, -10, -5 $eÅ^{-5}$ are solid lines; 3, 6, 9, 12, 15, 18, 21, 24, 27, 30 $eÅ^{-5}$ are dotted lines.

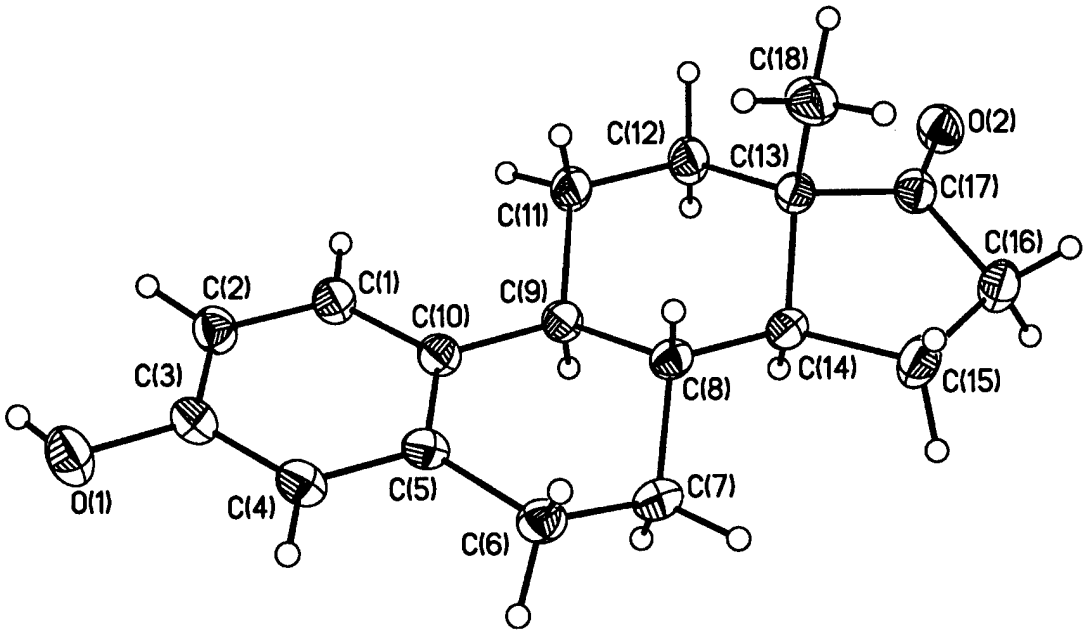

Figure 1a. The estrone molecule with 50% probability thermal ellipsoids for non-hydrogen atoms.

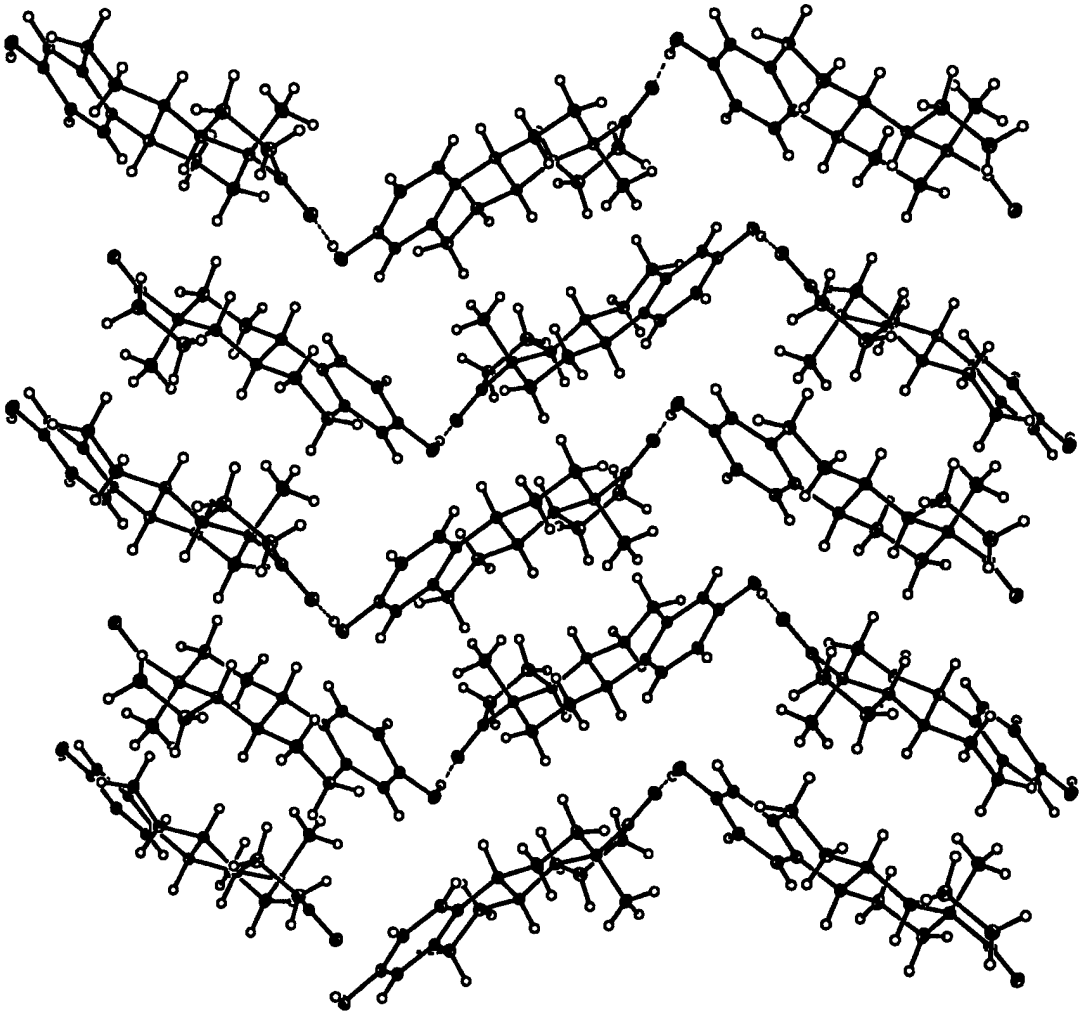

Figure 1b. Packing diagram showing the hydrogen bonds.

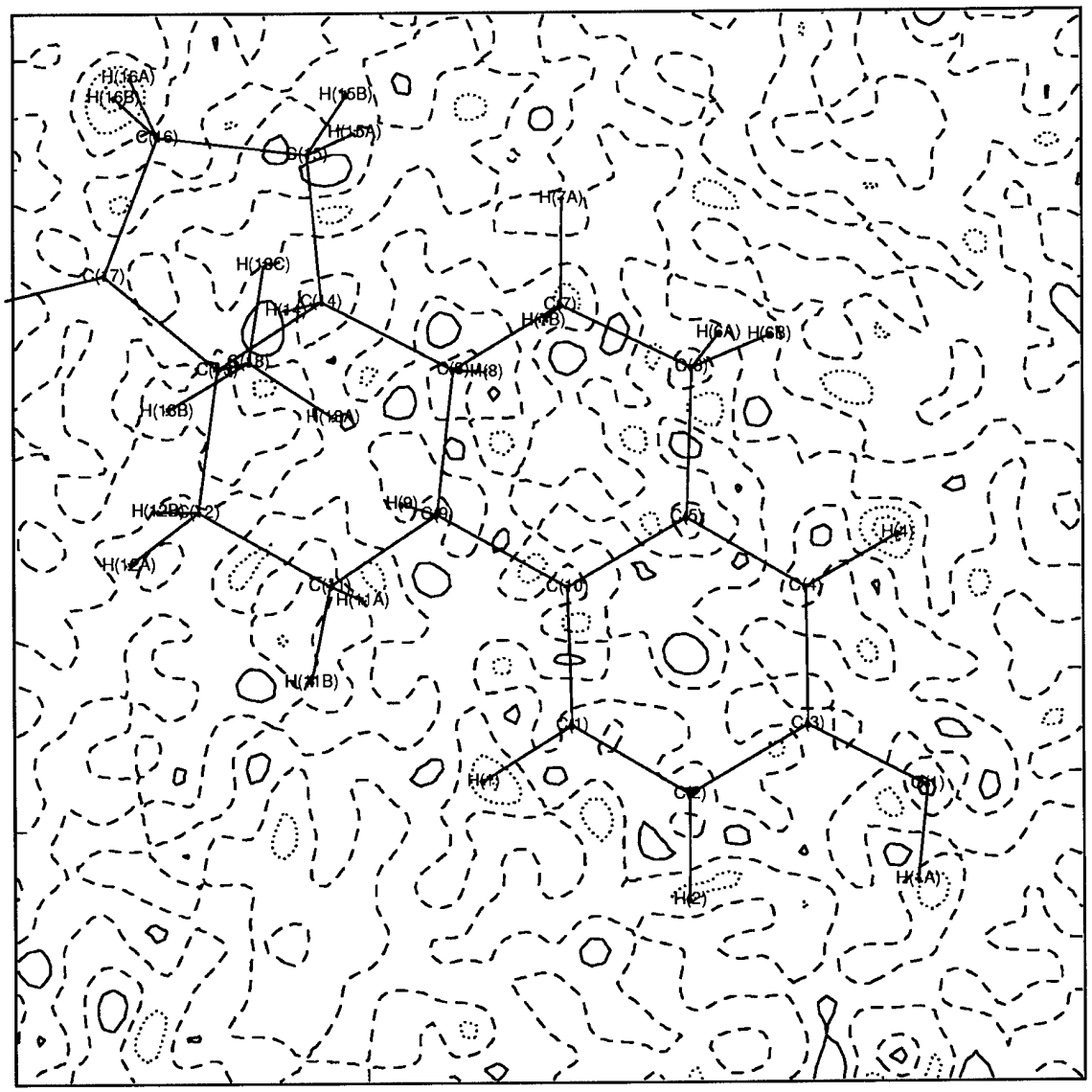

Figure 2. Residual electron density ($\delta\rho_{resid}=\rho_{exper}-\rho_{mult}$) map in the aromatic ring plane. Contour interval is 0.05 eÅ^{-3}. The solid lines show positive values, the negative contours are dashed lines, the zaro one is dashed.

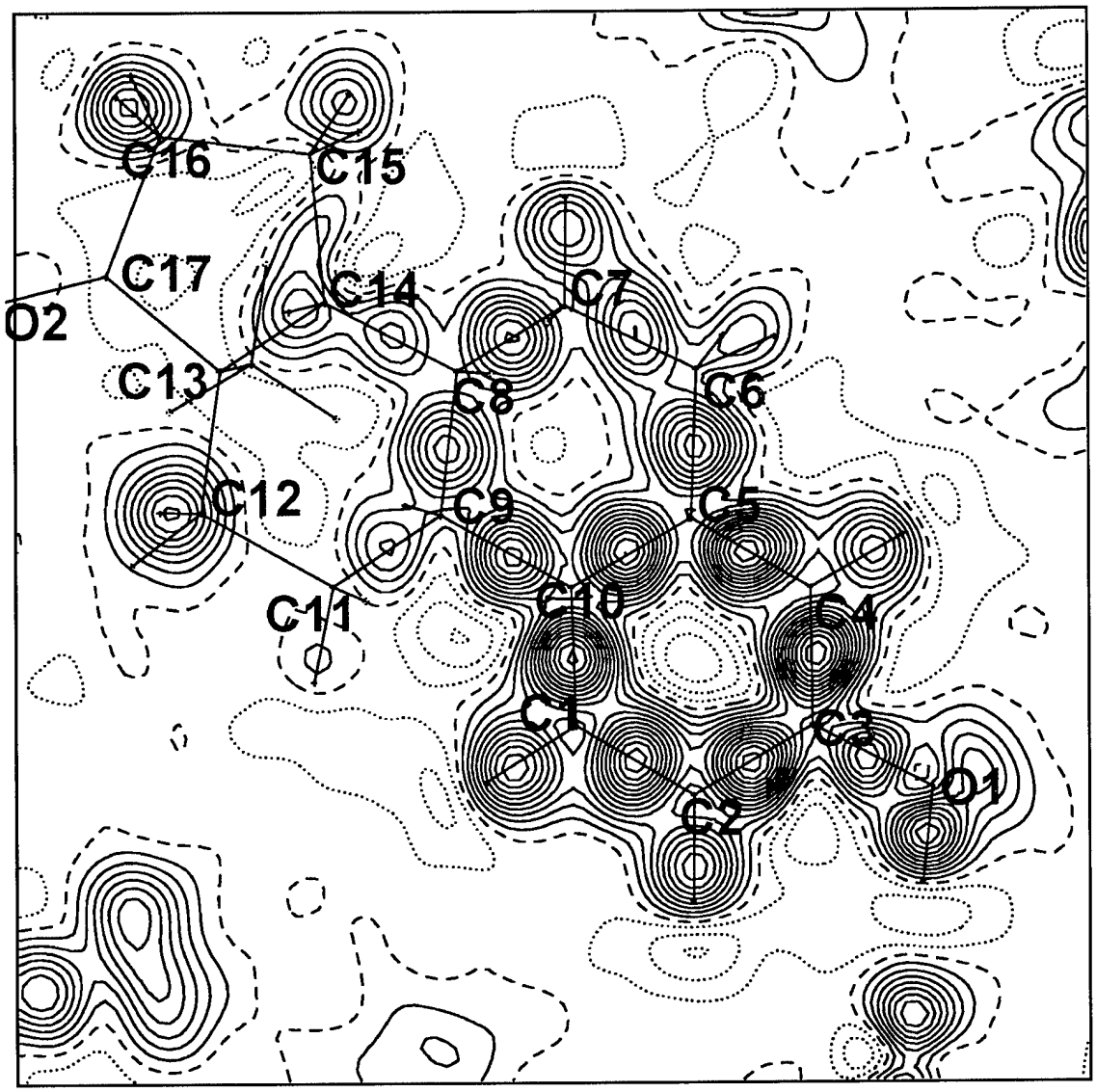

Figure 3a. The multipole deformation electron density ($\delta\rho_{mult}=\rho_{mult}-\rho_{sph}$) map in the aromatic ring plane. Contours are the same as in Fig. 2.

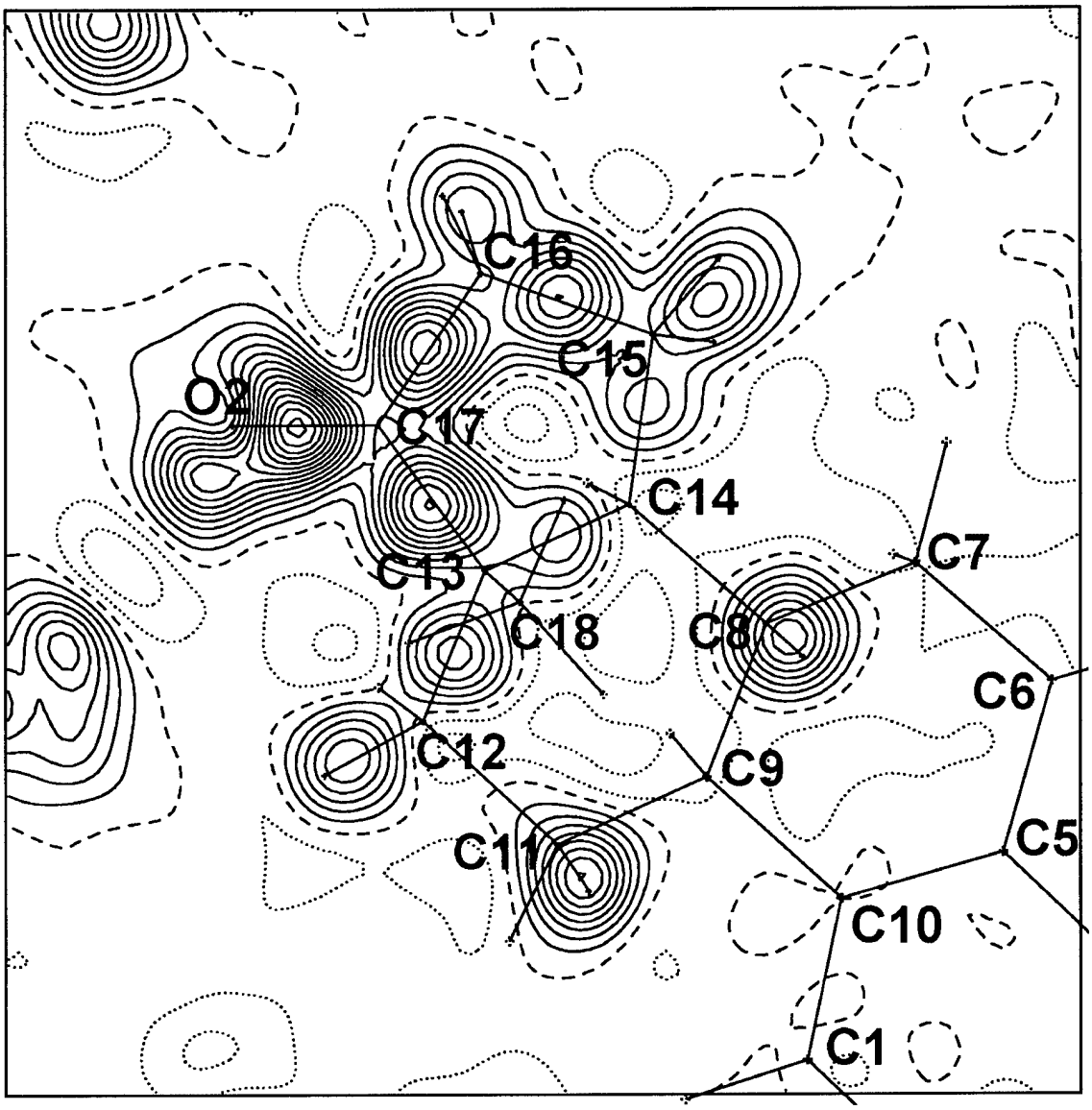

Figure 3b. The multipole deformation electron density ($\delta\rho_{mult}=\rho_{mult}-\rho_{sph}$) map in the O2, C17, C16 plane. Contours are the same as in Fig. 2.

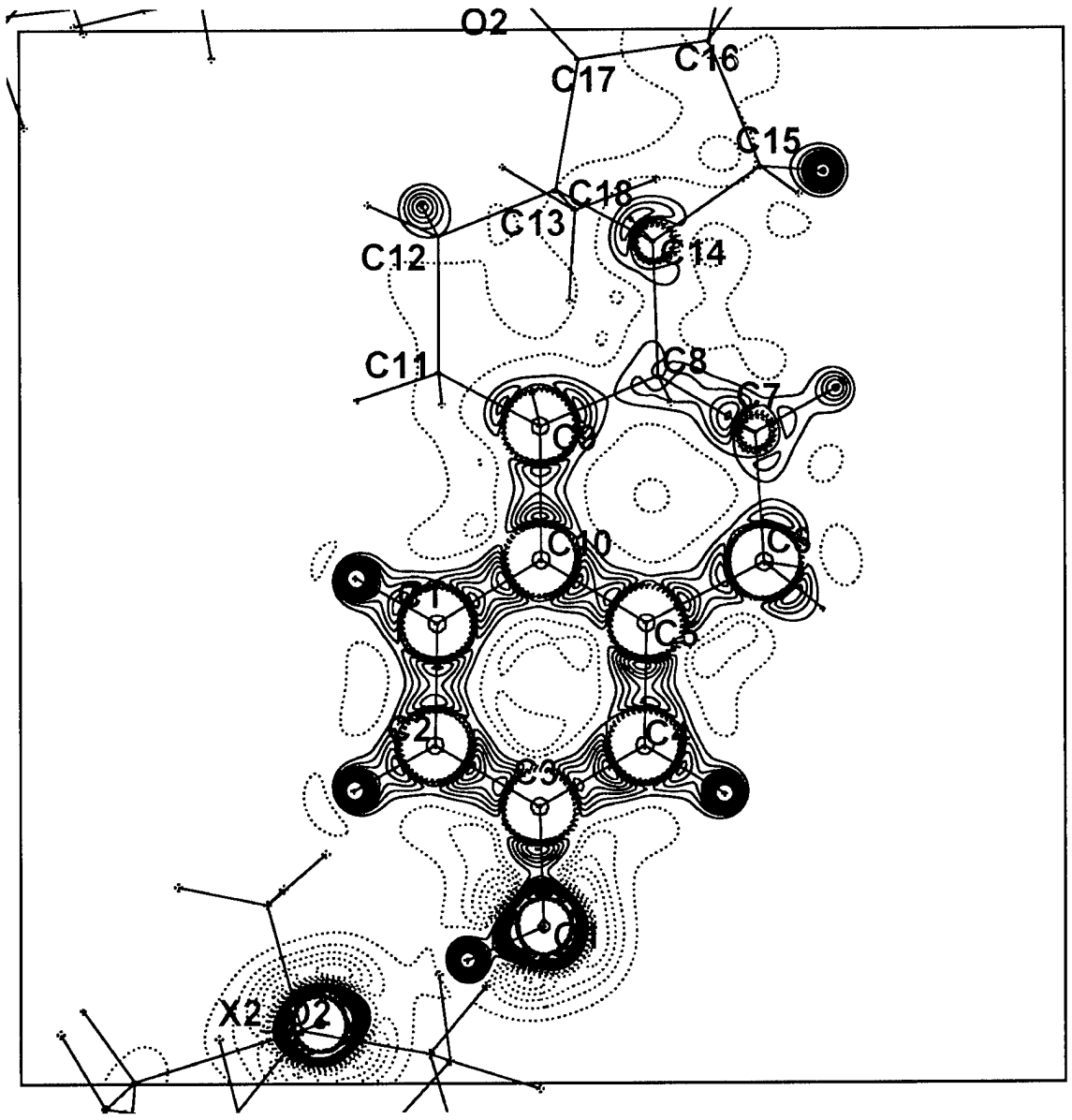

Figure 5. The Laplacian of the electron density of estrone in the aromatic ring plane. The solid lines show the negative Laplacian values, i.e they present the accumulation of electrons in the crystal. The contours are: -125, -110, -95, -80, -65, -50, -45, -40, -35, -30, -25, -20, -15, -10, -5, 3, 6, 9, 12, 15, 18, 21, 24, 27, 30 eA^{-5}.

The deposition material:

Fig.D1.

Table D1.

Table D2.

Figure D1.

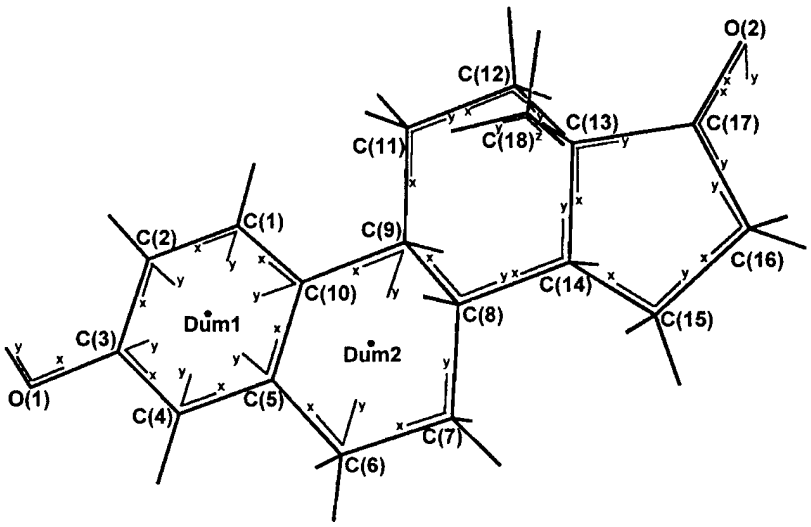

Local coordinate system in estrone

Table D1. The multipole population parameters for non-hydrogen atoms in estrone

Atom	P_v	κ'	κ''	D1+	D1-	D0	Q0	Q1+	Q1-	Q2+	Q2-	O0	O1+	O1-
O(1)	6.524(8)	0.963(1)	0.86(2)	-0.123(8)	0.036(8)				-0.042(9)	-0.070(9)	-0.020(9)			-0.08(1)
O(2)	6.413(8)	0.977(1)	0.79(2)	0.061(8)	-0.073(8)	-0.042(9)	-0.22(1)		-0.02(1)		0.07(1)	-0.01(1)		
C(1)	4.47(1)	0.943(2)	0.774(5)		0.03(2)	-0.07(1)	-0.40(2)							
C(2)	4.48(1)	0.943(2)	0.774(5)	0.02(1)			-0.39(2)		0.01(1)	0.06(1)	-0.01(1)		-0.06(2)	
C(3)	3.68(1)	0.990(4)	0.82(1)		0.03(2)		-0.18(2)	0.01(1)			0.03(2)	-0.05(2)	0.15(2)	0.12(2)
C(4)	4.46(1)	0.943(2)	0.774(5)	-0.15(2)		-0.03(1)	-0.40(2)		-0.09(1)		-0.17(2)	0.04(2)	0.14(3)	-0.12(2)
C(5)	4.20(1)	0.961(3)	0.836(7)		0.09(2)	-0.02(1)	-0.25(2)	-0.03(1)		-0.08(2)	-0.06(2)		0.02(2)	-0.05(2)
C(6)	4.33(1)	0.969(1)	0.800(3)	-0.04(1)			-0.06(1)		-0.05(1)	-0.06(1)		0.21(2)	-0.10(2)	-0.33(2)
C(7)	4.41(1)	0.969(1)	0.800(3)	-0.08(1)	-0.07(1)	-0.02(1)	0.02(1)	0.07(1)	-0.03(1)	-0.07(2)			-0.17(2)	-0.26(2)
C(8)	4.16(1)	0.969(1)	0.800(3)	0.05(2)		0.05(2)		-0.06(2)	-0.09(2)	-0.07(2)	0.03(2)	0.04(2)	-0.15(2)	-0.28(2)
C(9)	4.15(1)	0.969(1)	0.800(3)	-0.16(2)	-0.01(1)	-0.11(2)	-0.03(2)	0.05(2)	0.08(1)	-0.04(2)	-0.02(2)	-0.28(2)		-0.17(2)
C(10)	4.20(1)	0.961(3)	0.836(7)	-0.03(2)	0.03(2)	0.06(2)	-0.29(1)		0.05(1)			-0.02(2)		-0.04(2)
C(11)	4.45(1)	0.969(1)	0.800(3)	-0.05(2)	-0.05(2)	0.04(2)		0.04(2)			0.12(2)		-0.21(2)	-0.21(2)
C(12)	4.48(1)	0.969(1)	0.800(3)	-0.06(2)	-0.07(2)	-0.06(2)	-0.08(2)		-0.03(2)	-0.06(2)	0.07(2)	-0.05(2)	-0.20(2)	-0.25(2)
C(13)	3.97(1)	0.969(1)	0.800(3)	0.06(2)	0.12(2)	-0.04(2)	-0.02(2)	0.04(2)		-0.11(2)		0.08(3)	-0.20(2)	-0.29(2)
C(14)	4.14(1)	0.969(1)	0.800(3)	-0.10(2)	-0.04(2)	-0.03(2)		0.07(2)		0.05(2)	0.02(2)	-0.11(2)	-0.17(2)	-0.31(2)
C(15)	4.38(1)	0.969(1)	0.800(3)	-0.11(2)	-0.13(2)	0.06(2)	-0.06(2)	0.08(2)	0.03(2)		0.13(2)	0.05(2)	-0.18(2)	-0.19(2)
C(16)	4.49(1)	0.969(1)	0.800(3)		-0.04(2)	0.03(2)	-0.13(2)	0.03(2)	-0.04(2)	-0.05(1)	0.07(2)	-0.07(2)	-0.21(2)	-0.25(2)
C(17)	3.88(1)	1.000(4)	0.86(1)	0.07(1)			-0.20(1)	-0.02(1)		0.11(2)	-0.06(2)	-0.04(2)		0.05(2)
C(18)	4.55(1)	0.969(1)	0.800(3)	0.02(1)	-0.02(1)	-0.13(1)	0.04(2)	0.05(2)	0.07(2)	-0.02(2)	-0.04(1)	0.51(2)	0.10(2)	0.04(2)

Table D1. (continued)

Atom	O2+	O2-	O3+	O3-	H0	H1+	H1-	H2+	H2-	H3+	H3-	H4+	H4-
O(1)	-0.03(1)		0.09(1)	-0.04(1)		0.05(2)				0.04(2)		0.04(1)	0.05(1)
O(2)	0.02(1)		0.06(1)		0.05(2)			0.01(1)	-0.05(2+	-0.03(2)			-0.05(1)
C(1)		0.07(2)	0.42(2)	0.07(2)	0.11(2)		0.02(2)	-0.05(2)		-0.10(3)	0.09(2)		
C(2)			0.45(2)		0.08(2)	-0.06(2)	0.05(2)	-0.06(2)	0.09(2)	-0.04(3)	0.13(2)		-0.04(2)
C(3)	0.06(2)	0.07(2)	0.51(2)				0.05(2)	0.13(2)	-0.02(2)	0.05(2)		-0.04(3)	
C(4)			0.40(2)		0.17(3)	0.06(2)		0.12(3)	0.14(3)		0.11(2)	-0.13(3)	-0.09(2)
C(5)			0.44(2)	-0.12(2)	0.03(2)		-0.04(2)	0.09(3)	0.10(2)	-0.06(2)			0.04(2)
C(6)	0.08(2)	0.12(2)	0.03(2)	0.30(2)	0.12(2)	-0.01(2)	-0.09(2)	-0.18(2)	-0.04(2)	0.06(2)			
C(7)			0.32(2)	-0.15(2)			-0.03(2)		0.22(3)	0.02(2)			
C(8)	0.06(2)		0.26(2)	-0.15(2)	0.05(3)	-0.10(3)		0.11(3)	0.18(3)	0.07(3)		0.17(3)	0.09(3)
C(9)	-0.06(2)	-0.13(2)		0.27(2)	0.18(3)	0.05(2)	0.08(2)	-0.05(3)	-0.08(2)	-0.06(2)	0.08(3)	-0.03(3)	0.07(3)
C(10)		-0.04(2)	0.42(2)	-0.03(2)	0.18(2)	-0.08(2)			-0.03(3)	0.06(3)		0.07(3)	-0.06(3)
C(11)	0.03(2)		0.29(2)	-0.08(2)		-0.12(2)	-0.10(2)	-0.08(3)	0.04(3)		0.04(3)	-0.05(2)	
C(12)	0.02(2)		0.34(2)	-0.08(2)	0.14(2)	-0.03(2)	-0.03(2)		0.10(3)	0.17(2)	-0.09(3)	0.07(2)	
C(13)			0.22(2)	-0.13(2)	0.14(3)	-0.09(3)	-0.04(3)		0.19(3)	-0.12(3)	0.03(3)	0.09(3)	
C(14)	0.06(2)	0.06(2)	0.27(2)	-0.19(2)	0.07(3)	-0.05(3)	0.05(3)	-0.10(3)	0.15(3)	0.19(3)	-0.11(3)	-0.06(2)	0.11(3)
C(15)	0.13(2)	0.05(2)	0.26(2)	-0.18(2)		-0.03(3)	-0.12(2)	0.05(2)		-0.08(3)	0.21(3)	-0.05(3)	
C(16)	0.03(2)	0.07(2)	0.29(2)	-0.07(2)	0.06(2)		0.11(2)	0.02(2)	0.25(3)	0.07(2)			0.04(2)
C(17)	0.03(2)	-0.02(2)	0.37(2)		-0.03(2)		0.02(2)	0.03(3)	0.04(3)	0.11(2)			
C(18)	-0.10(2)		0.12(2)		0.02(2)		-0.02(2)	0.11(2)	-0.04(2)	-0.07(2)		-0.04(2)	

Table D2. The multipole population parameters for hydrogen atoms in estrone

Atom	H(1A)	H(1)	H(2)	H(4)	H(6A)	H(6B)	H(7A)	H(7B)	H(8)	H(9)	H(11A)
P_v	0.574(8)	0.729(8)	0.702(8)	0.664(8)	0.658(6)	0.658(6)	0.716(6)	0.716(6)	0.729(8)	0.800(8)	0.756(6)
κ'	1.2	1.2	1.2	1.2	1.2	1.2	1.2	1.2	1.2	1.2	1.2
κ''	1.0	1.0	1.0	1.0	1.0	1.0	1.0	1.0	1.0	1.0	1.0
D1+	0.10(1)	0.20(1)	0.21(1)	0.18(1)	0.190(7)	0.190(7)	0.156(8)	0.156(8)	0.12(1)	0.15(1)	0.097(8)

Table D2. (continued)

Atom	H(11B)	H(12A)	H(12B)	H(14)	H(15A)	H(15B)	H(16A)	H(16B)	H(18A)	H(18B)	H(18C)
P_v	0.756(6)	0.835(6)	0.835(6)	0.777(8)	0.741(6)	0.741(6)	0.757(6)	0.757(6)	0.762(5)	0.762(5)	0.762(5)
κ'	1.2	1.2	1.2	1.2	1.2	1.2	1.2	1.2	1.2	1.2	1.2
κ''	1.0	1.0	1.0	1.0	1.0	1.0	1.0	1.0	1.0	1.0	1.0
D1+	0.097(8)	0.149(9)	0.149(9)	0.12(1)	0.15(1)	0.15(1)	0.198(8)	0.198(8)	0.140(7)	0.140(7)	0.140(7)

Appendix D.

Crystal structure of 4-Hydroxyestradiol

Table 1. Crystal data and Experimental details

Crystal Data	
Empirical formula	$C_{18}H_{24}O_3$
Formula weight	288.37
Temperature	120 K
Crystal system	Monoclinic
Space group	$P2_1$
Unit cell dimensions	
	a = 5.651(1)Å
	β = 107.394(3)°
	b = 19.169(3)Å
	c = 6.980(1)Å
Volume, Z	721.5(2)Å^3 ,2
Density (calculated)	1.327 Mg/m^3
Absorption coefficient	0.089 mm^{-1}
F(000)	312
Crystal size	0.35x 0.3 x 0.21 mm
Crystal color	Pale yellow
Data Collection	
Diffractometer	Brukers' SMART 1K CCD
Radiation, Wavelength	Mo Kα , λ=0.71073 Å
Scan method	ω-scan, Scan width= 0.3°
Crystal-Detector distance	4.53cm
θ_{max} for data collection	25.37°
HKL Limiting indices	-6 ← h ←6, -22 ← k ← 22,
	-8 ← l ←7
R_{int}	0.031
Unique Data	2530
Refinement	
No. of Reflections	2340 [$F_o > 4\sigma(F_o)$]
R	0.044

wR	0.10
S (Goodness-of-fit)	1.11
No. of parameters refined	286
$(Shift/esd)_{max}$	0.001
$\Delta\rho_{max}/\Delta\rho_{min}$	0.18/-0.24 $eÅ^{-3}$

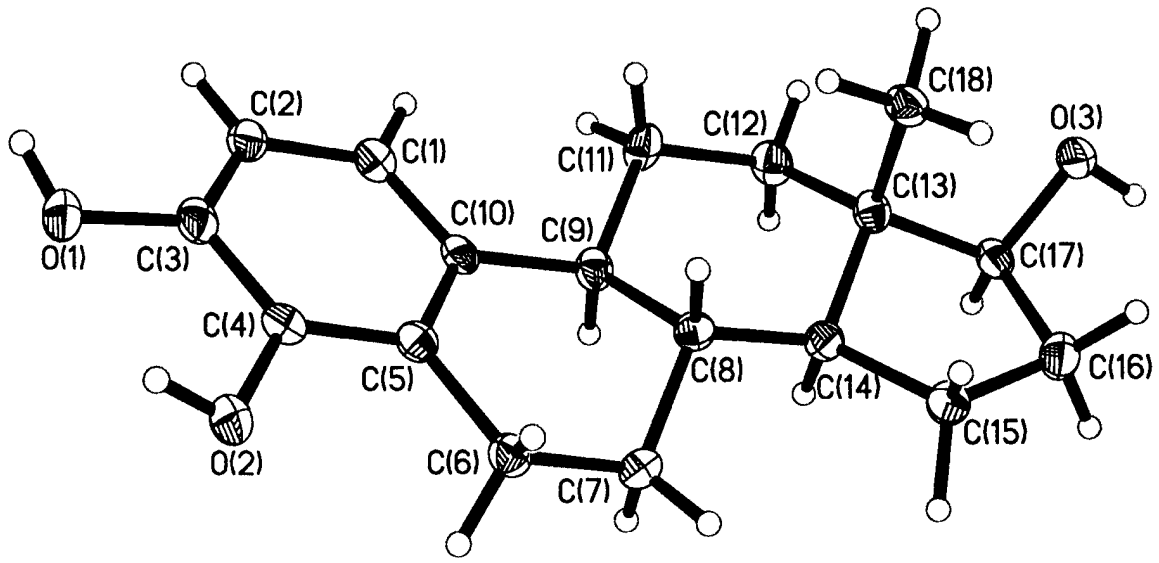

Figure 1. ORTEP view of 4-Hydroxyestradiol showing 50% probability thermal ellipsoids.

Table 2. Fractional atomic coordinates ($x10^{-4}$) and equivalent isotropic displacement Parameters ($Å^2x10^3$).

Atom	x	y	z	U(eq)
O(1)	5626(4)	826(1)	1077(3)	24(1)
O(2)	6651(3)	276(1)	4721(3)	22(1)
O(3)	-4509(3)	-3830(1)	2856(3)	22(1)
C(1)	339(5)	-384(1)	362(4)	20(1)
C(2)	1866(5)	117(1)	-122(4)	20(1)
C(3)	3992(5)	330(1)	1324(4)	20(1)
C(4)	4551(5)	43(1)	3244(4)	18(1)
C(5)	3066(5)	-457(1)	3750(4)	18(1)
C(6)	3879(5)	-762(1)	5854(4)	19(1)
C(7)	1970(5)	-1253(1)	6276(4)	21(1)
C(8)	769(5)	-1711(1)	4465(4)	17(1)
C(9)	-757(5)	-1241(1)	2745(4)	18(1)
C(10)	900(4)	-680(1)	2258(4)	17(1)
C(11)	-2263(5)	-1657(1)	903(4)	22(1)
C(12)	-3810(5)	-2244(2)	1434(4)	22(1)
C(13)	-2211(4)	-2720(1)	3060(4)	18(1)
C(14)	-888(5)	-2273(1)	4900(4)	18(1)
C(15)	227(5)	-2807(1)	6573(4)	23(1)
C(16)	-1728(5)	-3397(1)	6130(4)	23(1)
C(17)	-3598(5)	-3225(1)	4064(4)	18(1)
C(18)	-399(5)	-3135(1)	2239(4)	21(1)

U_{eq} is defined as one third of the trace of the orthogonalized U_{ij} tesor.

Table 3. Bond lengths(Å)

O(1)-C(3)	1.371(3)
O(1)-H(1A)	0.86(4)
O(2)-C(4)	1.393(3)
O(2)-H(2A)	0.82(4)
O(3)-C(17)	1.436(3)
O(3)-H(3A)	0.90(4)
C(1)-C(10)	1.387(3)
C(1)-C(2)	1.398(4)
C(1)-H(1)	0.98(2)
C(2)-C(3)	1.380(4)
C(2)-H(2)	0.95(3)
C(3)-C(4)	1.395(3)
C(4)-C(5)	1.387(4)
C(5)-C(10)	1.416(3)
C(5)-C(6)	1.518(3)
C(6)-C(7)	1.525(4)
C(6)-H(6B)	0.98(3)
C(6)-H(6A)	1.02(3)
C(7)-C(8)	1.523(4)
C(7)-H(7B)	0.99(3)
C(7)-H(7A)	0.95(3)
C(8)-C(14)	1.517(3)
C(8)-C(9)	1.542(3)
C(8)-H(8)	0.99(3)
C(9)-C(10)	1.530(3)
C(9)-C(11)	1.536(4)
C(9)-H(9)	0.99(3)
C(11)-C(12)	1.536(4)
C(11)-H(11B)	1.00(3)
C(11)-H(11A)	0.95(3)
C(12)-C(13)	1.525(4)
C(12)-H(12A)	0.94(3)
C(12)-H(12B)	0.95(3)
C(13)-C(18)	1.536(4)
C(13)-C(14)	1.539(3)

C(13)-C(17)	1.539(3)
C(14)-C(15)	1.538(4)
C(14)-H(14)	1.00(3)
C(15)-C(16)	1.547(4)
C(15)-H(15A)	0.98(3)
C(15)-H(15B)	1.06(3)
C(16)-C(17)	1.547(3)
C(16)-H(16B)	0.95(3)
C(16)-H(16A)	1.01(3)
C(17)-H(17)	1.00(3)
C(18)-H(18B)	1.01(3)
C(18)-H(18A)	0.98(3)
C(18)-H(18C)	0.97(3)

Bond angles(°)

C(10)-C(1)-C(2)	122.0(2)
C(3)-C(2)-C(1)	119.5(2)
O(1)-C(3)-C(2)	125.8(2)
O(1)-C(3)-C(4)	115.3(2)
C(2)-C(3)-C(4)	118.9(2)
C(5)-C(4)-O(2)	118.6(2)
C(5)-C(4)-C(3)	122.5(2)
O(2)-C(4)-C(3)	118.9(2)
C(4)-C(5)-C(10)	118.5(2)
C(4)-C(5)-C(6)	118.8(2)
C(10)-C(5)-C(6)	122.7(2)
C(5)-C(6)-C(7)	113.4(2)
C(8)-C(7)-C(6)	111.2(2)
C(14)-C(8)-C(7)	113.1(2)
C(14)-C(8)-C(9)	109.6(2)
C(7)-C(8)-C(9)	108.4(2)
C(10)-C(9)-C(11)	113.7(2)
C(10)-C(9)-C(8)	110.3(2)
C(11)-C(9)-C(8)	112.9(2)
C(1)-C(10)-C(5)	118.6(2)
C(1)-C(10)-C(9)	121.3(2)
C(5)-C(10)-C(9)	120.1(2)
C(12)-C(11)-C(9)	113.0(2)
C(13)-C(12)-C(11)	111.4(2)
C(12)-C(13)-C(18)	110.2(2)
C(12)-C(13)-C(14)	108.7(2)
C(18)-C(13)-C(14)	112.8(2)
C(12)-C(13)-C(17)	116.5(2)
C(18)-C(13)-C(17)	109.3(2)
C(14)-C(13)-C(17)	99.0(2)
C(8)-C(14)-C(15)	119.2(2)
C(8)-C(14)-C(13)	113.8(2)
C(15)-C(14)-C(13)	104.5(2)
C(14)-C(15)-C(16)	103.2(2)
C(15)-C(16)-C(17)	106.1(2)

O(3)-C(17)-C(13)	112.5(2)
O(3)-C(17)-C(16)	113.6(2)
C(13)-C(17)-C(16)	105.0(2)
C(3)-O(1)-H(1A)	108(2)
C(4)-O(2)-H(2A)	104(2)
C(17)-O(3)-H(3A)	105(3)
C(10)-C(1)-H(1)	119.1(15)
C(2)-C(1)-H(1)	118.8(15)
C(3)-C(2)-H(2)	120.4(15)
C(1)-C(2)-H(2)	120.2(15)
C(5)-C(6)-H(6B)	108.8(18)
C(7)-C(6)-H(6B)	110.3(18)
C(5)-C(6)-H(6A)	109.3(16)
C(7)-C(6)-H(6A)	110.1(17)
H(6B)-C(6)-H(6A)	104(2)
C(8)-C(7)-H(7B)	111.9(17)
C(6)-C(7)-H(7B)	108.2(17)
C(8)-C(7)-H(7A)	109.4(17)
C(6)-C(7)-H(7A)	112.6(17)
H(7B)-C(7)-H(7A)	103(2)
C(14)-C(8)-H(8)	112.6(15)
C(7)-C(8)-H(8)	107.4(15)
C(9)-C(8)-H(8)	105.3(15)
C(10)-C(9)-H(9)	109.5(14)
C(11)-C(9)-H(9)	106.6(14)
C(8)-C(9)-H(9)	103.3(14)
C(12)-C(11)-H(11B)	114.8(17)
C(9)-C(11)-H(11B)	106.7(16)
C(12)-C(11)-H(11A)	109.0(16)
C(9)-C(11)-H(11A)	110.3(16)
H(11B)-C(11)-H(11A)	103(2)
C(13)-C(12)-H(12A)	112.0(19)
C(11)-C(12)-H(12A)	112.8(18)
C(13)-C(12)-H(12B)	107.3(17)
C(11)-C(12)-H(12B)	112.3(18)
H(12A)-C(12)-H(12B)	101(2)
C(8)-C(14)-H(14)	105.1(15)
C(15)-C(14)-H(14)	108.1(15)

C(13)-C(14)-H(14)	105.3(15)
C(14)-C(15)-H(15A)	111.0(17)
C(16)-C(15)-H(15A)	113.6(18)
C(14)-C(15)-H(15B)	111.0(16)
C(16)-C(15)-H(15B)	115.4(16)
H(15A)-C(15)-H(15B)	103(2)
C(15)-C(16)-H(16B)	110.4(17)
C(17)-C(16)-H(16B)	108.7(16)
C(15)-C(16)-H(16A)	111.1(16)
C(17)-C(16)-H(16A)	109.5(15)
H(16B)-C(16)-H(16A)	111(2)
O(3)-C(17)-H(17)	106.7(14)
C(13)-C(17)-H(17)	109.9(15)
C(16)-C(17)-H(17)	109.1(13)
C(13)-C(18)-H(18B)	110.5(17)
C(13)-C(18)-H(18A)	111.9(16)
H(18B)-C(18)-H(18A)	103(2)
C(13)-C(18)-H(18C)	112.0(15)
H(18B)-C(18)-H(18C)	112(2)
H(18A)-C(18)-H(18C)	107(2)

Table 4. Anisotropic displacement parameters (Å x 10^3) for non hydrogen atoms.

Atom	U11	U22	U33	U23	U13	U12
O(1)	27(1)	20(1)	25(1)	2(1)	9(1)	-7(1)
O(2)	23(1)	19(1)	23(1)	-1(1)	6(1)	-6(1)
O(3)	26(1)	18(1)	22(1)	-2(1)	9(1)	-5(1)
C(1)	19(1)	17(1)	21(1)	-2(1)	4(1)	0(1)
C(2)	25(1)	15(1)	18(1)	2(1)	5(1)	2(1)
C(3)	24(1)	13(1)	27(1)	-1(1)	12(1)	2(1)
C(4)	18(1)	16(1)	18(1)	-4(1)	4(1)	0(1)
C(5)	21(1)	14(1)	20(1)	-1(1)	9(1)	4(1)
C(6)	20(1)	17(1)	18(1)	-1(1)	3(1)	0(1)
C(7)	26(2)	22(1)	16(1)	2(1)	7(1)	-2(1)
C(8)	16(1)	18(1)	16(1)	0(1)	5(1)	1(1)
C(9)	18(1)	16(1)	22(1)	1(1)	8(1)	1(1)
C(10)	20(1)	12(1)	20(1)	-3(1)	7(1)	1(1)
C(11)	21(1)	24(1)	15(1)	6(1)	-4(1)	-5(1)
C(12)	19(1)	22(1)	22(1)	-1(1)	2(1)	-4(1)
C(13)	16(1)	16(1)	21(1)	0(1)	6(1)	-1(1)
C(14)	19(1)	17(1)	18(1)	0(1)	6(1)	1(1)
C(15)	28(2)	21(1)	18(1)	0(1)	3(1)	-5(1)
C(16)	26(1)	20(2)	23(1)	3(1)	6(1)	-2(1)
C(17)	20(1)	15(1)	22(1)	-2(1)	9(1)	-1(1)
C(18)	22(1)	19(1)	22(1)	-4(1)	8(1)	-5(1)

The anisotropic displacement factor exponent takes the form:

$-2\pi^2 [h^2 a^{*2} U_{11} + \ldots + 2hka^*b^* U_{12}]$

Table 5. Hydrogen coordinates (Å x 10^4) and isotropic displacement parameters (Å^2 x 10^3).

Atom	x	y	z	U_{eq}
H(9)	-1980(50)	-1019(13)	3320(40)	13(7)
H(8)	2120(50)	-1905(13)	3990(40)	10(6)
H(12A)	-4740(60)	-2497(16)	300(50)	27(8)
H(18B)	-1320(50)	-3379(17)	950(40)	30(8)
H(16B)	-2590(50)	-3401(15)	7120(40)	20(7)
H(2)	1450(50)	304(14)	-1440(40)	13(6)
H(15A)	1870(60)	-2960(16)	6540(40)	26(8)
H(6B)	4250(60)	-379(17)	6830(50)	29(8)
H(11B)	-1070(50)	-1814(15)	190(40)	19(7)
H(16A)	-930(50)	-3867(17)	6060(40)	22(7)
H(18A)	750(50)	-2827(15)	1820(40)	18(7)
H(11A)	-3330(50)	-1357(15)	-40(40)	14(6)
H(7B)	2810(50)	-1532(16)	7480(50)	23(7)
H(6A)	5520(60)	-1013(16)	6080(40)	26(8)
H(7A)	720(50)	-1011(15)	6660(40)	18(7)
H(15B)	610(50)	-2572(16)	8020(50)	31(8)
H(12B)	-5110(60)	-2068(15)	1910(40)	18(7)
H(1)	-1130(50)	-546(13)	-690(40)	11(6)
H(18C)	610(50)	-3455(15)	3230(40)	15(7)
H(1A)	5230(60)	933(17)	-170(50)	35(9)
H(14)	-2240(50)	-2016(14)	5250(40)	16(7)
H(2A)	7460(60)	470(20)	4090(50)	39(10)
H(3A)	-5470(70)	-4060(20)	3490(60)	59(12)
H(17)	-5070(50)	-2987(14)	4270(30)	9(6)

Table 6. Selected torsion angles(°)

C(10)-C(1)-C(2)-C(3)	-0.4(4)
C(1)-C(2)-C(3)-O(1)	-178.5(2)
C(1)-C(2)-C(3)-C(4)	-0.6(4)
O(1)-C(3)-C(4)-C(5)	179.0(2)
C(2)-C(3)-C(4)-C(5)	0.9(4)
O(1)-C(3)-C(4)-O(2)	0.3(3)
C(2)-C(3)-C(4)-O(2)	-177.8(2)
O(2)-C(4)-C(5)-C(10)	178.4(2)
C(3)-C(4)-C(5)-C(10)	-0.2(4)
O(2)-C(4)-C(5)-C(6)	-3.8(3)
C(3)-C(4)-C(5)-C(6)	177.5(2)
C(4)-C(5)-C(6)-C(7)	174.5(2)
C(10)-C(5)-C(6)-C(7)	-7.8(3)
C(5)-C(6)-C(7)-C(8)	40.0(3)
C(6)-C(7)-C(8)-C(14)	172.3(2)
C(6)-C(7)-C(8)-C(9)	-65.9(3)
C(14)-C(8)-C(9)-C(10)	-178.9(2)
C(7)-C(8)-C(9)-C(10)	57.2(3)
C(14)-C(8)-C(9)-C(11)	-50.4(3)
C(7)-C(8)-C(9)-C(11)	-174.3(2)
C(2)-C(1)-C(10)-C(5)	1.1(4)
C(2)-C(1)-C(10)-C(9)	-178.4(2)
C(4)-C(5)-C(10)-C(1)	-0.7(3)
C(6)-C(5)-C(10)-C(1)	-178.4(2)
C(4)-C(5)-C(10)-C(9)	178.7(2)
C(6)-C(5)-C(10)-C(9)	1.1(4)
C(11)-C(9)-C(10)-C(1)	25.5(3)
C(8)-C(9)-C(10)-C(1)	153.5(2)
C(11)-C(9)-C(10)-C(5)	-154.0(2)
C(8)-C(9)-C(10)-C(5)	-26.0(3)
C(10)-C(9)-C(11)-C(12)	177.0(2)
C(8)-C(9)-C(11)-C(12)	50.3(3)
C(9)-C(11)-C(12)-C(13)	-53.4(3)
C(11)-C(12)-C(13)-C(18)	-68.0(3)
C(11)-C(12)-C(13)-C(14)	56.1(3)
C(11)-C(12)-C(13)-C(17)	166.8(2)

C(7)-C(8)-C(14)-C(15)	-58.7(3)
C(9)-C(8)-C(14)-C(15)	-179.8(2)
C(7)-C(8)-C(14)-C(13)	177.3( )
C(9)-C(8)-C(14)-C(13)	56.2(3)
C(12)-C(13)-C(14)-C(8)	-59.5(3)
C(18)-C(13)-C(14)-C(8)	63.0(3)
C(17)-C(13)-C(14)-C(8)	178.4(2)
C(12)-C(13)-C(14)-C(15)	168.9(2)
C(18)-C(13)-C(14)-C(15)	-68.6(3)
C(17)-C(13)-C(14)-C(15)	46.9(2)
C(8)-C(14)-C(15)-C(16)	-163.5(2)
C(13)-C(14)-C(15)-C(16)	-35.1(3)
C(14)-C(15)-C(16)-C(17)	9.0(3)
C(12)-C(13)-C(17)-O(3)	79.3(3)
C(18)-C(13)-C(17)-O(3)	-46.4(3)
C(14)-C(13)-C(17)-O(3)	-164.5(2)
C(12)-C(13)-C(17)-C(16)	-156.6(2)
C(18)-C(13)-C(17)-C(16)	77.7(2)
C(14)-C(13)-C(17)-C(16)	-40.5(2)
C(15)-C(16)-C(17)-O(3)	143.4(2)
C(15)-C(16)-C(17)-C(13)	20.0(3)